Proceedings of the Master's Programme Cognitive Neuroscience of the Radboud University

Table of Contents

From the Editors-in-Chief

Dear reader,

We are very proud to present our first issue of the 13th volume of the *Proceedings of the Master's Programme Cognitive Neuroscience.*

As you can see, the journal is currently run by two women. More so, of its 31 members (the most members we ever had!), 27 are female! This is rather the exception than the rule in most fields inside and outside of science. In 2017, 19.3% of all Dutch professors were female - a very sad percentage. This needs to change, and as the current occupation of the journal proves, it is already changing! Going through our journal, not only will you find mostly excellent theses written by our very own female alumni, but also two more editorials written by an influential female scientist and a cognitive neuroscience master alumnus here at the Donders Institute and connected research institutes. Putting the focus on women in science is not the only change we made this issue.

This year, we decided to implement a few changes in our public appearance and internal proceedings, some of them still in progress, others already implemented. One of these changes can be seen on this very issue you are holding right now. For the first time we had a photo cover contest. The journal team invited current master students to submit pictures of their data to demonstrate the art attributes of science produced in our master's programme. This year Nicholas Bechet won, and you can admire the Kabuki Syndrome neurons, retrieved and grown from stem cells from a Kabuki Syndrome patient on this cover.

As usual, we show our diverse research in the master's programme Cognitive Neuroscience and the Donders Institute for Brain, Cognition and Behaviour, ranging from speech-gesture combinations, predictive processing in adults with autism to spatial navigation, hand choice for action and exercise in Parkinson's Disease in the current printed issue. This issue also shows our diverse range of methods used in our programme ranging from eye-tracking, electroencephalography (EEG), electromyography (EMG) to transcranial magnetic stimulation (TMS) or functional magnetic resonance imaging (fMRI).

Every thesis selected for publication went through a rough selection procedure, being reviewed, asked to be revised and resubmitted. Only the very best, and most creative articles were selected and the whole team worked very hard to publish this issue on time. Further submissions that are not included in the printed version of our journal can be found on our website.

Lastly, we want to thank our amazing team for their hard work on this issue. Without them, it would not have been possible to publish this issue.

Enjoy discovering our diverse research, beautiful data and be inspired!

Nijmegen, December 2017

Your Editors-in-Chief
Lisanne and Katharina

Our minds are like wardrobes, we need to clear it out once in a while

In the second year of my PhD I visited an international conference on one of my favourite topics in neuroscience - multisensory integration. A woman gave a talk that was related to the well-known Shams illusion (i.e. a single flash of light is perceived as two flashes if you simultaneously hear two beeps). First, I was surprised that the speaker was called Shams. Then, I was shocked and ashamed that I obviously had assumed that the audiovisual phenomenon was named after a male scientist.

Implicit biases are everywhere. I have them. You have them. They spare nobody, not even scientists who consider themselves to be objective. How come, women on average earn less than men (even when one corrects for age and experience)? Why do you find fewer women, the higher you look in an organization? If we are objective researchers, it must be that women are not good or not motivated enough, right? That's not it. Many factors contribute to inequality in science, and they are mainly due to the scientific culture. In 2012 an experiment demonstrated a clear favour for male candidates. The application by the fictional student John was evaluated better than the one by the fictional Jennifer although the two applications were identical (Moss-Racusin et al., 2012). Remember this citation since you might need it in the future.

Currently, a lot of time and energy is spent on convincing scientists that they are not always objective even if they would like to be. Luckily, good scientists do not only try to be objective, but are also critical and reflective so that they can ask themselves whether they really are objective. While it is almost impossible to get rid of implicit biases, the good news is that we can change our behaviour. It is up to each and every one of us what we do with them. Do we act upon them or not? If you organize a symposium, invite women and men from around the world to give a talk since they all serve as role models for the next generation of scientists. If you sit in a meeting and a good point is made, take it seriously, no matter who brought it up, PI or student, woman or man. The first step in making science a better place, is admitting implicit biases and critically reflecting on how we currently evaluate science and scientists. Academics often claim that they look for excellence. However, if you ask what they mean by that, it turns out that the majority simply believes that they recognize it once they see it or they describe an ideal candidate that does not exist (Van den Brink & Benschop, 2011). We tend to be more generous in forgiving male candidates if they do not meet all these unrealistic criteria than female candidates. Fortunately, science nowadays is in transition and reconsiders the current evaluation system – a shift from quantity (e.g. publication list) to quality (e.g. five most influential publications) gives hope.

It is great to see the high quality theses by the next generation of scientists in this issue. That is what you are, whether you choose a career in science or not. Your critical thinking and cleverness are valuable qualities. Do not let any biases stop you from pursuing your dreams.

Claudia Lüttke

Sustainable Science Officer 2017 of the Donders Insitute and
Policy Officer for Gender and Diversity at FNWI and CNS Alumnus 2012

A headstart for women

When you go to the RU homepage these days (as on December 18), the two top posts each show a picture with a group of female academics. The first photo's caption reads "26,5 percent female professors: Radboud University raises the bar", the second one comes with the headline "Christine Mohrmann Grant for 10 promising female researchers". Apparently, gender diversity is quite high on the agenda of our university these days. And rightly so: even though the percentage of female professors in Nijmegen (26.5%) is way above the national average (19.3%), there are still many microcosms within the RU that are men's worlds, one among which is the realm of senior positions at the Donders Institute. The Donders has more than 65% women among its PhD students, but only 15% female professors, so it is clear that something has to be done if we do not want to lose much of our female talent in the 'leaky pipeline' along the way to the academic top.

There are many explanations for this leaky pipeline, some of which can be attributed to women themselves (dislike of power games and competition, lack of self-confidence and ambition, etc.), but not all of them can. A few weeks ago, I was asked to give a talk about gender equality in science for the new arrivals of the Max Planck Graduate School (IMPRS). I was asked for this because I am a member of the 'Donders gender steering group', an advisory committee that develops suggestions for the Donders board of directors to improve the gender balance at the Donders Institute, something that has been criticized as very much less-than-optimal in previous external evaluations. I had never given such a talk and I delved into the literature (which was fun!). The part that struck me most was that on gender bias: given the exact same qualifications, women are consistently perceived as less competent than men, with sometimes far-reaching consequences for women's careers.

In one of many, very well-controlled studies (Moss-Racusin et al., 2012), 127 members of natural science faculties in the US were given a fictitious students CV and motivation letter who applied for an (also fictitious) lab manager position. Apparently, within this specific academic environment in the US, it is common for excellent students to take on a lab manager position after graduation, with the aim to acquire relevant research skills and experience before they apply for a PhD position. The participants were told that the study investigated the factors that determine the selection process for this kind of position. Thus, they evaluated the candidate in terms of his/ her competence and likelihood to be hired, and they indicated the salary they would be prepared to offer this person. Now, crucially, all participants received exactly the same application, with one exception: for half of the participants, the candidate's first name was 'John', for the others, it was 'Jennifer'. The result was very similar to those of many other studies with similar research designs: while John received an average competence rating of 4.1 on a five-point scale, Jennifer only got 3.3. As a consequence, John was a lot more likely to be hired (3.8) than Jennifer (2.9), and the yearly salary he was offered was about $3500 higher than hers.

This is sad. What's even worse is the additional finding that female judges, i.e. female researchers who made it all the way to academic faculty in the natural sciences, were just as 'bad' as men were in terms of how strongly they displayed this gender bias. Who on earth should know better than these women that the gender of the first name on a CV says nothing about this person's qualifications? Apparently, simply getting more women into higher positions does not solve the problem; awareness and self-reflection seem to be crucial,

too. We are all implicitly biased, out of reasons I'm not sure I understand, and chances are that I am biased, too. Only when we consciously make an effort to counteract those biases that, by the way, concern every aspect of scientific achievement (receiving grants, getting publications, being cited, becoming tenured, etc.), can we change something.

I am really happy that the current issue of the CNS journal is a start in this direction. The majority (about 60%) of our CNS master students are women. Therefore, in this issue, there was the explicit policy to have a majority of women among the first authors. As talent is certainly very likely to be equally distributed across our male and female students, making sure that the gender proportion in the selected population matches that in the sampling population is surely a good start to fight those biases that sneak in every time you don't pay attention.

As a result, you will find five excellent papers from various fields within Cognitive Science in this issue, four of which written by women and one by a man who graduated from the CNS research master course this year. These top-level articles demonstrate not only the excellence of research at the Donders Institute, but above all the high incidence of outstanding talent in our Master students. All five of these young research talents deserve every possible encouragement to pursue an academic career, and every chance to make it as far in science as their aptitude and ambitions take them, unhindered by gender and other biases. Hopefully, their first publication in this journal provides a first step in this encouragement.

Kristin Lemhöfer

Principal Investigator and Associate Professor
at the Donders Institute for Brain, Cognition and Behavior

About the cover

What we are looking at in this particular image is two astrocytes, which are used to support the growth of neurons, which we derive from induced pluripotent stem cells (IPSC's). The cells themselves were transfected with a particular fluorescent protein isolated from reef coral (dsRed), which localizes throughout the cells thus permitting their visualization when utilizing fluorescence microscopy. The cells seen on the cover were used in support of a control line of IPSC-derived neurons and fall under a project wherein we were looking to investigate an in vitro model for a multiple congenital anomaly syndrome named Kabuki Syndrome (KS), which is strongly associated with epigenetic dysregulation. As such the project was carried out in the RadboudUMC in the Nadif Kasri Lab, which is making groundbreaking work in the application of IPSC models to better understand disorders bounded by intellectual disability and linked to such epigenetic dysregulation. The reason we transfect and image the IPSC-derived neurons is to morphologically characterize how neurons derived from control lines might differ in complexity to those derived from a patient suffering from a particular disorder or syndrome. By extrapolating how cells differ morphologically, and when coupling this readout to network and single cell electrophysiological data, we have the capacity to gain a greater understanding of the molecular mechanisms that underlie these disorders and furthermore test novel therapeutic agents in a personalized, patient specific, modus.

Nicholas Bechet

Winner of the photo cover contest

The ParkCycle Study: Investigating the Effects of Aerobic Exercise on Resting-State Functional Connectivity in Parkinson's Disease

Eva Klimars[1]
Supervisor: Ian Cameron[1]

[1]*Radboud University Nijmegen, Donders Institute for Brain, Cognition and Behaviour, the Netherlands*

Parkinson's disease is characterised by nigro-striatal dopamine depletion and it has been suggested that this depletion influences cortico-striatal functional connectivity. Aerobic exercise is known to promote neuroplasticity, suggesting it might induce partial neurorestoration in cortico-striatal circuits. Therefore, we investigated if a six-month aerobic exercise intervention can partially normalise disease-related changes in functional connectivity in a randomised controlled trial. Patients with Parkinson's disease underwent resting-state fMRI scanning before and after the exercise intervention or control intervention where subjects simply maintained their activity level, and we performed a longitudinal group comparison of the resting-state functional connectivity between different subdivisions of the putamen and the rest of the brain, because distinct striatal subregions are differentially affected by dopamine depletion. Aside from the whole-brain search volume, we also performed a region of interest analysis focusing on changes in connectivity between the putamen and the right inferior parietal cortex, a region previously identified as showing changes in cortico-striatal connectivity because of Parkinson's disease. At the whole brain-level, we observed an increase in resting-state functional connectivity between the right dorsoposterior putamen and the posterolateral cerebellum for the aerobic exercise intervention group, and the opposite pattern (i.e., a decrease) for the control group. When restricting the search volume to the right inferior parietal cortex, we also found that the intervention group showed a decrease in functional connectivity between a subregion of this area and the dorsoanterior putamen, while an increase was observed in the control group. These results do support the possibility for changes in functional connectivity to occur as the results of aerobic training, however, the small sample size necessitates a larger, sufficiently powered study to verify our results.

Keywords: Parkinson's disease, basal ganglia, aerobic exercise, functional connectivity

Corresponding author: Eva Klimars**;** **E-mail:** e.klimars@donders.ru.nl

Parkinson's disease (PD) is a neurodegenerative disorder, characterised by prominent motor symptoms of tremor, bradykinesia, and rigidity. PD is hallmarked by loss of dopaminergic neurons in the substantia nigra, leading to subsequent dopamine deficiency (Bernheimer, Birkmayer, Hornykiewicz, Jellinger, & Seitelberger, 1973; Kish, Shannak, & Hornykiewicz, 1988; Macdonald & Monchi, 2011). The dopaminergic system innervates basal ganglia (BG) structures and their projection targets, for instance the thalamus and brainstem motor center, hence the BG and their target regions are strongly affected by the degeneration of dopamine-producing cells occurring in PD (Dirkx et al., 2017). However, the various BG regions are differentially affected in PD, because degeneration can occur at different stages and to varying degrees throughout disease progression. This is because different regions receive divergent dopaminergic inputs. For example, the ventral striatum, including the ventral putamen, is innervated by dopamine produced in the relatively spared ventral tegmental area, while the dorsal striatum, containing the bulk of the putamen, receives dopaminergic inputs from the more affected substantia nigra (Djaldetti et al., 2011; Fearnley & Lees, 1991; Macdonald & Monchi, 2011; McRitchie, Cartwright, & Halliday, 1997). Additionally to this ventral/dorsal gradient, the posterior and anterior striatum can be distinguished based on their relative dopamine decline. The largest dopamine depletion in PD has been observed in caudal portions of the striatum, especially the posterior putamen. This is important, because motor deficits, typical for idiopathic PD, are mostly the consequence of dopamine loss in the putamen (Guttman et al., 1997; Kish et al., 1988; Ueda & Kimura, 2003; Yu, Liu, Wang, Chen, & Liu, 2013). In contrast, the anterior putamen starts declining at a later stage of PD, but then displays the same rate of progression, meaning a disparity is maintained throughout the course of the disease (Bruck et al., 2006; Nurmi et al., 2001). It has been proposed that the local impairments in the BG processing may propagate through various cortico-striatal connections and thereby alter the activity in other brain areas, which in turn could cause some of the PD symptoms (Obeso, Marin, et al., 2008).

Although, Parkinson's disease is mainly thought to be a movement disorder, there are also more behavioural and cognitive domains impaired aside from motor control. For example, impairments in associative learning, planning, attentional control, working memory, and emotion have been documented. Many of these functions are mediated by the BG through cortico-striatal loops (Grande et al., 2006; McNab & Klingberg, 2008; Muller, Philiastides, & Newsome, 2005; Obeso, Rodriguez-Oroz et al., 2008; Tommasi et al., 2015). These functionally segregated loops have a parallel topology and reciprocally connect the BG to several widespread cortical areas, including prefrontal and fronto-parietal regions (Alexander, DeLong, & Strick, 1986; Yelnik, 2008). According to the parallel loop model of Alexander et al. (1986) there are five segregated functional loops, in which each striatal subpart receives input from another cortical area and sends back connections to the same part of the cortex through specific BG nuclei and the thalamo-cortical connections. Based on the associated cortical regions, each loop was designated to process a specific set of motor and cognitive tasks. Following this study, multiple slightly modified, and further or less subdivided loop models have been proposed (Lawrence, Sahakian, & Robbins, 1998; Nakano, Kayahara, Tsutsumi, & Ushiro, 2000; Saint-Cyr, 2003). Regardless, the various model versions consistently link the caudal and dorsolateral striatum, including most of the putamen, to motor and premotor areas, thus implicating these BG regions in motor functions. The models also agree on cognitive cortico-striatal circuits incorporating more anterior regions of the striatum, such as the rostral putamen and the caudate nucleus (Alexander et al., 1986; Haber, Fudge, & McFarland, 2000; Postuma & Dagher, 2006). Considering the local and regionally specific changes in BG activity in PD and the spatial specificity as well as functional segregation of the cortico-striatal loops, it can be concluded that dysfunctional striatal dopaminergic function differentially affects the loops and thus leads to changes in the balance of activity between the cortico-striatal circuits. These differential changes in the circuits and subsequent altered functional connectivity have been implicated in the development of the PD pathology explaining among others motor symptoms (Shine et al., 2013) and the occurrence of other PD features (Monchi, Petrides, Mejia-Constain, & Strafella, 2007; Owen, 2004; Zgaljardic, Borod, Foldi, & Mattis, 2003). As alterations in the cortico-striatal network are thus causally implicated in the PD pathology, it is of major interest to characterize the distinct disease-related connectivity profile of the network. This can be done using functional magnetic resonance imaging (fMRI) to examine the functional connectivity. Many studies have focused on investigating functional connectivity differences in PD related to performance of a specific task (Helmich, Aarts, de

Lange, Bloem, & Toni, 2009; Palmer, Eigenraam, et al., 2009; Palmer, Li, Wang, & McKeown, 2010; Wu, Chan, & Hallett, 2010; Wu et al., 2012), but recently exploration of resting-state functional connectivity (RSFC) is of growing interest as findings are not limited to a specific brain process and functions.

In a previous study, Helmich et al. (2010) analysed the RSFC in PD and showed decreased coupling between the posterior putamen and a portion of the sensorimotor system, the inferior parietal cortex (IPC), while this region showed increased functional connectivity with the anterior putamen. This shift in recruitment follows the above described dopamine gradient present in PD (i.e., the anterior putamen is relatively spared compared to the posterior putamen), hence dopamine depletion in the posterior putamen could be causing the remapping of cortico-striatal connectivity. On the one hand, the connectivity change observed may reflect a *compensatory* process in PD patients, which is beneficial for some behavioural functions as certain parts of the cortex are redirected to less affected parts of the striatum. On the other hand, however, this remapping may not be optimal if it results in inefficient processing by the anterior putamen, thereby affecting cognitive functions. Because of this, it is critical to further examine if there are compensatory processes occurring in the cortico-striatal network in PD, and if those are beneficial or maladaptive. Moreover, it is also crucial to investigate if those compensatory processes could be influenced with cost-efficient, non-invasive interventions. A potentially effective intervention, aerobic exercise, will be discussed here in detail.

In addition to overt motor impairments, physical activity is found to be generally lower in PD patients and decreases along with disease progression, meaning that their health and quality of life are reduced even further. This is especially concerning, as physical activity has been shown to induce beneficial adaptive neuroplasticity in healthy subjects (Hillman, Erickson, & Kramer, 2008; Thomas, Dennis, Bandettini, & Johansen-Berg, 2012), namely larger prefrontal and temporal white and grey matter (Gordon et al., 2008), which have been shown to be predictive of better cognitive performance in older adults (Erickson et al., 2007; Marks et al., 2007). There are several lines of evidence that physical activity is beneficial to healthy aging, and to neuroprotection. First, in MPTP-lesioned mice (a murine model of PD), aerobic exercise (AE) induces neurorestoration, or in other words, increases dopaminergic transmission and reduces glutamate transmission in the nigrostriatal

system and promotes behavioural recovery (Fisher et al., 2004; Petzinger et al., 2007; Tillerson, Caudle, Reveron, & Miller, 2002). Similarly, exercise-induced neuroplasticity in dopaminergic signalling was also observed in PD patients (Fisher et al., 2013). Furthermore, in PD patients, positive behavioural responses were stimulated by AE as it generally improved motor action, balance and gait as well as postural control (Shu et al., 2014). More specifically, forced stationary cycling improved UPDRS motor scores and bimanual dexterity (Alberts, Linder, Penko, Lowe, & Phillips, 2011; Ridgel, Vitek, & Alberts, 2009). Finally, the pedalling rate during an eight week forced-rate lower-extremity exercise intervention could be positively correlated to functional connectivity changes between the most affected primary motor cortex and the ipsilateral thalamus (as well as a trend towards an increase in connectivity to the putamen) during a bilateral finger tapping task (Shah et al., 2016).

Taken together, there is sufficient evidence that exercise may be able to restore neuronal function in the more strongly impaired motor networks of the BG. Therefore, the effects of AE on functional connectivity networks in PD were investigated in a randomised controlled trial involving AE in one group of patients, compared to a six-month waiting period in another group of PD patients. Based on the previous findings from Helmich et al. (2010) we were specifically interested in the influence of AE on functional connectivity between the putamen and the sensorimotor system, but we were also interested in non-motor areas to examine the breadth of AEs influence in the brain. Therefore, we performed a whole-brain analysis, as well as a region of interest (ROI) analysis focusing on connectivity between the putamen and the inferior parietal cortex, a portion of the sensorimotor system. In both analyses, voxel-wise temporal correlations with the putamen seed regions were determined for the defined search volume (i.e., whole brain or ROI), to identify if there is statistical dependency among activation time-series of the putamen seed regions and other brain areas, which will be referred to as functional connectivity from now on. The main question addressed by this study, is whether AE can (partially) restore those changes documented by Helmich et al. (2010), who observed a shift in cortico-striatal connectivity from the posterior to the anterior putamen. We hypothesised that disease-related network connectivity changes will indeed (partially) normalize after AE.

Methods

Recruitment of Subjects

Twenty-one participants, between 30 and 75 years of age, with the diagnosis of idiopathic Parkinson's disease were recruited from the neurology department of the Radboudumc Nijmegen, the Netherlands during a 24-month period. Before the baseline assessments all subjects signed an informed consent form according to institutional guidelines of the local ethics committee (CMO region Arnhem-Nijmegen, the Netherlands). For inclusion, patients had to fulfil all of the following criteria:

- early disease stage (i.e., Hoehn & Yahr stage I-II)
- ability to cycle unaffected
- normal cognitive function (i.e., Mini-Mental State Examination score > 24)
- low risk of cardiovascular disease, thus no hypertension, diabetes mellitus, cardiac valve defects, rhythm disorder, heart failure; also a body mass index (BMI) < 30
- untreated for PD or receiving anti-Parkinson medication for less than two years and a stable dopaminergic response for at least one month
- medical history that did not include stroke or transient ischemic attack,
- no use of beta-blockers or daily institutionalized care
- sedentary lifestyle
- MRI compatibility
- computer with internet access at home
- ability to complete Dutch or English questionnaires

The Hoehn & Yahr stage I and II are defined as "unilateral involvement only, usually with minimal or no functional impairment" and "bilateral or midline involvement, without impairment of balance" respectively, hence patients were only minimally disabled (Hoehn & Yahr, 1967). Patients who did not have moderate intensity aerobic physical activity for a minimum of 30 minutes on five days each week or vigorous intensity aerobic activity for a minimum of 20 minutes on three days each week were considered sedentary according to the recommendations of the American College of Sports Medicine and American Heart Association for older adults (65+ years) and adults aged 50–64 with clinically significant chronic conditions or functional limitations (Nelson et al., 2007). Of the 21 originally recruited subjects, one subject dropped out and three more were excluded from the analysis due to scanner artefacts and excessive motion. Therefore, the remaining 17 subjects were included in the analysis.

Randomization and Concealment

After completion of the baseline assessment participants were randomly assigned, by an independent biostatistician, to either the AE group or the control group with an allocation ratio of 1:1. Permuted blocks of varying size (maximally three consecutive patients with the same allocation) were employed to ensure balance over time.

Intervention

Patients in the AE group performed three to five individual training sessions per week, of at least 30 minutes on a stationary bike, at home for about six months. They were instructed to exercise at 60-80% of their heart rate reserve, which was calculated using the Karvonen formula (Karvonen, Kentala, & Mustala, 1957). Usage of the equipment was explained during a home visit and also a practice session was performed to see if the patient understood the instructions and training objectives. The stationary bikes (Amada Sport, Velp, the Netherlands) were equipped with a computer, which provided feedback on the current heart rate, exercise time, pedalling cadence and power in Watts. Participants could select from a range of real-life videos of well-known cycling routes, such as the Alpe d'Huez, to create diverse training sessions of 30 to 45 minutes. The playback speed of the video was influenced by their pedalling rate. All exercise and performance data of each patient were automatically uploaded to a cloud-based database and monitored by the exercise physiologist on a biweekly basis. Training performance was evaluated through an online monitoring system and training goals and preferences were adjusted by the exercise physiologist based on the participant's improvements. For instance, if a patient was able to complete the created routes too easily and the target heart rate was not met, a more challenging route was created and alternatives were sought corresponding with the participant's preferences. Adherence to the intervention was determined halfway the training period (after three months) and at the end of the intervention (after six months).

Patients in the control group continued their usual physical activities and were instructed to keep those as stable as possible. They also kept receiving

the usual care related to their PD, which was provided by their own neurologist. In the case of changes in activity level or medication they were instructed to inform the research team. There was no additional contact with the control group during the trial besides the baseline and follow-up assessments. The actual time interval between the two assessments was comparable between the two groups, with on average 216.4 (σ = 28.1) days for the AE group and 195.5 (σ = 24.7) days for the control group.

Clinical assessments and statistical analysis

All clinical measurements were obtained during two identical sessions: one at baseline and one at the end of the six-month intervention period. All assessments were done in OFF medication state and the baseline and follow-up ratings for each participant were done by the same assessor. All assessors received extensive training before the first assessment. Baseline tests were done before randomisation. The severity of motor symptoms was assessed during both sessions using part III of the Unified Parkinson's Disease Rating Scale in order to estimate disease progression visible from motor symptoms. To ensure that our results are not confounded by the development of cognitive impairments or changes in the usual everyday physical activity, the Mini-Mental State Examination Questionnaire and the LASA Physical Activity Questionnaire were also filled in twice by participants.

The clinical data were analysed using IBM SPSS Statistics (23.0, SPSS Inc., Chicago, USA). Independent-samples t-tests were performed to assess between-group differences in clinical score development from baseline to follow-up. Moreover, between-session differences for clinical scores of both groups were tested for using paired-samples t-tests. Additionally, baseline characteristics of the two groups were compared by performing a Mann-Whitney U test to validate that the two patient populations are comparable. Statistical significance was assumed when $p < .05$.

Image Acquisition

Imaging data were acquired during two identical MRI sessions: one at baseline and one six months later after the intervention period. Structural and functional images were acquired in the morning, at least 12 hours after the last dose of dopaminergic medication, which is defined as off-condition

(Langston et al., 1992). Imaging was performed on a 1.5-Tesla MRI scanner (Siemens Avanto, Erlangen, Germany) equipped with an 8-channel phased-array head coil. For each subject a high-resolution T1-weighted MPRAGE anatomical scan was obtained (TR = 2730 ms, TE = 2.95 ms, TI = 1000 ms, flip angle = 7°, 176 sagittal slices, matrix size = 350 × 263 × 350 mm, voxel size = 1.0 × 1.0 × 1.0 mm, field of view [FOV] = 256 mm, scanning time approximately 11.5 minutes). Furthermore, about 8.5 minutes of resting-state functional MRI (rsfMRI) data were collected consisting of 266 interleaved whole-brain functional volumes using a gradient-echo echo-planar imaging (GE-EPI) sequence (TR = 1870 ms, TE = 35 ms, flip angle = 80°, 39 axial slices, matrix size = 224 × 224 × 137 mm, voxel size = 3.5 × 3.5 × 3.5 mm, FOV = 224 mm). Participants were verbally instructed to lie still with their eyes open, to think of nothing in particular and to stay awake. The subject's eyes were monitored by the experimenter to confirm wakefulness during the scanning.

Preprocessing of Functional MRI Images

Imaging preprocessing was performed using FSL software, version 5.0.9 (http://fmrib.ox.ac.uk/fsl; Jenkinson, Beckmann, Behrens, Woolrich, & Smith, 2012). The functional data were preprocessed using the FMRI Expert Analysis Tool (FEAT v6.00), including motion correction with MCFLIRT (Jenkinson, Bannister, Brady, & Smith, 2002), slice-timing correction, grand mean scaling, spatial smoothing using a Gaussian kernel of 5 mm full width at half-maximum (FWHM) and deletion of the first four volumes to allow the magnetisation to reach dynamic equilibrium, leaving 262 volumes for later analysis. Also, for the higher-level analysis required registration transformations were generated. First, the anatomical scans were brain extracted with the brain extraction tool implemented in FSL (BET v2.1; Smith, 2002) as needed for the boundary based linear registration method (Greve & Fischl, 2009) of the FMRIB's Linear Image Registration Tool (FLIRT; Jenkinson et al., 2002; Jenkinson & Smith, 2001), which was used to find the linear transformation to the structural space. Second, the non-linear transformation for transferring the anatomical images to the standard space was estimated using the FMRIB tool for small-displacement non-linear registration (FNIRT; Andersson, Jenkinson, & Smith, 2007). Third, both transformations were concatenated and

saved for later use in the group-level analysis. In the following, ICA-AROMA (Pruim et al., 2015) was used to identify and remove motion-related artefacts using non-aggressive denoising. Mean displacement for subjects of the AE and control group during the baseline session was 0.19 mm and 0.20 mm, respectively. Mean displacement during the follow-up session was comparable, 0.19 mm for the AE group and 0.22 mm for the control group. Two-sample t-tests did not reveal any significant differences in motion between the two groups for the baseline session ($t_{df=15} = -0.951$, $p = .360$), follow-up session ($t_{df=15} = -0.643$, $p = .530$) and both combined ($t_{df=32} = -1.019$, $p = .316$) or between the two session ($t_{df=32} = -0.574$, $p = .571$). Additionally, nuisance regression was done, including 24 motion parameters and signals from white matter (WM) and cerebrospinal fluid (CSF) to filter out residual effects of motion using linear regression. Lastly, a high-pass filter with a cut-off frequency of 0.01 Hz was applied. Global signal regression was not performed as it has been shown to introduce anti-correlations in resting-state data (Murphy, Birn, Handwerker, Jones, & Bandettini, 2009).

Longitudinal Seed-Based Analysis

First-Level Time-Series Analysis. The putamen was segmented from each subject's whole-head native space anatomical images using the model-based subcortical segmentation tool FIRST (Patenaude, Smith, Kennedy, & Jenkinson, 2011). The output was then linearly transformed to the native functional space using FLIRT. Next, the segmented putamen was first split manually into a left and right part. Then, to further subdivide the left and right putamen, four masks were created for the dorsoanterior-, dorsoposterior-, ventroanterior- and ventroposterior part of the brain. The borders between these masks were drawn at y = 0 and z = 0 in MNI (Montreal Neurological Institute) space based on previous work (Helmich et al., 2015; Postuma & Dagher, 2006) such that they passed through the anterior commissure. A gap of 4 mm was left between the different masks to minimise partial volume effects, so dorsal was defined as z ≥ 2 mm, ventral as z ≤ 2 mm, anterior as y ≥ 2 mm and posterior as ≤ 2 mm. The four masks were transformed non-linearly to the subject's functional space using the *applywarp* command and by multiplying them with the masks of the left and right putamen both were subdivided into four regions, resulting in a total of eight seed regions.

Afterwards, it was verified in all subjects that the various transformations were successful and it was ensured that there was no overlap between any seed regions. This procedure made it possible to run the time-series analysis in native space. Next, the mean time course was calculated for each seed region and input as regressor into the first-level analysis. For each subject a multiple regression analysis was performed including the time courses from all eight seed regions, and whole-brain voxels. Thereby eight zstat images were obtained, reflecting the degree of correlation of each voxel's time course with the regressors.

Group-Level Analysis. The first-level zstat images were registered to the MNI standard space applying the earlier, FEAT-generated transformation using *applywarp*. As longitudinal effects were of interest for this analysis, the paired difference (post − pre) of the zstats was calculated. Next, we performed two separate seed-based analyses for different search volumes using non-parametric tests, as due to the small number of subjects we cannot assume that our results are normally distributed. First, whole-brain analysis was performed, including only the voxels present in all participants. To identify group (i.e., intervention-induced) differences in the longitudinal connectivity change, non-parametric permutation testing with 5000 permutations was performed on the paired difference zstat images using the *Randomise* tool of FSL (v2.9; Winkler, Ridgway, Webster, Smith, & Nichols, 2014). The family-wise error (FWE) rate was controlled by applying cluster-based thresholding with an initial cluster-forming threshold of z = 3.1, chosen based on methods of Woo et al. (2014) and Eklund et al. (2016). The significance level was set at one-tailed $p < .05$. Second, another group comparison was done using *Randomise*, also applying 5000 permutations, focusing on a target region in the right inferior parietal cortex (IPC), which had been identified by previous studies (Helmich et al., 2010; Helmich et al., 2015). Voxel-wise tests were masked with a 12 mm sphere around the MNI coordinates [+56, −20, +28]. Threshold-Free Cluster Enhancement (TFCE; Smith & Nichols, 2009) was applied and between-group effects were considered significant if a one-tailed p-value < .05 (FWE corrected) was reached. Gender and age were also added to both models as covariates of no interest.

Supplementary Analyses

Furthermore, we performed four post hoc

analyses to confirm that the two intervention groups did not differ at baseline and to examine the validity of the results from the seed-based analysis (i.e., test if the observed differences might indeed be caused by intervention effects). First, it was explored if RSFC differences between the AE and control group were already present at baseline. This was done for the whole brain as well as for the previously defined IPC target region. In both cases non-parametric permutation testing was performed, using the zstat images from the baseline session of each subject as input. Second, we tested for an intervention effect by doing a non-parametric two-sample paired t-test, comparing the baseline and follow-up session of the subjects from the AE group. Again, this was done for the whole brain and the 12 mm sphere in the IPC. All analyses were done with *Randomise*, applying 5000 permutations. For the two whole-brain analyses, cluster-based thresholding with a cluster-forming threshold of z = 3.1 was applied. TFCE was used for the ROI analyses, for which the search volume was restricted to the IPC.

After the longitudinal seed-based analysis, we also carried out an fMRI-based power analysis, to estimate the number of subjects required for detecting significant intervention effects in a study that would test for between session differences in a group of PD patients, who all undergo a six-month aerobic exercise intervention. This was done using novel methods developed by Mumford and Nichols (2008), which are implemented in the fMRIpower software package (fmripower.org). This method uses pilot data, in this case our outcome data from the post hoc analysis comparing the baseline and follow-up session of the subjects from the AE group. The estimation is done under the assumption that the data acquired in this future study will have similar characteristics (e.g., similar number of runs per subject and a comparable length of the runs) and that the scanner noise characteristics will be about the same. The power calculation was based on the previously by Helmich et al. (2010) identified target region in the right IPC, consisting of a 12 mm sphere drawn around the MNI coordinates [+56, −20, +28]. The significance level was set at one-tailed $p < .05$. The effect size was expressed in standard deviation units, which is analogous to the Cohen's D measure.

Table 1.

Baseline characteristics and clinical score development from baseline to follow-up per allocation

	Aerobic exercise (n = 9)	Control (n = 8)	*p*-value
Baseline characteristics			
Mean age in years (SD)	54.7 (10.7)	58.5 (6.7)	.387
No. of men (%)	6 (66.7%)	5 (62.5%)	.888
Disease duration in months	10 (10.5)	10 (8.8)	.888
No. of patients using medication (%)	7 (77.8%)	7 (87.5%)	.541
Levodopa	7 (77.8%)	6 (75%)	.963
Dopamine agonist	-	1 (12.5%)	.673
LED	375 (343.8)	375 (328.1)	.815
No. of patients with H&Y grade I (%)	4 (44.4%)	4 (50%)	.721
UPDRS III	17 (11)†	15 (4.8)	.852
MMSE	29 (1.5)	29 (1.8)	.370
LAPAQ outdoor	17.1 (15)	23.6 (33.8)	.236
Clinical score development from baseline to follow-up session			
Mean UPDRS III difference [95% CI]	2.0 [−2.8, 6.8] †	6.8 [1.5, 12.0]	.128
Mean MMSE difference [95% CI]	0.1 [−0.6, 0.8]	−0.3 [−1.3, 0.8]	.522
Mean LAPAQ outdoor difference [95% CI]	1.0 [−8.9, 10.8]	11.2 [−4.4, 26.9]	.216

Note. Numbers express the median followed by the interquartile range in brackets unless indicated otherwise. LED = Levodopa Equivalent Dose; H&Y = Hoehn and Yahr scale; UPDRS = Unified Parkinson's Disease Rating Scale; MMSE = Mini-Mental State Examination; LAPAQ = LASA Physical Activity Questionnaire (only outdoor and sports activities, reported in minutes per day); SD = Standard Deviation; CI = Confidence Interval. †Missing data from three subjects.

Results

Patients

In total 17 patients (11 men, 6 women) were included in the analysis. Nine subjects were assigned to the AE group and the remaining eight subjects were allocated to the control group. Baseline characteristics were similar between the two groups as depicted by Table 1. Within the six months between the assessments, the Unified Parkinson's Disease Rating Scale Part III (UPDRS III) score significantly increased in the control group subjects by 6.8 units on average $(t_{df=7} = -3.021, p = .019)$, which might indicate disease progression, while the not changing significantly for participants in the AE group (mean difference = 2.0 units, $t_{df=5} = -1.074, p = .332$). The cognitive function, as examined by the Mini-Mental State Examination, stayed about the same for subjects of the AE group $(t_{df=8} = -0.359, p = .729)$ as well as the control group $(t_{df=7} = 0.552, p = .598)$ and also the physical activity, determined using the LASA Physical Activity Questionnaire, was not significantly altered when comparing the follow-up and baseline assessment for the intervention $(t_{df=8} = -0.224, p = .829)$ and control group $(t_{df=7} = -1.698, p = .133)$. Importantly, the two groups did not show any differences in the clinical score change from baseline to follow-up (Table 1).

Longitudinal Functional Connectivity Differences Between Groups

The whole-brain analysis of voxel-wise connectivity with the striatal seed regions revealed a significant cluster in the cerebellum, which showed a greater increase in resting-state functional connectivity (RSFC) with the right dorsoposterior putamen for the AE group, but the opposite pattern for the control group (MNI coordinates peak voxel: +28; -78; -20, p-value = .0292, cluster size = 173 voxels [2 mm isotropic]). The cluster was located in the right cerebellar lobule VI and crus I regions (Fig. 1).

When restricting the search volume to a 12 mm
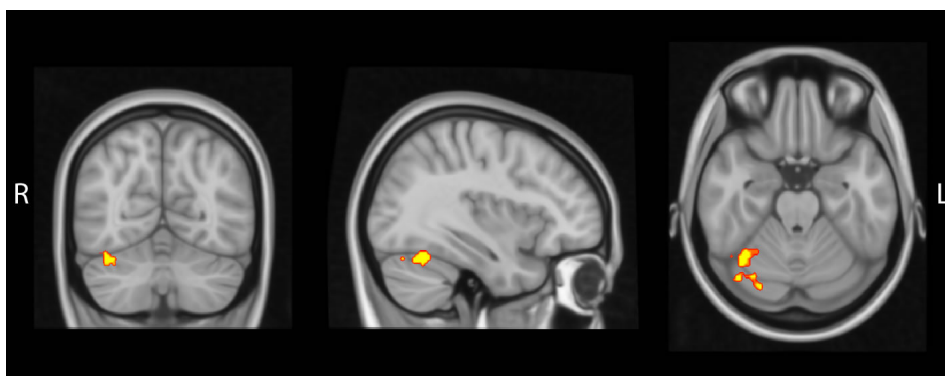
Fig. 1. Between-group difference in the longitudinal change of RSFC of the whole brain with the putamen. Significant differences were found in the posterolateral cerebellum, which showed a larger increase in RSFC with the right dorsoposterior putamen for the AE group compared to the control group. Displayed slices are in line with the center of gravity of the cluster, located at MNI coordinates [+36, -64, -23].

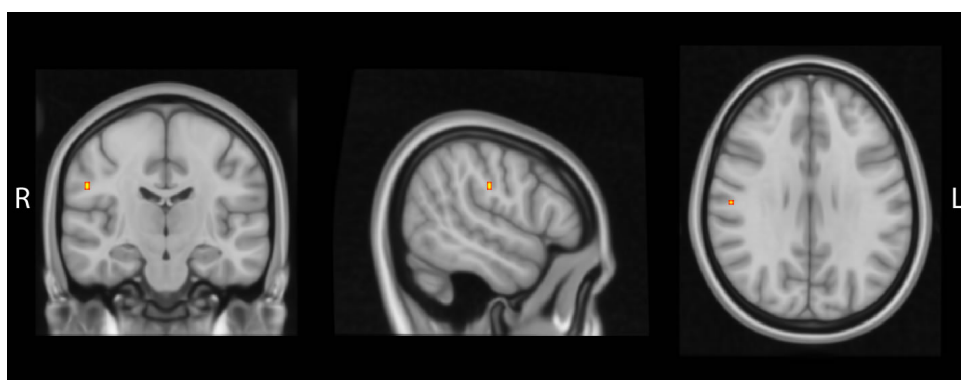**Fig. 2.** Between-group difference in the longitudinal change of RSFC between the putamen and the right IPC. A small cluster in the right IPC showed a larger increase in RSFC with the right dorsoanterior putamen for the control group compared to the AE group. Displayed slices are in line with the peak voxel of the cluster at MNI coordinates [+54, -18, +30].

sphere in the right IPC, which had been previously identified as region displaying altered functional connectivity with distinct putamen subdivisions (Helmich et al., 2010), a small significant cluster was found, for which the RSFC with the right dorsoanterior putamen increased in the control group within the six months, while decreasing in the AE group (MNI coordinates peak voxel: +54; -18; +30, p-value = .0228, cluster size = 2 voxels [2 mm isotropic]). This peak in the parietal lobe, shown in Figure 2, was part of a larger cluster of activation

that was found at p = .08 (cluster size = 11 voxels [2 mm isotropic]).

Note however, that these group differences observed in both longitudinal seed-based analyses were driven by *opposing changes* in RSFC between the putamen and the posterolateral cerebellum or right IPC for both groups. That means that on the group-level, the RSFC between seed and target region increased from the baseline session to the follow-up for one group, while decreasing for the other. For the cerebellar cluster, shown in Figure 1, all
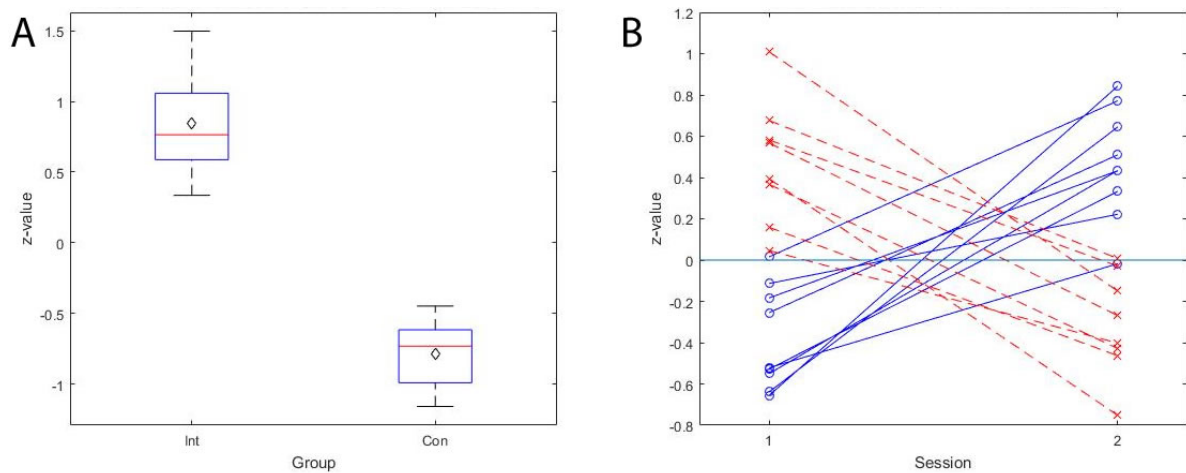

Fig. 3. Between session z-value difference in the posterolateral cerebellum. **A.** The variation in between-session z-value change is depicted for both groups. Whiskers represent the full range from minimum to maximum value. The mean between-session z-score difference is indicated with diamonds. Subjects of the AE group (Int) increased in z-value from baseline to follow-up, while the subjects of the control group (Con) showed a z-score decrease. **B.** The individual changes in z-value from baseline (session 1) to follow-up (session 2). Subjects of the AE group are shown in blue with a continuous line, control subjects in red with a dashed line.

Fig. 4. Between session z-value difference in the right IPC. **A.** The variation in between-session z-value change is depicted for both groups. Whiskers represent the full range from minimum to maximum value. The mean between-session z-score difference is indicated with diamonds. Subjects of the AE group (Int) decreased in z-value from baseline to follow-up, while the subjects of the control group (Con) showed a z-score increase. **B.** The individual changes in z-value from baseline (session 1) to follow-up (session 2). Subjects of the AE group are shown in blue with a continuous line, control subjects in red with a dashed line.
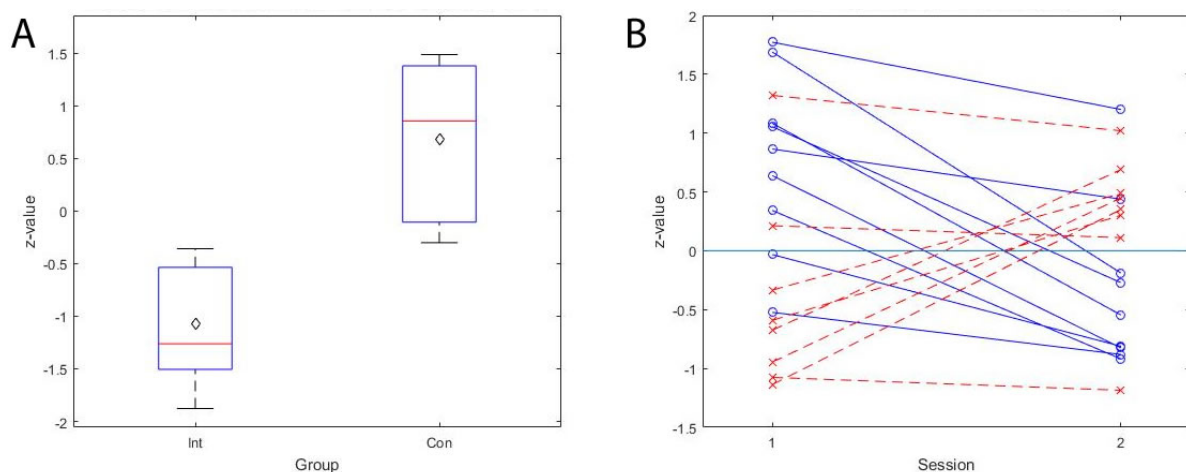
subjects of the AE group increased in z-value from baseline to follow-up, with a mean z-score increase of 0.84, while all the control subjects showed a z-score decrease, which was −0.79 on average (Fig. 3A). Note, however, that the connectivity of the dorsoposterior putamen with the posterolateral cerebellum seems to differ between the two groups at baseline (Fig. 3B). A similar, but reversed pattern was found for the IPC. There was a mean decrease in the z-score of −1.08 for the AE group and a mean increase of 0.68 for the control group (Fig. 4A). The individual time-series correlation scores of the IPC cluster with the dorsoanterior putamen are shown in Figure 4B.

Supplementary Analyses

The whole-brain analysis comparing the baseline RSFC for both intervention groups did not reveal any significant group differences at baseline. In addition, intervention effects could not be confirmed by the whole-brain two-sample paired t-test comparing both sessions of the participants that underwent the AE training. Also for an adjusted search volume, including only the 12 mm sphere in the right IPC, no group differences were detected for the baseline session. However, when testing for an intervention effect in the AE group in the right IPC, a small cluster showed a significant increase in connectivity from baseline to follow-up with the left dorsoposterior putamen (MNI coordinates peak voxel: +50; -22; +28, p-value = .0466, cluster size = 2 voxels [2 mm isotropic]) (Fig. S1). Note that the coordinates and the associated seed region did not match the coordinates and corresponding seed regions of the clusters found by the initial longitudinal seed-based analysis. The power analysis revealed that with 134 subjects we will have at least

80% power to detect a mean differences between the two sessions of 0.216 standard deviation units in the right IPC (Fig. S2).

Discussion

Our longitudinal seed-based analysis revealed two clusters, in the posterolateral cerebellum and right IPC, driven by a group difference in the alteration of functional connectivity with the putamen from baseline to follow-up assessment. Initially, the group comparison of the longitudinal change in RSFC between the putamen and the rest of the brain showed differences in the posterolateral cerebellum. This is striking, because the cerebellum has been implicated in both pathological and compensatory processes in PD, implying a functional relevance to changes in the BG-cerebellar connectivity. The cerebellum has been found to display hyperactivation during motor execution and motor learning in PD patients (Wu & Hallett, 2013) and other changes in the cerebellum such as altered dopaminergic neurotransmission and decrease in gray matter volume have been suggested to be associated with the motor symptoms in PD (Lewis et al., 2013). More specifically, modifications of striato-cerebellar connections in PD have been reported by previous studies. For example, during a self-initiated movement task, decreased effective connectivity was observed for striato-thalamo-cortical and striato-cerebellar connections (Wu et al., 2011), which might reflect abnormal signalling from the BG influencing cerebellar function (Bostan, Dum, & Strick, 2010). In addition, many studies have suggested that cerebello-thalamo-cortical pathways are involved in pathological, as well as compensatory processes in PD.

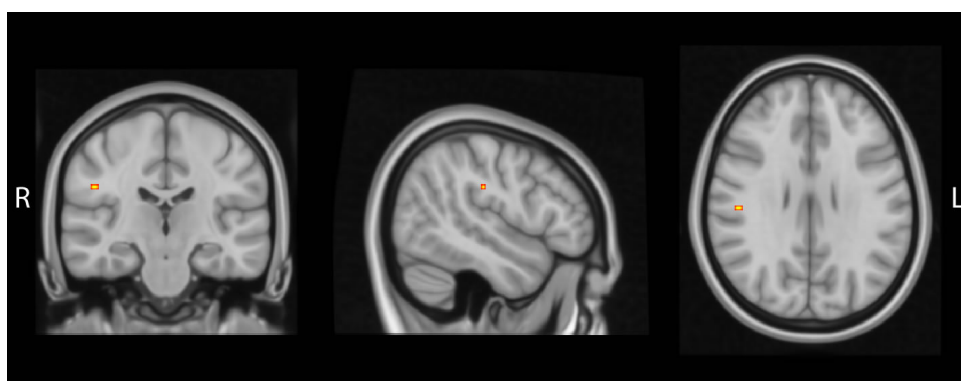On the one hand, tremor-dominant Parkinson's

Fig. S1. Longitudinal RSFC change between the putamen and the right IPC of the intervention group. A small cluster in the right IPC showed a significant increase in connectivity from baseline to follow-up with the left dorsoposterior putamen for the AE group. Displayed slices are in line with the peak voxel of the cluster at MNI coordinates [+50, -22, +28].
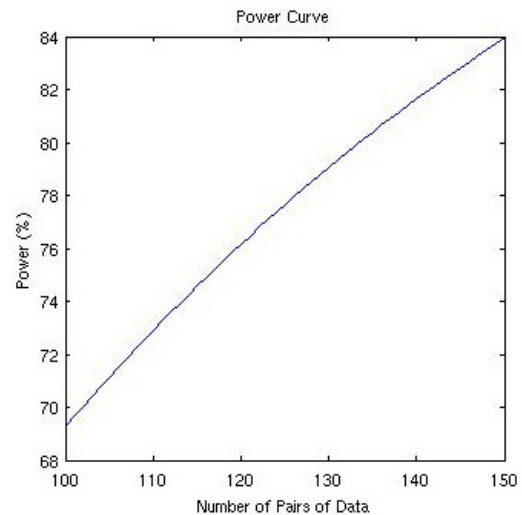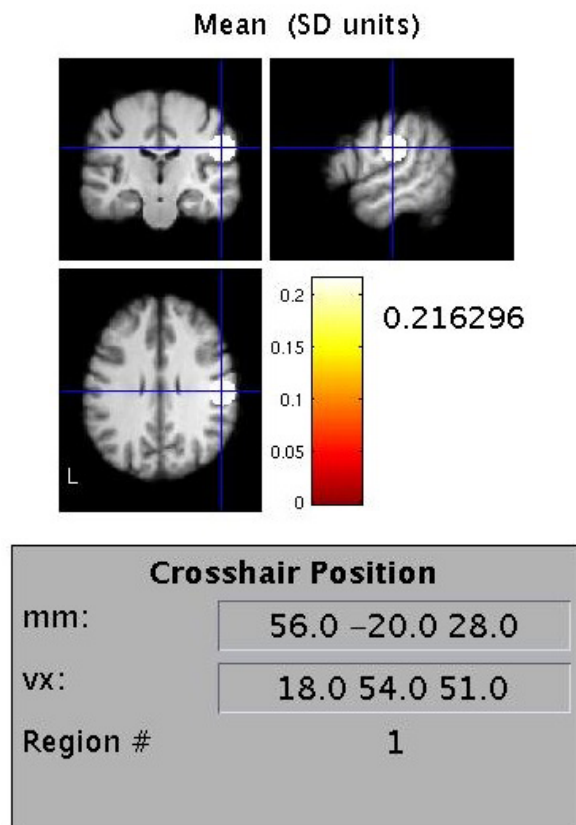
Fig. S2. Effect size estimation and power curve for the right IPC as determined by fmripower. Calculations were done based on a between-session comparison of the resting-state fMRI data from the AE group. The effect size is expressed in standard deviation (SD) units. In total 134 subjects would be required, to have at least 80% power to detect a between-session mean differences of about 0.216 standard deviation units in the right IPC.

patients showed increased functional connectivity between the BG and cerebello-thalamo-cortical circuits and tremor amplitude-related activity correlated with the latter, indicating that the cerebellum could be involved in the propagation and transmission of the resting tremor, which might be underlain by a pathological interaction between the BG and these circuits (Helmich, Janssen, Oyen, Bloem, & Toni, 2011). On the other hand, the cerebello-thalamo-cortical network was increasingly engaged in a visually guided sinusoidal force task as it became more challenging (Palmer, Ng, Abugharbieh, Eigenraam, & McKeown, 2009) and recruitment of these circuits positively correlated with the severity and progression of symptoms during early stages of PD (Sen, Kawaguchi, Truong, Lewis, & Huang, 2010; Wu et al., 2009). It has been proposed that this increased connectivity in cerebello-thalamo-cortical loops compensates for hypofunction in the striato-thalamo-cortical, which induces a decline in motor performance (Wu & Hallett, 2008), thereby preserving near-normal motor function. Recently, also altered functional connectivity between the putamen and the cerebellum was found, which seemed to be compensating for pathological changes in the connectivity of the putamen with the primary motor cortex (Simioni, Dagher, & Fellows, 2016).

Taken together, the group difference in RSFC

change between the putamen and the posterolateral cerebellum that we observed, could be driven by opposing processes occurring in subjects AE group compared to control subjects. That means that the increase in RSFC in the intervention group might reflect a potentially compensatory alteration to improve motor function induced by AE. In contrast, in the absence of the additional physical activity, pathological processes might dominate in the control group and the decrease in functional connectivity could simply represent progression of PD. The notion that disease progression might occur in control subjects, but not in subjects of the AE group, as it is counteracted by compensatory processes induced by AE, is not fully supported by the clinical data: while the UPDRS III score worsens for control subjects, there is no significant change in participants undergoing the physical training, but a direct comparison of the change in the UPDRS III score within the six months between groups did not reveal significant differences. Still, it is possible that disease-related functional connectivity changes in the posterolateral cerebellum are indeed restored by a long-term moderately intensive aerobic exercise intervention. That being said, our results might be influenced by methodological confounds, which will be described in the study limitations section.

It is also interesting that we detected group

differences in RSFC between the putamen and the region previously identified by Helmich et al. (2010) in the right IPC. The authors interpreted the shift in cortico-striatal functional connectivity from the posterior putamen to the anterior putamen as a compensatory mechanism in idiopathic PD, which was dependent on the spatial pattern of dopamine depletion in the striatum. Transferring this hypothesis to our study and assuming that AE is able to (partially) restore the connectivity pattern present in the healthy brain, we would have expected to see the largest group differences in cortico-striatal functional connectivity in the heavily dopamine depleted dorsoposterior and less affected ventroanterior putamen. Specifically, the RSFC of the ventroanterior putamen with the right IPC should have increased or not changed for the control group, while the AE group should have displayed a decrease in RSFC between the two regions from baseline to follow-up. The reversed pattern would be expected for the dorsoposterior putamen. In contrast to this, we found a differential longitudinal functional connectivity change with the right IPC in the dorsoanterior putamen only; RSFC decreased during the six months for subjects of the AE group and increased in the control group. It could be that effects were observed in this putamen subregion as the dopamine gradient might not be perfectly in line with the dorsoposterior-ventroanterior axis and the borders between the subdivisions of the putamen were drawn at arbitrary coordinates. Moreover, there is a chance that partial volume effects were not fully eliminated when creating the seed regions. More general study limitations, applying to all analyses carried out in this study, will be covered in the next section.

Study Limitations

There are a number of methodological constraints, which could have potentially influenced the outcome of our analyses. First of all, we have to acknowledge that the small sample size limits the detection power, while at the same time increasing the chance to find false positives as explained by Button et al. (2013) in detail. We cannot fully remove the doubts about our findings reflecting a true effect as, for example, the cluster size was generally quite small. Moreover, the post hoc analyses could not provide support for the intervention leading to the group differences detected by the longitudinal group comparison: no effect of AE on the functional connectivity with the putamen was found in the whole-brain analysis. Additionally, when restricting the target area to the right IPC, the post hoc analysis only revealed a between-session difference in RSFC between the left dorsoposterior putamen and another IPC area that did not align with the coordinates of the significant cluster in the right IPC observed before. We, therefore, cannot confirm potential effects of aerobic exercise on resting-state functional connectivity in Parkinson's disease with absolute certainty. It is possible that we discovered a true effect here, still the power analysis performed, points towards it rather being a false positive, as it suggests that the number of participants required to detect significant effects is much higher. It remains unclear how the significant cluster in the right IPC identified by the post hoc analysis should be interpreted. The between-session difference was marginally significant, but not large enough to also be observed in the whole-brain analysis. We cannot draw any conclusions about the nature of this cluster due to the small sample size and subsequent limited number of data points.

Second, it is possible that our methods restrict us to finding only the largest group differences, which are driven by *opposing* longitudinal changes in both groups. For example, as Figure 3B shows, the mean cluster z-values of the groups seem to be dissimilar at baseline already for the posterolateral cerebellum, despite this segregation not being confirmed by post hoc analyses. A similar distinction, although to a lesser extent, could be observed in the right IPC (Fig. 4B). This is striking, because assuming that differences in the RSFC change between the two groups are caused by the intervention, we would expect the groups to not differ at baseline and then diverge until the follow-up session. In addition, there is a surprisingly large change in RSFC in both groups, which leads to an almost inverted connectivity pattern in the follow-up assessment. It seems that our methods are such that only the largest group differences in longitudinal RSFC alteration are detected and we are prone to finding this kind of distinctness in which the functional connectivity pattern is reversed from baseline to follow-up.

Conclusion

In this study we identified the posterolateral cerebellum as a region in which both pathological changes in RSFC with the putamen, as a consequence of PD, as well as restoration of those connectivity changes, induced by aerobic exercise, might occur. By comparing PD patients undergoing physical

training and patients not receiving this six-month intervention, we also found opposing longitudinal changes in cortico-striatal connectivity in the right IPC, a region that previously had been shown to display altered connectivity with distinct putamen subregions in Parkinson's patients, potentially reflecting compensatory mechanisms taking place in PD. However, we have to acknowledge that there is the possibility of the small sample size undermining the reliability of our results. A larger follow-up study is required to confirm potential effects of aerobic exercise on resting-state functional connectivity in Parkinson's disease.

References

Alberts, J. L., Linder, S. M., Penko, A. L., Lowe, M. J., & Phillips, M. (2011). It is not about the bike, it is about the pedaling: Forced exercise and Parkinson's disease. *Exercise and Sport Sciences Reviews, 39*(4), 177-186.

Alexander, G. E., DeLong, M. R., & Strick, P. L. (1986). Parallel organization of functionally segregated circuits linking basal ganglia and cortex. *Annual Review of Neuroscience, 9*, 357-381.

Andersson, J. R., Jenkinson, M., & Smith, S. (2007). Non-linear registration, aka Spatial normalisation FMRIB technical report TR07JA2. *FMRIB Analysis Group of the University of Oxford, 2.*

Bernheimer, H., Birkmayer, W., Hornykiewicz, O., Jellinger, K., & Seitelberger, F. (1973). Brain dopamine and the syndromes of Parkinson and Huntington. Clinical, morphological and neurochemical correlations. *Journal of Neurological Science, 20*(4), 415-455.

Bostan, A. C., Dum, R. P., & Strick, P. L. (2010). The basal ganglia communicate with the cerebellum. *Proceedings of the National Academic of Sciences U S A, 107*(18), 8452-8456.

Bruck, A., Aalto, S., Nurmi, E., Vahlberg, T., Bergman, J., & Rinne, J. O. (2006). Striatal subregional 6-[18F] fluoro-L-dopa uptake in early Parkinson's disease: A two-year follow-up study. *Movement Disorder, 21*(7), 958-963.

Button, K. S., Ioannidis, J. P., Mokrysz, C., Nosek, B. A., Flint, J., Robinson, E. S., & Munafo, M. R. (2013). Power failure: Why small sample size undermines the reliability of neuroscience. *National Review of Neuroscience, 14*(5), 365-376.

Dirkx, M. F., den Ouden, H. E., Aarts, E., Timmer, M. H., Bloem, B. R., Toni, I., & Helmich, R. C. (2017). Dopamine controls Parkinson's tremor by inhibiting the cerebellar thalamus. *Brain, 140*(3), 721-734.

Djaldetti, R., Lorberboym, M., Karmon, Y., Treves, T. A., Ziv, I., & Melamed, E. (2011). Residual striatal dopaminergic nerve terminals in very long-standing Parkinson's disease: A single photon emission computed tomography imaging study. *Movement Disorders, 26*(2), 327-330.

Eklund, A., Nichols, T. E., & Knutsson, H. (2016). Cluster failure: Why fMRI inferences for spatial extent have inflated false-positive rates. *Proceedings of National Academic of Sciences U S A, 113*(28), 7900-7905.

Erickson, K. I., Colcombe, S. J., Wadhwa, R., Bherer, L., Peterson, M. S., Scalf, P. E., . . . Kramer, A. F. (2007). Training-induced plasticity in older adults: Effects of training on hemispheric asymmetry. *Neurobiology of Aging, 28*(2), 272-283.

Fearnley, J. M., & Lees, A. J. (1991). Ageing and Parkinson's disease: Substantia nigra regional selectivity. *Brain, 114*(Pt 5), 2283-2301.

Fisher, B. E., Li, Q., Nacca, A., Salem, G. J., Song, J., Yip, J., . . . Petzinger, G. M. (2013). Treadmill exercise elevates striatal dopamine D2 receptor binding potential in patients with early Parkinson's disease. *Neuroreport, 24*(10), 509-514.

Fisher, B. E., Petzinger, G. M., Nixon, K., Hogg, E., Bremmer, S., Meshul, C. K., & Jakowec, M. W. (2004). Exercise-induced behavioral recovery and neuroplasticity in the 1-methyl-4-phenyl-1,2,3,6-tetrahydropyridine-lesioned mouse basal ganglia. *Journal of Neuroscience Research, 77*(3), 378-390.

Gordon, B. A., Rykhlevskaia, E. I., Brumback, C. R., Lee, Y., Elavsky, S., Konopack, J. F., . . ., Fabiani, M. (2008). Neuroanatomical correlates of aging, cardiopulmonary fitness level, and education. *Psychophysiology, 45*(5), 825-838.

Grande, L. J., Crosson, B., Heilman, K. M., Bauer, R. M., Kilduff, P., & McGlinchey, R. E. (2006). Visual selective attention in Parkinson's disease: Dissociation of exogenous and endogenous inhibition. *Neuropsychology, 20*(3), 370-382.

Greve, D. N., & Fischl, B. (2009). Accurate and robust brain image alignment using boundary-based registration. *Neuroimage, 48*(1), 63-72.

Guttman, M., Burkholder, J., Kish, S. J., Hussey, D., Wilson, A., DaSilva, J., & Houle, S. (1997). [11C]RTI-32 PET studies of the dopamine transporter in early dopa-naive Parkinson's disease: Implications for the symptomatic threshold. *Neurology, 48*(6), 1578-1583.

Haber, S. N., Fudge, J. L., & McFarland, N. R. (2000). Striatonigrostriatal pathways in primates form an ascending spiral from the shell to the dorsolateral striatum. *Journal of Neuroscience, 20*(6), 2369-2382.

Helmich, R. C., Aarts, E., de Lange, F. P., Bloem, B. R., & Toni, I. (2009). Increased dependence of action selection on recent motor history in Parkinson's disease. *Journal of Neuroscience, 29*(19), 6105-6113.

Helmich, R. C., Derikx, L. C., Bakker, M., Scheeringa, R., Bloem, B. R., & Toni, I. (2010). Spatial remapping of cortico-striatal connectivity in Parkinson's disease. *Cerebral Cortex, 20*(5), 1175-1186.

Helmich, R. C., Janssen, M. J., Oyen, W. J., Bloem, B. R., & Toni, I. (2011). Pallidal dysfunction drives a cerebellothalamic circuit into Parkinson tremor. *Ann Neurol, 69*(2), 269-281.

Helmich, R. C., Thaler, A., van Nuenen, B. F., Gurevich, T., Mirelman, A., Marder, K. S., . . . Consortium, L.

A. J. (2015). Reorganization of corticostriatal circuits in healthy G2019S LRRK2 carriers. *Neurology, 84*(4), 399-406.

Hillman, C. H., Erickson, K. I., & Kramer, A. F. (2008). Be smart, exercise your heart: Exercise effects on brain and cognition. *National Review of Neuroscience, 9*(1), 58-65.

Hoehn, M. M., & Yahr, M. D. (1967). Parkinsonism: Onset, progression and mortality. *Neurology, 17*(5), 427-442.

Jenkinson, M., Bannister, P., Brady, M., & Smith, S. (2002). Improved optimization for the robust and accurate linear registration and motion correction of brain images. *Neuroimage, 17*(2), 825-841.

Jenkinson, M., Beckmann, C. F., Behrens, T. E., Woolrich, M. W., & Smith, S. M. (2012). Fsl. *Neuroimage, 62*(2), 782-790.

Jenkinson, M., & Smith, S. (2001). A global optimisation method for robust affine registration of brain images. *Medical Image Analysis, 5*(2), 143-156.

Karvonen, M. J., Kentala, E., & Mustala, O. (1957). The effects of training on heart rate: A longitudinal study. *Annales Medicinae Experimentalis Et Biologiae Fenniae, 35*(3), 307-315.

Kish, S. J., Shannak, K., & Hornykiewicz, O. (1988). Uneven pattern of dopamine loss in the striatum of patients with idiopathic Parkinson's disease. Pathophysiologic and clinical implications. *The New England Journal of Medicine, 318*(14), 876-880.

Langston, J. W., Widner, H., Goetz, C. G., Brooks, D., Fahn, S., Freeman, T., & Watts, R. (1992). Core assessment program for intracerebral transplantations (CAPIT). *Movement Disorders, 7*(1), 2-13.

Lawrence, A. D., Sahakian, B. J., & Robbins, T. W. (1998). Cognitive functions and corticostriatal circuits: Insights from Huntington's disease. *Trends in Cognitive Science, 2*(10), 379-388.

Lewis, M. M., Galley, S., Johnson, S., Stevenson, J., Huang, X., & McKeown, M. J. (2013). The role of the cerebellum in the pathophysiology of Parkinson's disease. *Canadian Journal of Neurological Science, 40*(3), 299-306.

Macdonald, P. A., & Monchi, O. (2011). Differential effects of dopaminergic therapies on dorsal and ventral striatum in Parkinson's disease: Implications for cognitive function. *Parkinsons Disease, 2011*, 572743.

Marks, B. L., Madden, D. J., Bucur, B., Provenzale, J. M., White, L. E., Cabeza, R., & Huettel, S. A. (2007). Role of aerobic fitness and aging on cerebral white matter integrity. *Annals of the New York Academy of Sciences, 1097*, 171-174.

McNab, F., & Klingberg, T. (2008). Prefrontal cortex and basal ganglia control access to working memory. *Nature Neuroscience, 11*(1), 103-107.

McRitchie, D. A., Cartwright, H. R., & Halliday, G. M. (1997). Specific A10 dopaminergic nuclei in the midbrain degenerate in Parkinson's disease. *Experimental Neurology, 144*(1), 202-213.

Monchi, O., Petrides, M., Mejia-Constain, B., & Strafella, A. P. (2007). Cortical activity in Parkinson's disease during executive processing depends on striatal involvement. *Brain, 130*(Pt 1), 233-244.

Muller, J. R., Philiastides, M. G., & Newsome, W. T. (2005). Microstimulation of the superior colliculus focuses attention without moving the eyes. *Proceedings of the National Academy of Sciences U S A, 102*(3), 524-529.

Mumford, J. A., & Nichols, T. E. (2008). Power calculation for group fMRI studies accounting for arbitrary design and temporal autocorrelation. *Neuroimage, 39*(1), 261-268.

Murphy, K., Birn, R. M., Handwerker, D. A., Jones, T. B., & Bandettini, P. A. (2009). The impact of global signal regression on resting state correlations: Are anti-correlated networks introduced? *Neuroimage, 44*(3), 893-905.

Nakano, K., Kayahara, T., Tsutsumi, T., & Ushiro, H. (2000). Neural circuits and functional organization of the striatum. *J Neurology, 247*(Supplement 5), V1-V15.

Nelson, M. E., Rejeski, W. J., Blair, S. N., Duncan, P. W., Judge, J. O., King, A. C., . . ., Castaneda-Sceppa, C. (2007). Physical activity and public health in older adults: Recommendation from the American College of Sports Medicine and the American Heart Association. *Medicine & Science in Sports & Exercise, 39*(8), 1435-1445.

Nurmi, E., Ruottinen, H. M., Bergman, J., Haaparanta, M., Solin, O., Sonninen, P., & Rinne, J. O. (2001). Rate of progression in Parkinson's disease: A 6-[18F]fluoro-L-dopa PET study. *Movement Disorders, 16*(4), 608-615.

Obeso, J. A., Marin, C., Rodriguez-Oroz, C., Blesa, J., Benitez-Temino, B., Mena-Segovia, J., . . . Olanow, C. W. (2008). The basal ganglia in Parkinson's disease: current concepts and unexplained observations. *Annals of Neurology, 64*(Supplement 2), S30-S46.

Obeso, J. A., Rodriguez-Oroz, M. C., Benitez-Temino, B., Blesa, F. J., Guridi, J., Marin, C., & Rodriguez, M. (2008). Functional organization of the basal ganglia: Therapeutic implications for Parkinson's disease. *Movement Disorders, 23*(Supplement 3), S548-S559.

Owen, A. M. (2004). Cognitive dysfunction in Parkinson's disease: The role of frontostriatal circuitry. *Neuroscientist, 10*(6), 525-537.

Palmer, S. J., Eigenraam, L., Hoque, T., McCaig, R. G., Troiano, A., & McKeown, M. J. (2009). Levodopa-sensitive, dynamic changes in effective connectivity during simultaneous movements in Parkinson's disease. *Neuroscience, 158*(2), 693-704.

Palmer, S. J., Li, J., Wang, Z. J., & McKeown, M. J. (2010). Joint amplitude and connectivity compensatory mechanisms in Parkinson's disease. *Neuroscience, 166*(4), 1110-1118.

Palmer, S. J., Ng, B., Abugharbieh, R., Eigenraam, L., & McKeown, M. J. (2009). Motor reserve and novel area recruitment: Amplitude and spatial characteristics of compensation in Parkinson's disease. *European Journal of Neuroscience, 29*(11), 2187-2196.

Patenaude, B., Smith, S. M., Kennedy, D. N., & Jenkinson,

M. (2011). A Bayesian model of shape and appearance for subcortical brain segmentation. *Neuroimage, 56*(3), 907-922.

Petzinger, G. M., Walsh, J. P., Akopian, G., Hogg, E., Abernathy, A., Arevalo, P., . . . Jakowec, M. W. (2007). Effects of treadmill exercise on dopaminergic transmission in the 1-methyl-4-phenyl-1,2,3,6-tetrahydropyridine-lesioned mouse model of basal ganglia injury. *Journal of Neuroscience, 27*(20), 5291-5300.

Postuma, R. B., & Dagher, A. (2006). Basal ganglia functional connectivity based on a meta-analysis of 126 positron emission tomography and functional magnetic resonance imaging publications. *Cerebral Cortex, 16*(10), 1508-1521.

Pruim, R. H., Mennes, M., van Rooij, D., Llera, A., Buitelaar, J. K., & Beckmann, C. F. (2015). ICA-AROMA: A robust ICA-based strategy for removing motion artifacts from fMRI data. *Neuroimage, 112*, 267-277.

Ridgel, A. L., Vitek, J. L., & Alberts, J. L. (2009). Forced, not voluntary, exercise improves motor function in Parkinson's disease patients. *Neurorehabilation Neural Repair, 23*(6), 600-608.

Saint-Cyr, J. A. (2003). Frontal-striatal circuit functions: context, sequence, and consequence. *Journal of the International Neuropsychological Society, 9*(1), 103-127.

Sen, S., Kawaguchi, A., Truong, Y., Lewis, M. M., & Huang, X. (2010). Dynamic changes in cerebello-thalamo-cortical motor circuitry during progression of Parkinson's disease. *Neuroscience, 166*(2), 712-719.

Shah, C., Beall, E. B., Frankemolle, A. M., Penko, A., Phillips, M. D., Lowe, M. J., & Alberts, J. L. (2016). Exercise Therapy for Parkinson's Disease: Pedaling Rate Is Related to Changes in Motor Connectivity. *Brain Connect, 6*(1), 25-36.

Shine, J. M., Matar, E., Ward, P. B., Frank, M. J., Moustafa, A. A., Pearson, M., . . . Lewis, S. J. (2013). Freezing of gait in Parkinson's disease is associated with functional decoupling between the cognitive control network and the basal ganglia. *Brain, 136*(Pt 12), 3671-3681.

Shu, H. F., Yang, T., Yu, S. X., Huang, H. D., Jiang, L. L., Gu, J. W., & Kuang, Y. Q. (2014). Aerobic exercise for Parkinson's disease: A systematic review and meta-analysis of randomized controlled trials. *PLoS One, 9*(7), e100503.

Simioni, A. C., Dagher, A., & Fellows, L. K. (2016). Compensatory striatal-cerebellar connectivity in mild-moderate Parkinson's disease. *Neuroimage Clinical, 10*, 54-62.

Smith, S. M. (2002). Fast robust automated brain extraction. *Human Brain Mapping, 17*(3), 143-155.

Smith, S. M., & Nichols, T. E. (2009). Threshold-free cluster enhancement: Addressing problems of smoothing, threshold dependence and localisation in cluster inference. *Neuroimage, 44*(1), 83-98.

Thomas, A. G., Dennis, A., Bandettini, P. A., & Johansen-Berg, H. (2012). The effects of aerobic activity on brain structure. *Frontiers in Psychology, 3*, 86.

Tillerson, J. L., Caudle, W. M., Reveron, M. E., & Miller, G. W. (2002). Detection of behavioral impairments correlated to neurochemical deficits in mice treated with moderate doses of 1-methyl-4-phenyl-1,2,3,6-tetrahydropyridine. *Experimental Neurology, 178*(1), 80-90.

Tommasi, G., Fiorio, M., Yelnik, J., Krack, P., Sala, F., Schmitt, E., . . ., Chelazzi, L. (2015). Disentangling the role of cortico-basal ganglia loops in top-down and bottom-up visual attention: An investigation of attention deficits in Parkinson disease. *Journal of Cognitive Neuroscience, 27*(6), 1215-1237.

Ueda, Y., & Kimura, M. (2003). Encoding of direction and combination of movements by primate putamen neurons. *European Journal of Neuroscience, 18*(4), 980-994.

Winkler, A. M., Ridgway, G. R., Webster, M. A., Smith, S. M., & Nichols, T. E. (2014). Permutation inference for the general linear model. *Neuroimage, 92*, 381-397.

Woo, C. W., Krishnan, A., & Wager, T. D. (2014). Cluster-extent based thresholding in fMRI analyses: Pitfalls and recommendations. *Neuroimage, 91*, 412-419.

Wu, T., Chan, P., & Hallett, M. (2010). Effective connectivity of neural networks in automatic movements in Parkinson's disease. *Neuroimage, 49*(3), 2581-2587.

Wu, T., & Hallett, M. (2008). Neural correlates of dual task performance in patients with Parkinson's disease. *Journal of Neurol Neurosurgical Psychiatry, 79*(7), 760-766.

Wu, T., & Hallett, M. (2013). The cerebellum in Parkinson's disease. *Brain, 136*(Pt 3), 696-709.

Wu, T., Long, X., Zang, Y., Wang, L., Hallett, M., Li, K., & Chan, P. (2009). Regional homogeneity changes in patients with Parkinson's disease. *Human Brain Mapping, 30*(5), 1502-1510.

Wu, T., Wang, J., Wang, C., Hallett, M., Zang, Y., Wu, X., & Chan, P. (2012). Basal ganglia circuits changes in Parkinson's disease patients. *Neurosci Letters, 524*(1), 55-59.

Wu, T., Wang, L., Hallett, M., Chen, Y., Li, K., & Chan, P. (2011). Effective connectivity of brain networks during self-initiated movement in Parkinson's disease. *Neuroimage, 55*(1), 204-215.

Yelnik, J. (2008). Modeling the organization of the basal ganglia. *Revue Neurologique (Paris), 164*(12), 969-976.

Yu, R., Liu, B., Wang, L., Chen, J., & Liu, X. (2013). Enhanced functional connectivity between putamen and supplementary motor area in Parkinson's disease patients. *PLoS One, 8*(3), e59717.

Zgaljardic, D. J., Borod, J. C., Foldi, N. S., & Mattis, P. (2003). A review of the cognitive and behavioral sequelae of Parkinson's disease: Relationship to frontostriatal circuitry. *Cognitive and Behavioural Neurology, 16*(4), 193-210.

Cognitive Mapping: Metrics of Neural Representations of Space

Loes Ottink[1]
Supervisors: Naomi de Haas[1], Christian F. Doeller[1,2]

[1]*Radboud University Nijmegen, Donders Institute for Brain, Cognition and Behaviour, The Netherlands*
[2]*Norwegian University of Science and Technology, Kavli Institute for Systems Neuroscience, Trondheim, Norway*

For successful spatial navigation, accurate memory or representation of the environment is required. The hippocampus has been shown to be highly involved in spatial navigation. Also, the frontal cortex has been suggested to be implicated. The hippocampus is thought to play a role in the formation of a cognitive map of the environment. In such a map, the representation of distances between locations is important. Previous research has suggested that similarity in neural activation pattern between pairs of locations correlates with the distance between these locations. In our study, we aimed to take a more fine-grained look at cognitive map formation. We investigated whether the represented distances were Euclidean or path distances, or both. Thereby, we looked at the hippocampus and the frontal pole. We used navigational tasks in a virtual city, functional magnetic resonance imaging (fMRI), and representational similarity analysis to investigate neural representations of distances between locations in the virtual environment. We furthermore wanted to investigate the use of different navigational strategies and their effect on neural distance representations. To this end, participants performed several additional behavioural spatial tasks. Our results suggest that both objective and remembered path distances are represented in a right lateral frontal region. We found no evidence for representations in the hippocampus. We also did not find evidence for Euclidean distance representations. However, based on previous research, it is more likely that we did not pick up on these effects rather than that they are not present. Further analyses on our data may give a clearer view on this, but that lies beyond the scope of this thesis. Considering navigational abilities, we show that there are clear behavioural differences between people. These suggest differential use of navigational strategies.

Keywords: spatial navigation, hippocampus, frontal cortex, representational similarity analysis, navigational strategies

---

Corresponding author: Loes Ottink**; E-mail:** loes.ottink@gmail.com

Finding our way in familiar and unfamiliar environments is a very important aspect of our daily lives. For successful navigation, we have to adequately remember or represent the environment in some sort of mental map. The hippocampus has been shown to be highly involved in spatial memory and spatial navigation (Burgess, Maguire, & O'Keefe, 2002; Eichenbaum, Dudchenko, Wood, Shapiro, & Tanila, 1999; O'Keefe & Dostrovsky, 1971; O'Keefe & Nadel, 1978). This structure seems to be the region where a cognitive map of the spatial environment is formed, which we can use to navigate in this environment (Burgess et al., 2002; Iglói, Doeller, Berthoz, Rondi-Reig, & Burgess, 2010; O'Keefe & Nadel, 1978). Cognitive map formation was already suggested by Tolman in 1948 as a mental representation of a spatial environment in the rat brain. A cognitive map as considered in this paper is a neural representation of a map of a spatial environment (Burgess et al., 2002; McNaughton, Battaglia, Jensen, Moser, & Moser, 2006; O'Keefe & Nadel, 1978). It can be used to efficiently navigate to goals in that environment. Representation of distances between locations in the environment is very important when forming such a map. Thereby, locations with a low distance between each other are suggested to be neurally represented more similarly than locations with a higher distance (Deuker, Bellmund, Navarro Schröder, & Doeller, 2016; Morgan, MacEvoy, Aguirre, & Epstein, 2011). In the current study, we aimed to further investigate the formation of a cognitive map in humans.

Spatial navigation, memory and cognitive mapping have been studied a lot in rodents. Using single-cell recordings, a few types of cells have been found in the rodent brain that are active in relation to the spatial environment the animal is in (Moser, Kropff, & Moser, 2008). Importantly, they are also related to spatial navigation. These cell types are, for instance, place cells in the hippocampus, which fire when the rat is in a specific location (O'Keefe & Conway, 1978; O'Keefe & Dostrovsky, 1971; Wilson & McNaughton, 1993), and grid cells in the entorhinal cortex, which fire when the rat is at a node of a hypothetical grid that covers the environment (Hafting, Fyhn, Molden, Moser, & Moser, 2005). These specific cells stably represent the location of animal in its environment. These findings indicate that such cells contribute to a general representation of a map of the spatial environment in the brain. This suggests the formation of a cognitive map of space (O'Keefe & Nadel, 1978; Hafting et al., 2005).

Findings about such spatially tuned neurons also extend to the human brain. Neuronal recordings in the human hippocampus during a spatial navigation task showed that some neurons respond only at certain locations (Ekstrom et al., 2003). This is similar to the place cells found in rats. Furthermore, evidence for grid-cell-like representations in the entorhinal cortex have been found in humans, using functional magnetic resonance imaging (fMRI) during a spatial navigation task in a virtual environment (Doeller, Barry, & Burgess, 2010). More research has been conducted investigating spatial navigation and its neural underpinnings in humans, using spatial tasks in virtual environments (Deuker et al., 2016; Doeller, Barry, & Burgess, 2012; Ekstrom et al., 2003; Hartley, Lever, Burgess, & O'Keefe, 2014; Iglói et al., 2015; Kaplan, Horner, Bandettini, Doeller, & Burgess, 2014; Viard, Doeller, Hartley, Bird, & Burgess, 2011), supporting the use of virtual environments in this field of research.

These findings suggest that the hippocampal formation is also highly involved in spatial navigation in humans and that the human hippocampus forms a cognitive map of the environment. This has been assessed more specifically in a study by Deuker et al. (2016), where participants navigated through a virtual city called Donderstown. In this city, 16 objects were placed with various spatial and temporal distances between them. Participants had to learn the locations of these objects during an object location task. Using representational similarity analysis (RSA; see Methods for details; Kriegeskorte et al., 2008), they could analyse neural pattern similarity between objects. In other words, they analysed how similar pairs of objects were represented in the hippocampus in relationship to their temporal and spatial distance in the task. Participants also had to estimate the distance between the objects. These remembered distances were correlated with the neural similarity. They found a negative correlation in the right hippocampus. This suggests that objects that were remembered as closer together in space, were represented more similarly in the hippocampus than objects that were remembered further apart (Deuker et al., 2016). It furthermore indicated that remembered spatial distances were represented in the hippocampus. These findings are therefore in accordance with the theory of the hippocampus forming a cognitive map of the environment. Similar results were obtained for temporal distances between objects.

The study by Deuker and colleagues (2016) thus shows interesting results suggesting that spatial and temporal distances between locations are represented in the hippocampus. We aimed to expand these findings by taking a closer look at

representations of spatial distances in a cognitive map. It might be that the represented distances are the length of a straight line between two locations (Euclidean distance), or the distance of the path navigated between two locations (path distance). In the current study, we wanted to investigate whether one or the other distance type is represented in a cognitive map, or both.

A study by Howard et al. (2014) suggests that both distance types are represented. Here, the path distance was encoded by the posterior hippocampus, and Euclidean distance by the entorhinal cortex. In this study, when the path distance to the goal suddenly changed because the goal was moved, the signal change in the posterior hippocampus correlated with the distance change. In a similar fashion, when the Euclidean distance to their goal suddenly changed, the signal change in the entorhinal cortex correlated with this distance change. These representations, however, were not representations in the sense of similarity in neural activation patterns between locations, in contrast to the study by Deuker et al. (2016). Furthermore, the fMRI measures were done during navigation, not before and after learning locations. Therefore, this study may suggest retrieval of spatial memory or a cognitive map rather than storage of a cognitive map. Besides, the navigation was no real, active navigation, but a movie of a path with several navigational decisions. In the current study, we used a different approach to investigate Euclidean versus path distance representation, adapted from Deuker and colleagues (2016).

Not only the hippocampus has been shown to be involved in human spatial navigation. Also frontal areas were found in relation to navigation, and for instance related to navigational goals and spatial planning. More specifically, the medial prefrontal cortex (mPFC; Doeller et al., 2010; Iglói et al., 2010; Spiers & Maguire, 2007; Viard et al., 2011), as well as the lateral prefrontal cortex (lPFC; Viard et al., 2011), anterior cingulate and orbitofrontal cortex (Ekstrom et al., 2003) are shown to be involved. Therefore, we did not only focus on the hippocampus, but also looked at frontal regions. In the interest of time, we looked at the predefined mask of the frontal pole.

In the current study, we aimed to take a more fine-grained look at the formation of a cognitive map for spatial navigation. Therefore, we analysed neural representations of distances between locations in an environment, and assessed whether differences in these representations correlated with Euclidean or path distance, or with both. In other words, we tested whether the formed cognitive map is based on Euclidean distances or on path distances. Additionally, we wanted to test whether these representations adapt when routes change. This, however, goes beyond the scope of this thesis, and was not further addressed for this paper. We let participants navigate in a virtual city marked with certain locations. The virtual city was adapted from 'Donderstown' (Deuker et al., 2016), using Unreal Development Kit (Unreal Engine 3, Epic Games, Inc.). Figure 1 shows a bird's-eye view of the city. Our experimental sessions took place on two consecutive days. On day 1, participants first performed a Training task (Fig. 2), to learn the locations and the shortest routes between them. There were eight locations marked by a black box (Fig. 1). Different than in the task by Deuker et al. (2016), participants freely navigated from location to location, thereby approaching the locations from different directions. Additionally, the order in which they encountered locations was pseudo-randomised (see Methods), while in Deuker et al. (2016) this order was always the same. There were also three roadblocks placed (Fig. 1). These roadblocks allowed us to manipulate some routes and to introduce clear distinctions between the Euclidean and path distances between location pairs. The path distances were the shortest possible routes between the locations, which the participants were instructed to learn. We chose the locations and the roadblocks such that some location pairs have a similar Euclidean and path distance, but other pairs have large differences. For example, the two objects in Figure 1 have a much larger path distance (dashed arrow) than Euclidean distance (continuous arrow). This was done in order to be able to distinguish between neural representations of Euclidean and path distances. The whole Training task was divided into four blocks. To test knowledge of the locations, a short test phase started after each block. Here, the black boxes were removed from the city. Participants had to navigate around, and 'drop' boxes at the eight locations as they remember. On day 2, participants performed a second navigation task (Object Location task). Here, the locations were associated with an object. Participants had to learn the locations of the objects, and the shortest routes between them. Associating objects with the locations allowed us to later analyse the neural representations of distances between the locations (objects). On the second day, participants furthermore performed a third navigation task (Route Change). Here, the locations and objects remained the same, but two of the roadblocks were relocated. This introduced a change in some routes and thus also in their path distance. This was done to answer our additional research question concerning whether distance

representations adapted when routes change, and was not further analysed for this thesis. For a more detailed description of the navigation tasks, see the Methods section. We presented the objects before the Training on day 1, and after the Object Location and the Route Change task on day 2, in a picture
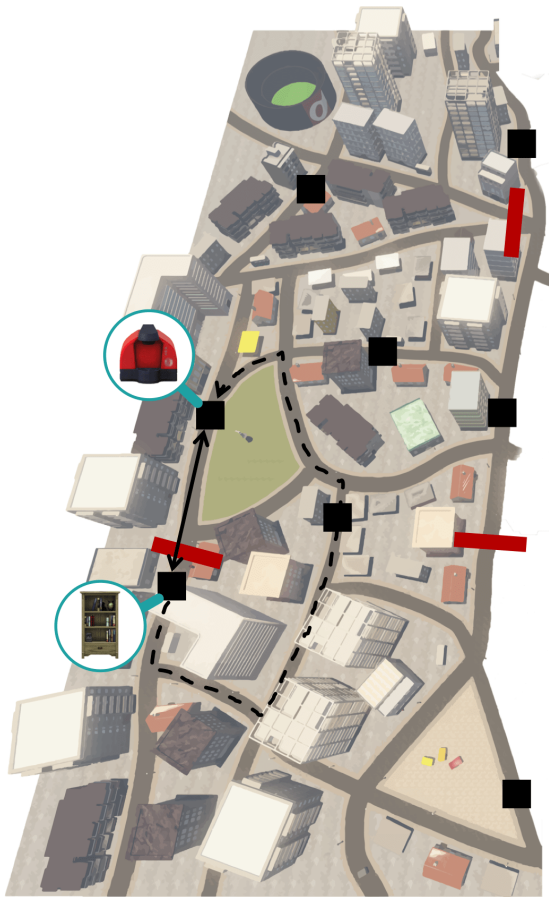

Fig. 1. Bird's-eye view of the virtual city environment. The eight locations are marked with a black square, and the three roadblocks with a red bar. Examples of two objects are pointed out on two locations. Their Euclidean distance is indicated by the straight arrow, and their path distance by the dashed arrow.

viewing task during fMRI sessions (Fig. 2, RSA_{pre}, RSA_{post}, and RSA_{post_2}). The objects were presented in a random order, different for each participant, but in the same order during the three fMRI sessions. Using RSA, we analysed the change in neural pattern similarity between each object pair from before to after the Object Location task. Data from RSA_{post_2} was not analysed for this thesis. RSA further allowed us to test whether these changes correlated with the Euclidean or path distance between the object pairs. Thereby we investigated whether the distance representations were based on the Euclidean or the path distance between objects, or on both. Based on the results of Deuker et al. (2016), we hypothesised that the change in neural similarity between each object pair would correlate negatively with the distances.

It may furthermore be the case that individual differences in for example navigational strategies may affect representations of distances in a cognitive map. For instance, representations of the environment in spatial memory can be egocentric (perspective from own body or location) or allocentric (based on distal cues in the environment), and thus differ in point of view (Burgess, 2006; Klatzky, 1998). Therefore, spatial navigation could also be egocentric or allocentric. Egocentric navigation is based on remembered left and/or right turns (sequence or stimulus-response memory), and allocentric navigation is based on environmental cues (place memory; Astur, Purton, Zaniewski, Cimadevilla, & Markus, 2016; Iglói et al., 2010). Previous research has shown that a distinction can be made between the stable use of these two navigational strategies (Astur et al., 2016; Iglói et al., 2010).

In the current study, we also wanted to address the use of different navigational strategies and their impact on representation of distances in a cognitive map. For example, some people may have a kind
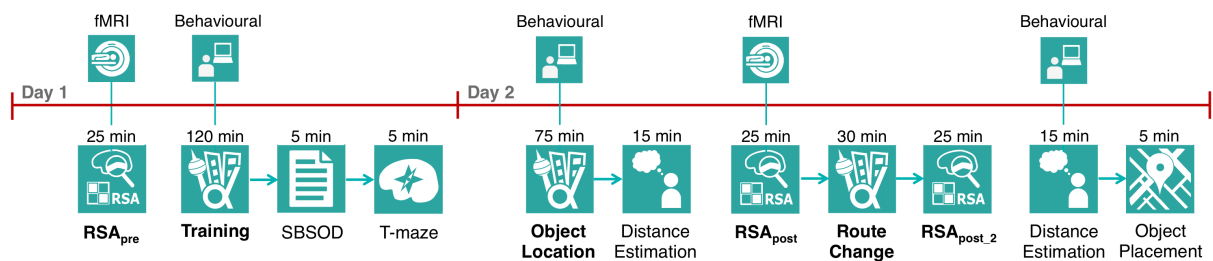
Fig. 2. Experimental 2-day design overview. On day 1, the RSA_{pre}-block was executed during an fMRI session. The Training task, Santa Barbara Sense of Direction Scale, and T-maze task were performed during a behavioural session. On day 2, The Object Location, Distance Estimation and Object Placement tasks were performed during a behavioural session. The RSA_{post} and RSA_{post_2}-blocks and Route Change task were executed during an fMRI session. The Route Change, RSA_{post_2}, and second Distance Estimation task were not analysed for this thesis.

of bird's-eye view map in their mind that they use to navigate. This can be called a map-based navigation strategy. On the contrary, some people may only remember the paths they took from their own point of view, and only remember which left or right turn they took where. This can be called a route-based navigation strategy. We conducted several behavioural spatial tasks to distinguish between a map- or route-based strategy. To this end, participants performed the Santa Barbara Sense of Direction Scale questionnaire (SBSOD; Hegarty, Richardson, Montello, Lovelace, & Subbiah, 2002) and a T-maze task (Astur et al., 2016) on day 1 (Fig 2). The SBSOD contains questions about general navigational abilities, and thus obtains a value that can be used as a measure of self-report about such abilities. The T-maze task is a short task that roughly classifies the participants as having a map- or route-based navigation strategy. On the second day, they performed a Distance Estimation task after the Object Location and Route Change tasks, and an Object Placement Task at the end of the session on day 2 (Fig. 2). We assumed that a higher performance on these spatial tasks indicates a map-based strategy, and lower performance a route-based strategy. For a more detailed description of the tasks, see the Methods section. To investigate whether there is a relationship between spatial behaviour and navigational strategies, we correlated performances of the spatial tasks with each other.

Furthermore, we investigated whether there was a link between the behavioural measures, and the neural similarity measures from the RSA. We tested whether there were correlations between performances on the SBSOD and Object Placement task and how well Euclidean and path distances are represented in the brain. Thereby we assessed whether different navigational strategies can affect neural representations of distances in a cognitive map that is formed during navigation.

Results

Neural representations of distances

To investigate neural representations of distances between the objects, we analysed data from the fMRI sessions using RSA. In our study, this analysis method generated changes in neural pattern similarity between object pairs, from before to after the navigation task (from the first RSA-block to the second). We wanted to assess how the representations change due to learning the locations

in the Object Location task, by testing whether the change in neural similarity correlated with the distance between each object pair.

The neural activation pattern for all objects was correlated with each other (so each object pair), both before (RSA_{pre}), and after (RSA_{post}) the Object Location task, to get the neural similarity. Data of the RSA_{pre}-block was then subtracted from data of the RSA_{post}-block (pre-post design; Fig. 3) for each object pair, yielding the change in neural similarity in a so-called similarity matrix (8×8). These matrices were symmetrical, so we only used the upper half of the matrix (above the diagonal) for analyses.

Subsequently, we tested whether neural representations of distances between objects (locations) were Euclidean or path distances. We compared the RSA results with predictions on how the neural similarity between objects would change based on either of the distance types. Besides the objective distances, we also used the behaviourally informed distances (those estimated by the participant) as predictions. Before the navigation tasks, there was presumably no association between the objects, so the neural similarity should be random and low. After the navigation tasks, so after learning the locations and the routes, the associations were predicted to be changed according to the distances between the object pairs. Therefore, the distances were predictions of how the neural similarity would change. These distances were stored in so-called 8 × 8 prediction matrices (Fig. 3). These matrices were symmetrical, so we only used the upper half of the matrix (above the diagonal) for analyses. There were four prediction matrices (objective Euclidean and path distances, and behaviourally informed Euclidean and path distances), so four conditions for which the neural data was further analysed. The behaviourally informed prediction matrices were obtained for each participant, using data from the Distance Estimation task. The change in neural similarity between each object pair, as obtained from the RSA, was then correlated with the four prediction matrices. This yielded a correlation value for each of the four conditions, respectively. We hypothesised that this correlation would be negative, since we expect an object pair with high distance having low neural similarity and a pair with a low distance having high similarity.

These analyses were performed using a whole-brain searchlight analysis. Thereby, the RSA was done on a sphere (searchlight) around each grey matter voxel in the brain. The correlation values for the four conditions were read back into the centre voxel of each searchlight, giving a
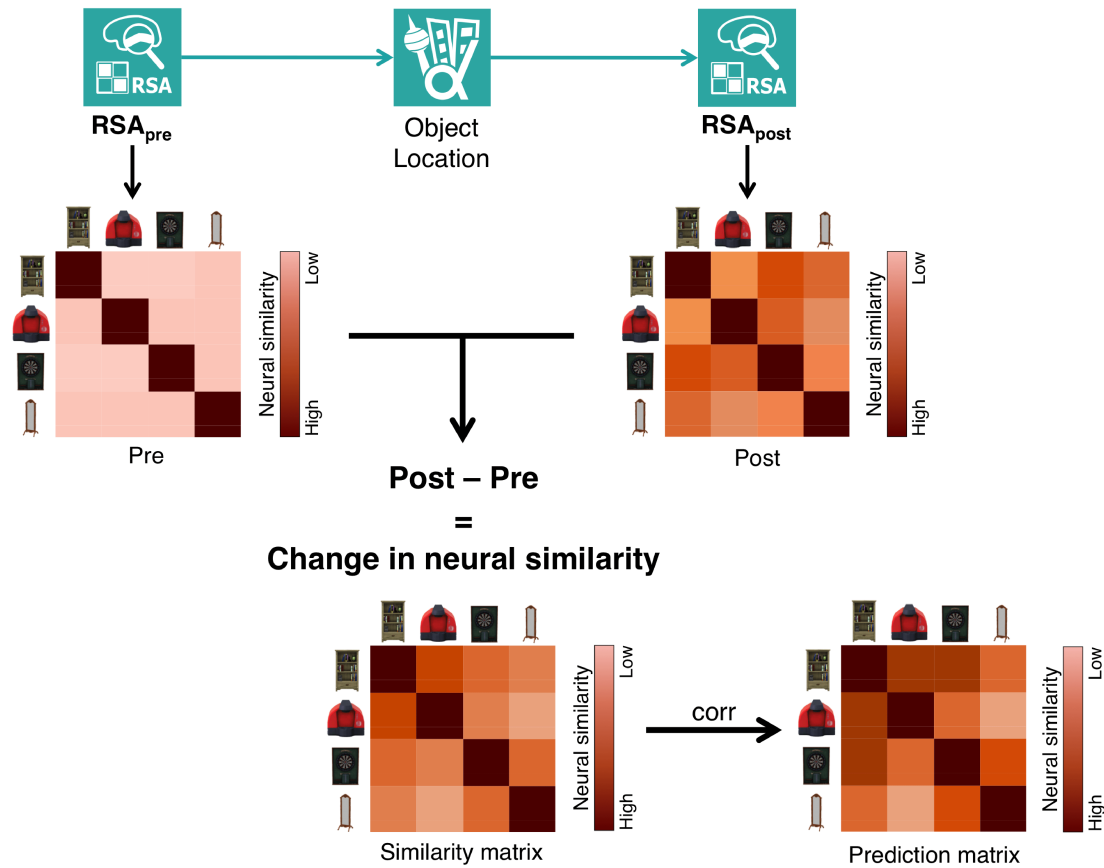
Fig. 3. Pre-post design of RSA. Neural similarity between each object pair was obtained from RSA$_{pre}$ and RSA$_{post}$. The data from RSA$_{pre}$ was subtracted from RSA$_{post}$, yielding the change in neural similarity for each object pair. This similarity matrix was correlated with the prediction matrices of all distance types (objective Euclidean and path distance, and behaviourally informed Euclidean and path distance). In the similarity and prediction matrices, all objects are on the rows and columns (four objects are shown as an example here). Neural similarity is colour-coded in these examples, with a darker colour indicating higher neural similarity. Since the matrices are symmetrical, only data from above the diagonal are analysed.

correlation value for each voxel, per condition. On these correlation values, a permutation test was performed to test in which voxels the correlation with the predictions was significantly different from zero. The *p*-values were FWE-corrected for multiple comparisons, for the whole brain. Small-volume correction was also applied for the left, right, and whole hippocampus, and for the frontal pole. In addition to the voxel-wise corrections, a Threshold-Free Cluster Enhancement (TFCE) analysis was performed. Peak voxels were extracted with a threshold of $p < .001$ (uncorrected).

There were no voxels in either conditions that were significant after whole-brain FWE-correction. The peak voxels that were extracted with a threshold of $p < .001$ (uncorrected) and $T \geq 3.7$ are listed in Table 1. These comprise mostly frontal areas. There was only one voxel in the left hippocampal formation that had an effect in the objective Euclidean and path distance conditions ($p < .001$ uncorrected, see

Table 1).

After small-volume correction, there were no voxels that survived in the left, right, or whole hippocampus. In the frontal pole, there was a cluster in a right lateral region that survived small-volume correction for both the objective and behaviourally informed path distance conditions (peak objective: $T = 4.81$, $p < .05$ FWE-corrected; Fig. 4; peak behaviourally informed: $T = 5.44$, $p < .01$ FWE-corrected; Fig. 5; Table 1). Both clusters survived small-volume correction after TFCE, but the behaviourally informed condition also survived without. For the behaviourally informed path distance condition, the peak T-value is higher than for the objective condition, suggesting a stronger effect for the behaviourally informed condition. The correlation of neural similarity with distance in the peak voxel in the RSA$_{pre}$ and RSA$_{post}$-blocks separately are also presented in Figure 4 and 5. For the peak voxel of both clusters, there was
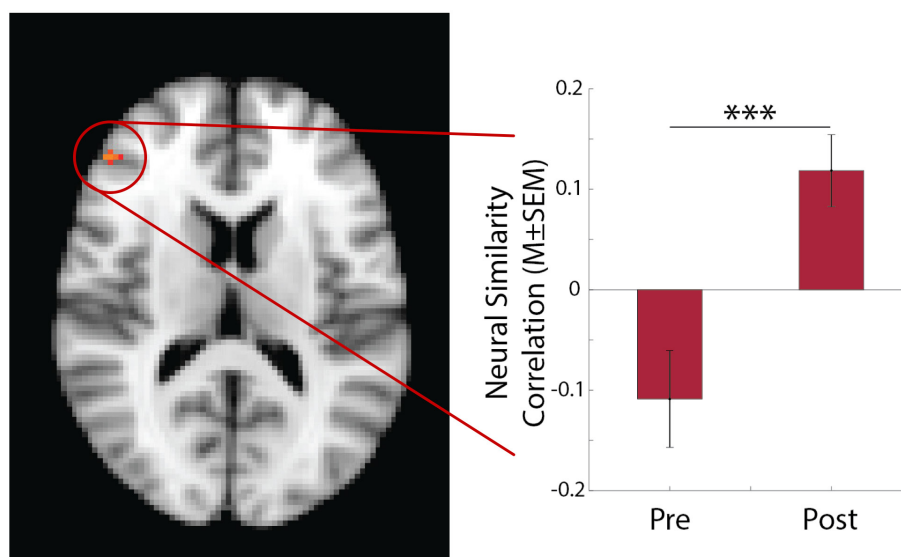
Fig. 4. Change in neural similarity between object pairs correlated with objective path distance in a cluster in a right lateral frontal pole area (peak voxel 48, 40, 14; T = 4.81, p < .05 FWE-corrected). This is the only cluster that survives small-volume correction, using TFCE. There was a significant increase in correlation between neural similarity and distance (neural similarity correlation) from RSA_{pre} (Pre) to RSA_{post} (Post). This indicates a significant positive correlation between neural similarity change and objective path distance. Brain is displayed in the radiological convention. ***p < .001.
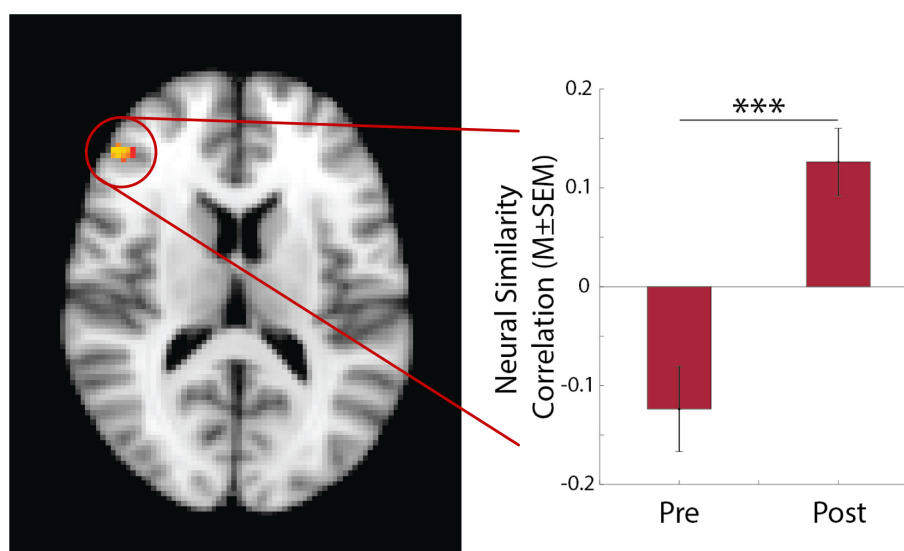
Fig. 5. Change in neural similarity between object pairs correlated with behaviourally informed path distance in a cluster in a right lateral frontal pole area (peak voxel 50, 40, 14; T = 5.44, p < .01 FWE-corrected). This was the only cluster that survived small-volume correction, using TFCE. There was a significant increase in correlation between neural similarity and distance (neural similarity correlation) from RSA_{pre} (Pre) to RSA_{post} (Post). This indicates a significant positive correlation between neural similarity change and behaviourally informed path distance. Brain is displayed in the radiological convention. ***p < .001.
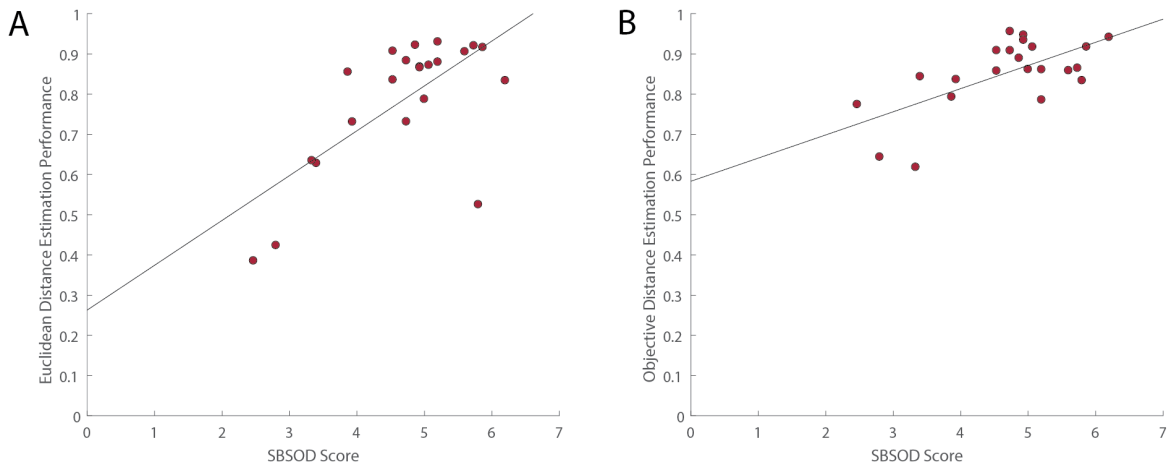
Fig. 6. Correlations of Distance Estimation performance with SBSOD score. **A.** Correlation of Euclidean distance estimation performance with SBSOD score ($r = 0.68$, $p < .001$), including a linear fitted trendline. Each dot refers to a participant. **B.** Correlation of path distance estimation performance with SBSOD score ($r = 0.65$, $p < .01$), including linear fitted trendline. Each dot is a participant.

a significant negative correlation in RSA_{pre}, and a significant positive correlation in RSA_{post}. The change in neural similarity (from pre to post) thus correlated positively with distance.

Spatial behaviour

To check whether participants learned the locations and the shortest routes between them, we calculated learning curves of the Training and Object Location tasks on how many mistakes they made when finding the shortest routes (supplementary Fig. S1, see online appendix). These learning curves went down of both navigation tasks, so they made less mistakes as they proceeded in the tasks. The learning curves of the Object Location tasks decrease faster and reach a lower level than those of the Training, suggesting that the participants remembered the shortest routes between the locations from the Training task. The mean percentage of correctly placed boxes in the test phases of Training task is 90% ($SD = 19\%$), suggesting the participants know the locations by the end of this task. There were four participants who did not complete the Training due to time issues. Hence, they navigated a reduced amount of times between some location pairs. To check whether this could cause a bias, we correlated this amount with the distance between the locations of those pairs. We found no significant correlation. Therefore, we found no indication that the fact that some participants did not finish the Training biased results concerning distances between objects (i.e., RSA results).

Of the SBSOD and Object Placement task,

we calculated the mean score and mean error per participant, respectively (supplementary Fig. S2 and S3). For both Distance Estimation tasks (Euclidean and path distance), we correlated the estimated distance with the objective distance for each participant, and tested whether the correlations across participants were different from zero, using a t-test. For both tasks, we found a positive mean correlation (Euclidean: $r = 0.78$; path: $r = 0.85$), which was significant (Euclidean: $t(21) = 22.41$, $p < .001$; path: $t(21) = 45.24$, $p < .001$). We additionally used a t-test to see whether there was a difference in performance between Euclidean and path distance estimation. We found no significant difference, but a trend ($t(42) = -1.73$, $p = .09$), with slightly better performance on path distance. Using the T-maze task, we found that 10 participants had a spatial strategy (Spatial strategy group), 10 participants had a response strategy (Response strategy group), and 2 participants had a mixed strategy (supplementary Fig. S4, and the Methods section for more details on this task). Data of participants in the Spatial and Response strategy groups (not the mixed group) were used to investigate whether there were differences in the other spatial tasks between these two strategy groups.

Relations between spatial tasks. To determine whether there is a relationship between spatial behaviour and navigational strategies, we correlated the performances of our behavioural tasks with each other. We found a significant correlation of SBSOD score with Distance Estimation performance for both Euclidean ($r = 0.68$, $p < .001$) and path distance ($r = 0.65$, $p < .01$; Fig. 6). There was a significant

Table 1.

Peak voxels of clusters found in the four conditions, with a threshold of $p < .001$, uncorrected, if not stated differently. They are ordered according to the cluster index given by FSL, from high to low index. *After TFCE. **Belong to the same cluster.

Condition	Region	Sig.	T-value	Peak (MNI)		
				x	y	z
Euclidean distance	Frontal pole	< .001	4.84	44	40	12
	Superior frontal gyrus	< .001	5.08	22	24	50
	Middle/inferior temporal gyrus	< .001	4.84	56	-18	-22
	Temporal pole	< .001	3.84	-54	6	-4
	Temporal pole	< .001	3.76	-54	6	-8
	Parahippocampal gyrus/left hippocampus	< .001	4.62	-32	-38	-8
Path distance	Frontal pole	< .05 FWE-corr.*	4.81	48	40	14
	Frontal pole/orbitofrontal cortex	< .001	4.02	30	34	-16
	Middle frontal gyrus	< .001	4.21	40	20	46
	Superior frontal gyrus	< .001	4.33	22	24	50
	Superior frontal gyrus	< .001	4.19	18	26	54
	Temporal pole	< .001	3.73	-54	6	-4
	Parahippocampal gyrus/left hippocampus	< .001	3.90	-32	-38	-8
	Cingulate gyrus/precuneous cortex	< .001	3.99	6	-34	48
	Superior frontal gyrus	< .001	3.73	-16	6	66
Euclidean distance (behaviourally informed)	Frontal pole	< .001	4.54	44	38	12
	Lingual gyrus	< .001	3.75	30	-42	-6
	Superior/middle frontal gyrus	< .001	4.14	24	24	50
	Temporal pole	< .001	4.71	36	12	-36
	Central opercular cortex	< .001	4.21	52	-8	8
	Post/precentral gyrus	< .001	3.96	-40	-22	52
Path distance (behaviourally informed)	Frontal pole**	< .01 FWE-corr.*	5.44	50	40	14
	Frontal pole**	< .05 FWE-corr.*	5.15	44	40	12
	Superior frontal gyrus	< .001	5.09	22	24	50
	Middle frontal gyrus	< .001	3.89	32	10	52
	Middle/superior frontal gyrus	< .001	3.84	28	6	56
	Lateral occipital cortex	< .001	4.15	12	-82	44
	Middle frontal gyrus	< .001	4.34	38	0	62
	Lateral occipital cortex	< .001	4.00	-40	-72	46
	Middle temporal gyrus	< .001	3.71	-50	2	-26
	Superior frontal gyrus	< .001	4.08	-16	6	66
	Frontal pole	< .001	3.99	-36	44	22
	Frontal pole/frontal orbital cortex	< .001	3.92	30	34	-16
	Temporal fusiform cortex	< .001	4.21	38	-4	-40
	Frontal pole	< .001	3.70	42	44	12
	Frontal pole	< .001	3.78	46	44	22
	Superior parietal lobule	< .001	3.92	32	-52	50
	Temporal fusiform cortex	< .001	3.97	36	-8	-34

Table 2.

Peak voxels in the whole brain and frontal pole mask, for the four conditions, used for post-hoc analyses. They are found using a threshold of $p < .001$, uncorrected, if not stated differently. *After TFCE.

Condition	Mask	Region	Sig.	T-value	Peak (MNI)		
					x	y	z
Euclidean distance	Whole brain	Superior frontal gyrus	< .001	5.08	22	24	50
	Frontal pole	Frontal pole	< .001	4.84	44	40	12
Path distance	Whole brain	Frontal pole	< .001	4.81	48	40	14
	Frontal pole	Frontal pole	< .05 FWE-corr.*	4.81	48	40	14
Euclidean distance (behaviourally informed)	Whole brain	Temporal pole	< .001	4.71	36	12	-36
	Frontal pole	Frontal pole	< .001	4.54	44	38	12
Path distance (behaviourally informed)	Whole brain	Frontal pole	< .001	5.44	50	40	14
	Frontal pole	Frontal pole	< .01 FWE-corr.*	5.44	50	40	14
	Frontal pole	Frontal pole	< .05 FWE-corr.*	5.15	44	40	12

negative correlation between SBSOD scores and mean errors on the Object Placement task ($r = -0.70$, $p < .001$; Fig. 7). When correlating the Distance Estimation performance with the Object Placement errors, we found a significant negative correlation for Euclidean ($r = -0.58$, $p < .01$) and path distance estimation ($r = -0.67$, $p < .001$; supplementary Fig. S5).

We furthermore tested whether there was a difference in performance for the behavioural tasks between the Spatial and Response strategy group from the T-maze task. Therefore, we compared performance of both groups using 2-sample t-tests. For the SBSOD scores, there was no difference between the strategy groups ($t(18) = 1.20$, $p = .25$; supplementary Fig. S6). For performance on the Distance Estimation task, there was a significant difference for Euclidean distance ($t(18) = 2.33$, $p < .05$; Fig. 8), with a higher performance in the Spatial strategy group (Spatial: $M = 0.87$, $SD = 0.06$; Response: $M = 0.71$, $SD = 0.20$). We found a trend for path distance estimation ($t(18) = 1.82$, $p = .08$, Fig. 8), with slightly higher performance in the Spatial strategy group (Spatial: $M = 0.89$, $SD = 0.05$; Response: $M = 0.82$, $SD = 0.12$). We found no difference in mean error in the Object Placement task between the Spatial and Response strategy group ($t(18) = -0.96$, $p = .35$; supplementary Fig. S7).

Post-hoc analysis: Correlating RSA results with spatial behaviour

To investigate whether there is a link between the RSA results and the behavioural data as a post-hoc analysis, we took the peak voxel from each region of interest (left, right, and whole hippocampus, frontal pole, and whole brain). For each peak voxel, we retrieved the correlation value (of neural similarity change with distance) in that voxel for each participant. Then, we correlated these peak voxel correlation values with scores on the SBSOD and Object Placement task, and also tested whether there were differences in peak voxel correlation between the Spatial and Response strategy groups of the T-maze task. The peak voxels and their regions taken here are shown in Table 2. The frontal pole peak voxels for the path distances are the peak voxels from the clusters that survived small-volume correction for RSA in the path distance conditions (Table 2). There was a second significant frontal pole peak voxel in the behaviourally informed path distance condition that survived FWE-correction (Table 1). This voxel was also included in the post-hoc analyses (Table 2). For all three hippocampal masks there were no peak voxels found.

For the SBSOD, there was no significant correlation with any peak voxel. For the Object Placement task, there was a significant positive correlation in the whole-brain peak voxel (superior frontal gyrus) in the objective Euclidean distance condition ($r = 0.48$, $p < .05$). In this peak voxel, there was a positive correlation of neural similarity change with distance ($T = 5.08$, $p < .001$ uncorrected). There were no significant differences between the Spatial and Response strategy groups for any peak voxel correlation values in any condition.
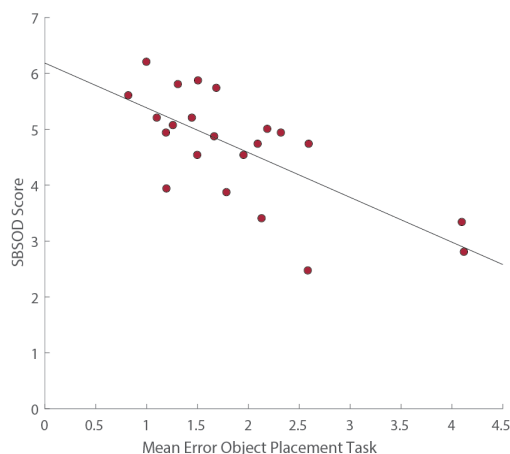
Fig. 7. Correlation of SBSOD score with mean error on the Object Placement task ($r = -0.70$, $p < .001$), including a linear fitted trendline. Each dot refers to a participant.

Fig. 8. The mean performance on the Distance Estimation tasks, for the Euclidean and path distance, for the Spatial and Response strategy group of the T-maze task. *$p < .05$.

Discussion

Path distances were represented in a right lateral frontal region

Analysis of behaviour during the Training and Object Location tasks suggested that the participants learned the locations and the shortest routes between them. When correlating the change in neural similarity from RSA_{pre} to RSA_{post} with the prediction matrices for the four types of distances (objective Euclidean and path distance, and behaviourally informed Euclidean and path distance), we found a cluster in the right lateral frontal pole for the path distance that survived correction for multiple comparisons. This effect was found for both the objective and behaviourally informed condition. This means that after learning certain locations in an environment and routes between them, the path distances were represented in the right lateral frontal pole. When not correcting for multiple comparisons, we found more clusters showing an effect ($p < .001$ uncorrected, Table 1), for instance in the superior frontal gyrus and the temporal pole. With a larger sample size than 22, so with data from the larger project, we might therefore find more brain regions where distances are represented, possibly in the other conditions as well.

The higher peak T-value for the behaviourally informed path distance condition suggests stronger path distance representations when they are behaviourally informed. The latter can be related to previous research (Deuker et al., 2016), where they also found a correlation of change in
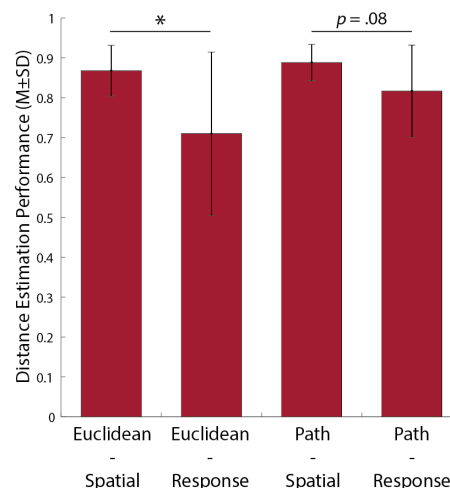
neural representation with the remembered, so behaviourally informed, distances. They furthermore found a neural representation of temporal distance judgements, and additionally that spatial judgements were influenced by temporal distances. Therefore, the behaviourally informed distance representation in our study may have been affected and strengthened by the experienced temporal distance between objects as well. Temporal distance was proportional to the path distance, therefore, it is a challenge to distinguish them in our task.

Finding an effect in a frontal region is in line with previous findings that also frontal regions, not only the hippocampus, are involved in spatial navigation (Doeller et al., 2010; Ekstrom et al., 2003; Iglói et al., 2010; Spiers & Maguire, 2007; Viard et al., 2011). Since the prefrontal cortex is involved in spatial planning (Iglói et al., 2010; Viard et al., 2011), our effects in the frontal pole region could for instance reflect distance representation of navigational goals. The effects in the right lateral frontal regions in our study, however, were in the opposite direction than hypothesised. We found a positive correlation of change in neural similarity with distance. This would mean that the closer the locations were together, the lower the neural similarity between the locations. A stronger effect could then be related to a less accurate representation of distances. This finding, however, seems to be in accordance with the results by Spiers and Maguire (2007). They found a positive correlation of mPFC activity with distance to goal, but a negative correlation of activity in the hippocampal formation. Together with our results and those of for example Deuker et al. (2016), this may suggest an opposite representation of distance

in frontal regions than in the hippocampal formation.

Furthermore, when looking at the neural similarity correlation with distance in RSA_{pre} and RSA_{post} separately, there already was an effect in RSA_{pre}. There we found a negative correlation before associations of the locations with objects. This was unexpected, since we assumed the associations between objects before the navigation tasks to be random and low. This could mean that the association between objects somehow correlated with distance before the navigation task, but randomisation of objects across participants makes this possibility very small. There was a larger spread around the mean in RSA_{pre}, which was in accordance with our expectation that the association should be random. In RSA_{post} there is an equally large effect as in RSA_{pre}, but in the opposite direction. On the one hand, for this kind of fMRI analyses (RSA), a population of 22 participants is rather small. It could be that the effects shown here have just become significant, but will disappear, or even change direction, with data from a larger sample size. On the other hand, it could very well be that there actually is a positive correlation in this frontal region. This was also supported by some other research (Spiers & Maguire, 2007). Although unexpected, correlation of neural similarity change with distance in the opposite direction is still some sort of representation of distance. It thus could still be some kind of neural representation of the spatial environment. In addition, because the effect was stronger for behaviourally informed distance, it could also point to an even less accurate behaviourally informed distance representation. When connecting this to earlier findings about temporal distance (Deuker et al., 2016), it could be the case that influences of temporal distance on spatial judgements distorted the representation of spatial distance. A positive correlation would also be in accordance with the peak voxel correlation with errors on the Object Placement task. There we found a significant positive correlation as well. In the context of the positive correlation of neural similarity change with distance, it would mean that a higher error on the task relates to a less accurate representation of Euclidean distance, as expected. This, however, is a different peak voxel and a different condition, so we should be very careful with interpreting this link.

No evidence for distance representations in the hippocampus

We find no evidence for representations of distances in the hippocampus. This is in contrast to our hypotheses, and not in line with earlier studies about spatial memory and cognitive mapping. Nevertheless, given the extended evidence that the hippocampus is involved in spatial navigation and the formation of a cognitive map of space (Deuker et al., 2016; Howard et al., 2014; Iglói et al., 2010; Morgan et al, 2011; O'Keefe & Nadel, 1978), it would be more likely that we did not pick up on the hippocampal effects with our sample size and design rather than that they were not there.

In the study by Deuker et al. (2016), however, they also did not find the effects using parametric tests. There, they assigned the distances between locations to four bins, ranging from very close to very far. Then they found an effect in the hippocampus comparing the lower with higher distances. Furthermore, they did not test for other regions than the hippocampus. It could be the case that in that study there actually was a frontal effect as well. Furthermore, in our study, we would possibly also find an effect in the hippocampus if we analysed our data similar to what has been done in Deuker et al. (2016). We could for example only compare the extreme distances (e.g., the eight highest and eight lowest distances) in some further analyses on our data.

Another possibility is that different navigational strategies affected neural representations of space, and thus of distances. This is further what we hypothesised. Since we found an effect in the behavioural tasks between the Spatial and Response strategy group, these groups could also have differential neural representations. They perhaps show contrasting effects that would cancel each other out when testing across all participants. For instance, Iglói et al. (2010) showed opposite hippocampal effects for allocentric and egocentric responses during spatial navigation. There, the right hippocampus was active during allocentric responses, and the left hippocampus during egocentric responses. Something similar could be the case in our study, in the sense that people showing one or the other strategy could have opposite effects on neural distance representations. We possibly do not distinguish those in our design. In the Distance Estimation task, the Spatial strategy group was better at estimating the Euclidean distance than the Response strategy group. Based on this finding, Euclidean distances might be neurally stronger represented in the Spatial strategy group. To further investigate this, we could do some additional analyses on our data. We could test whether in the Spatial group the Euclidean distance is better represented than the path distance, and in the Response group

the other way around. We could furthermore check whether this would give effects in hippocampus.

No evidence for Euclidean distance representation

Our results furthermore suggest that only the path distance is represented in the brain, but give no evidence for representations of Euclidean distance. However, it is unlikely that these distances are not represented in the brain at all (Howard et al., 2014; Spiers & Maguire, 2007). The effect of path distance could for instance also be the representation of the temporal aspect of spatial navigation that strengthens the path distance representation (see above). Temporal distance is proportional to the path distance, therefore, it is a challenge to distinguish this in our task. Nevertheless, the temporal aspect has been shown to be represented in the hippocampus as well (Deuker et al., 2016), of which we show no effects in our study. For our larger project, however, we additionally aimed to look at how representations would alter when routes between the locations change. Therefore, participants performed a third navigation task (Route Change task). Results from some preliminary RSA analyses on this data suggests that after this task, the objective, but not behaviourally informed, Euclidean distance was represented in a right lateral frontal pole region. This region was similar to where the path distances were represented. It might be the case that after walking more different routes, and approaching locations from even more directions, people are better at inferring the Euclidean distances between them. This could lead to a stronger neural representation of these distances as well.

Spatial behaviour may affect neural representation of distances

Considering the behavioural tasks, we found clear links between them. The SBSOD scores correlated with performance on the Distance Estimation and Object Placement tasks. Participants' self-reports on general navigational abilities thus correlated with how well they can estimate distances and replicate locations in a bird's-eye view map of an environment. These results suggest that performances on these tasks have some relation with navigational abilities, and that they are consistent across different measures. This is also supported by comparisons between the Spatial and Response strategy group from the T-maze task. The Spatial strategy group

was significantly better at estimating the Euclidean distance between objects. They were close to significantly better at estimating the path distance as well. There, however, were no differences between the groups considering SBSOD score and error in the Object Placement task. Although not consistent over all tasks, the results suggest that there are consistent differences on a neural basis between people considering navigational strategy, and that these are reflected in other behavioural measures. These findings are in line with our hypotheses about differences between people considering navigational strategies. They are furthermore consistent with other research on such strategies (Astur et al., 2016; Iglói et al., 2010), where they showed clear distinctions. These differential strategies may affect spatial representations in a cognitive map.

In the post-hoc analyses, we correlated behavioural performances with peak voxel correlations. Considering the Object Placement task, we found that the lower the error in placing objects in a bird's-eye view map, the stronger the neural effect for objective Euclidean distance was in the whole-brain peak voxel (superior frontal gyrus). Since we found positive correlations of neural similarity change with distance, this would mean that a lower error on the task would relate to better representation of Euclidean distance. This is according to our predictions, since a better representation of Euclidean distances would benefit the ability of locating locations in a bird's-eye view map. Furthermore, this link could support the prediction that Euclidean distances are more strongly represented than path distances in people with a map-based navigational strategy. Again, the distinction between the two strategies in neural data is supported by previous findings (Iglói et al., 2010). Our results, however, are not very robust. We only show a significant effect for one spatial task (Object Placement) in a peak voxel in one condition, and the Object Placement task is also related to the virtual city of the navigation tasks. Furthermore, the peak voxel where we found this effect was in the objective Euclidean distance condition. We, however, did not find a significant effect that indicated representation of Euclidean distances. Therefore, we should be careful with the interpretation of these findings. The post-hoc results may give a hypothesis for additional experiments, but further research is needed to give a more clear-cut indication.

Concluding remarks

In short, our results indicate that path distances between learned locations in a certain environment are represented in a right lateral frontal pole area. These effects become stronger when distances are behaviourally informed. The correlations between change in neural similarity and distances, however, were positive. This suggests that a stronger effect relates to less accurate representation of distances. In our study, we did not find evidence for representations in the hippocampus, nor for Euclidean distance representations. It however is likely, based on previous research, that we did not pick up on these effects rather than that they are not present at all. Further analyses on our data may give a clearer view on that. We furthermore show that there are clear behavioural differences between people considering navigational abilities, and these suggest differential use of navigational strategies. In addition, post-hoc analyses give some suggestion that these differences between people are related to differences in neural representations of locations. However, more research focused on such relationships is essential.

References

Astur, R. S., Purton, A. J., Zaniewski, M. J., Cimadevilla, J., & Markus, E. J. (2016). Human sex differences in solving a virtual navigation problem. *Behavioural Brain Research, 308*, 236-243.

Burgess, N. (2006). Spatial memory: how egocentric and allocentric combine. *TRENDS in Cognitive Sciences, 10*(12), 551-557.

Burgess, N., Maguire, E. A., & O'Keefe, J. (2002). The Human Hippocampus and Spatial and Episodic Memory. *Neuron, 35*, 625-641.

Deuker, L., Bellmund, J. L. S., Navarro Schröder, T., & Doeller, C. F. (2016). An event map of memory space in the hippocampus. *eLife, 5*, e16534.

Doeller, C. F., Barry, C., & Burgess, N. (2010). Evidence for grid cells in a human memory network. *Nature, 463*, 675-661.

Doeller, C. F., Barry, C., & Burgess, N. (2012). From cells to systems: Grids and boundaries in spatial memory. *The Neuroscientist, 18*(6), 556-566.

Eichenbaum, H., Dudchenko, P., Wood, E., Shapiro, M., & Tanila, H. (1999). The hippocampus, memory, and place cells: is it spatial memory or a memory space? *Neuron 23*, 209–226.

Ekstrom, A. D., Kahana, M. J., Caplan, J. B., Fields, T. A., Isham, E. A., Newman, E. L., & Fried, I. (2003). Cellular networks underlying human spatial navigation. *Nature, 425*, 184-187.

Hafting, T., Fyhn, M., Molden, S., Moser, M.-B., & Moser, E. I. (2005). Microstructure of a spatial map in the entorhinal cortex. *Nature, 436*, 801–806.

Hartley, T., Lever, C., Burgess, N., & O'Keefe, J. (2014). Space in the brain: how the hippocampal formation supports spatial cognition. *Philosophical Transactions of the Royal Society B, 369*, 20120510.

Hegarty, M., Richardson, A. E., Montello, D. R., Lovelace, K., & Subbiah, I. (2002). Development of a self-report measure of environmental spatial ability. *Intelligence, 30*, 425-448.

Howard, L. R., Homayoun Javadi, A., Yu, Y., Mill, R. D., Morrison, L. C., Knight, … & Spiers, H. J. (2014). The hippocampus and entorhinal cortex encode the path and Euclidean distances to goals during navigation. *Current Biology, 24*, 1331-1340.

Iglói, K., Doeller, C. F., Berthoz, A., Rondi-Reig, L., & Burgess, N. (2010). Lateralized human hippocampal activity predicts navigation based on sequence or place memory. *PNAS, 107*(32), 14466-14471.

Iglói, K., Doeller, C. F., Paradis, A.-L., Benchenane, K., Berthoz, A., Burgess, N., & Rondi-Reig, L. (2015). Interaction between hippocampus and cerebellum crus I in sequence-based but not place-based navigation. *Cerebral Cortex, 25*, 4146-4154.

Kaplan, R., Horner, A. J., Bandettini, P. A., Doeller, C. F., & Burgess, N. (2014). Human hippocampal processing of environmental novelty during spatial navigation. *Hippocampus, 24*, 740-750.

Klatzky, R. L. (1998). Allocentric and Egocentric Spatial representations: Definitions, Distinctions, and Interconnections. *Lecture Notes in Artificial Intelligence, 1404*, 1-17.

Kriegeskorte, N., Mur, M., Ruff, D. A., Kiani, R., Bodurka, J., Esteky, … & Bandettini, P. A. (2008). Matching categorical object representations in inferior temporal cortex of man and monkey. *Neuron, 60,* 1126–1141.

McNaughton, B. L., Battaglia, F. P., Jensen, O., Moser, E. I., & Moser, M.-B. (2006). Path integration and the neural basis of the 'cognitive map'. *Nature Reviews Neuroscience 7,* 663-678.

Morgan, L. K., MacEvoy, S. P., Aguirre, G. K., & Epstein, R. A. (2011). Distances between real-world locations are represented in the human hippocampus. *The Journal of Neuroscience, 31*(4), 1238-1245.

Moser, E. I., Kropff, E., & Moser, M.-B. (2008). Place Cells, Grid Cells, and the Brain's Spatial Representation System. *Annual Review of Neuroscience, 31*, 69-89.

O'Keefe, J. (1976). Place Units in the Hippocampus of the Freely Moving Rat. *Experimental Neurology, 51*, 78-109.

O'Keefe, J., & Conway, D. H. (1978). Hippocampal place units in the freely moving rat: why they fire where they fire. *Experimental Brain Research, 31*, 573–590.

O'Keefe, J., & Dostrovsky, J. (1971). The hippocampus as a spatial map. Preliminary evidence from unit activity in the freely-moving rat. *Brain Research, 34*, 171–175.

O'Keefe, J., & Nadel, L. (1978). *The Hippocampus as a Cognitive Map*. Oxford, UK: Oxford University Press.

Spiers, H. J., & Maguire, E. A. (2007). A navigational

guidance system in the human brain. *Hippocampus, 17,* 618-626.

Tolman, E. C. (1948). Cognitive maps in rats and men. *The Psychological Review, 55*(4), 189-208.

Viard, A., Doeller, C. F., Hartley, T., Bird, C. M., & Burgess, N. (2011). Anterior hippocampus and goal-directed spatial decision making. *The Journal of Neuroscience, 31*(12), 4613-4621.

Wilson, M.A., & McNaughton, B. L. (1993). Dynamics of the hippocampal ensemble code for space. *Science, 261*, 1055–1

Methods

Participants

A group of 22 participants was recruited (12 females, mean age 21.73, $SD = 2.10$) via the Research Participation System of Radboud University. A sample size of $N = 29$ was calculated using G*Power (http://www.gpower.hhu.de/), based on an effect size of $d = -1.07$ (found in a similar study by Deuker et al., 2016), and on an α-level of $p < .0001$ (required for fMRI multiple comparisons), two-tailed and a power of 0.9. Due to time limitations for this Master thesis, we were not able to include all 29 subjects in this study. Ethical approval of the study was given by the local ethics committee (CMO Regio Arnhem-Nijmegen). Written informed consent was given by all participants, and they filled out a screening form for fMRI to make sure they did not meet any fMRI exclusion criteria. Participants were paid for their participation time, 10 euros per hour for MRI, 8 euros per hour for behavioural time, and 2 euros per hour in addition outside office hours and during weekends. Participants who could not complete all tasks were excluded from further analysis. We also excluded participants for further analyses based on movement during one or more of the fMRI sessions (motion exceeding twice the voxel size: 4.0 mm).

Experimental sessions

The experiments took place on two consecutive days. Participants performed three navigation sessions in a virtual city environment, adapted from 'Donderstown' (Deuker et al., 2016; Fig. 1). This is an environment, developed using Unreal Development Kit (Unreal Engine 3, Epic Games, Inc.). Using this city, we simulated a life-like experience of wayfinding and navigating between certain locations. Eight locations in this city were marked with a black box. Participants first underwent a Training session to learn the city and the locations in the city (Fig.

2). On day two of the experiments, they performed a second navigation task (Object Location, Fig. 2), in which objects were associated with the locations. In this task, participants had to learn the locations of these objects. They furthermore performed a third navigation task in the same city on the second day, the Route Change task (Fig. 2). Here, two of the three roadblock had changed location. In this way, we modulated some of the routes and thereby their path distance. Participants had to learn the new shortest routes between objects. Before the Training, after the Object Location task, and after the Route Change task, participants performed a picture viewing task during an fMRI session (Fig. 2, RSA_{pre} and RSA_{post}, and RSA_{post_2}). Furthermore, they did several additional behavioural tasks that could give an indication about their navigational strategies (Fig. 2): The Santa Barbara Sense of Direction Scale questionnaire (SBSOD, Hegarty et al., 2002), a T-maze task (Astur et al., 2016), a Distance Estimation task, and an Object Placement task (see below for more details).

Navigation tasks

Training task. The Training navigational session took place in the virtual city environment, in which eight locations were marked with a black box (Fig. 1; Fig. 9A for a screenshot of the task). The aim of this task was for the participants to learn the eight locations, and the shortest routes between them. In all tasks in a virtual environment, participants navigated using the arrow keys on a keyboard. They could only walk on the streets. There were also three roadblocks placed in the city (Fig. 9B). Due to this, participants could not always take the shortest route, but sometimes had to take a detour. The roadblocks allowed us to make clear distinctions between the Euclidean and path distances of a location pair, and later, in the Route Change task, to manipulate distance of some routes. The path distances were the shortest possible routes between the locations, which the participants were instructed to learn. We chose the locations and the roadblocks such that some location pairs have a similar Euclidean and path distance, but other pairs have large differences. At the beginning of a trial, they received instructions to go to the next box, and find the shortest route possible. These instructions were presented on the screen for 1000 ms. The box on the target location for that trial would become multi-coloured (Fig. 9C). To give some sort of feedback whether they are walking in the right direction or not, a signal was also

presented on the screen, similar to a Wi-Fi signal ranging (Fig. 9B-D). This would become stronger (maximum eight bars) as the participant got closer to the target box. When the participant arrived at the target box, they received written feedback about whether they had walked the shortest possible route. This feedback was presented for 2000 ms. The program that was used to develop the task in the virtual city (Unreal Development Kit) tracked the routes the participants had taken, and could compare this to the optimal route. In this way, it could give feedback about whether they had walked the shortest path. Then the next trial would start, with another location as the target. In this way, by navigating from location to location, participants learned the eight locations in the city, and the

shortest routes between them. There was a total of 112 trials, which were pseudo-randomised. This was done so that the target location of one trial was the start location of the subsequent trial, and that the start and target location within a trial were never the same. Additionally, participants navigated an equal amount of times (twice) between each location pair, in both directions (so four times in total). Therefore, there were exactly 14 repetitions per location. The trials were divided into four blocks of 28 trials each. After each block, a test phase would start, to test knowledge about the locations. In this phase, the blocks were removed from the city. Participants had to walk around, and drop the eight boxes at the locations they remembered (Fig. 9E). The dropped box was considered correct when it was placed
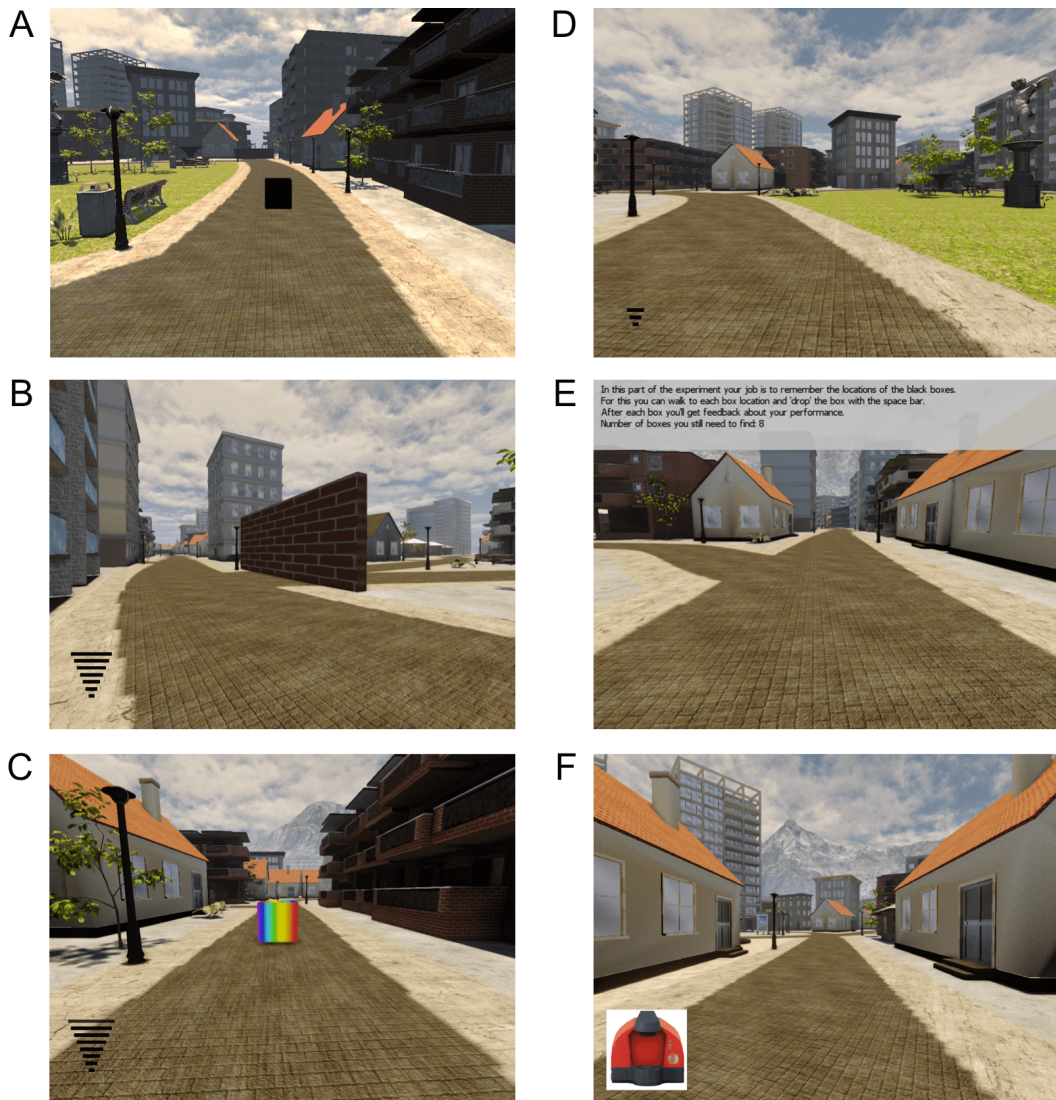
Fig. 9. Screenshots from the Training and Object Location tasks. **A.** An example of a black box that marks a location. **B.** An example of a roadblock (brick wall). The signal at the lower left corner is the signal until the target box. **C.** An example of a multi-coloured target box. The signal at the lower left corner is the signal until the target box. **D.** Screenshot of a weaker signal until the target box. **E.** Screenshot of one of the test phases during the Training task. **F.** Screenshot of the second half of the Object Location task, with the target object presented at the lower left corner.

within a radius of approximately eight times the box size of a correct location. When participants placed a box further away, a multi-coloured box appeared on the closest correct location. They first had to go to this box, before they could continue dropping the remaining boxes. During this test phase, they received feedback when they placed a box correctly. The amount of remaining boxes was presented on the screen during the whole test phase.

Object Location task. In the second navigational task, the Object Location task, the same city as in the Training task was used (Fig. 1). The same locations were marked and the roadblocks also remained at the same places. Only in this task, objects were associated with each location. Thus, objects were now 'placed' in the city. In this navigation task, participants had to learn the locations of the objects, and the shortest routes possible between them. For the first half of the task (56 trials), the trials were similar to the trials during the Training task. But here, when participants arrived at the target box, the object that was associated with that location, was presented on the screen for 2000 ms. For the second half of the task (56 trials), participants were not presented with

the signal reflecting distance until the target box anymore. During these trials, the object associated with the target location for that trial was visible at the lower left corner of the screen (Fig. 9F). They were instructed to navigate to the location of that object. This change in feedback while navigating was done to encourage participants to learn the object locations, instead of just following the signal. The Object Location task also had 112 trials in total, which were, similarly to the Training, pseudo-randomised. Participants navigated twice between each object pair, in both directions, so there were 14 repetitions per object. For each participant, the eight objects were randomly picked out of a pool of twelve objects (Fig. 10). Their associated locations were also randomised across participants.

Route Change task. The Route Change task was similar to the second half of Object Location task. However, here, two of the three roadblocks were placed on a different location (supplementary Fig. S8). Due to this, compared to the Object Location task, nine routes became shorter and nine became longer. We chose the new roadblocks such that some location pairs with small differences between

Fig. 10. All twelve objects used in the experiments. For each participant, eight objects were randomly picked out of these twelve, and associated with the locations in the city.

Euclidean and path distance in the Object Location task had large differences in the Route Change task or vice versa. The locations and associated objects in the city remained the same. Participants had to learn the new shortest routes between the objects. The Route Change task consisted of 56 pseudo-randomised (see Training and Object Location tasks) trials, with 7 repetitions per object. Similar to the second half of the Object Location task, the object of the target location was presented at the lower left corner of the screen during the whole trial. At the beginning of a trial, participants were instructed to navigate the shortest route to the location of that object. When the participant arrived at the target location, the associated object was again presented on the whole screen. The participants also received feedback about whether they walked the shortest route or not. Then, the next trial started.

Additional behavioural spatial tasks

Picture Viewing task. During the fMRI sessions (Fig. 2) before the Training (RSA$_{pre}$), after the Object Location task (RSA$_{post}$), and after the Route Change task (RSA$_{post\_2}$) participants performed a picture viewing task (PVT; Deuker et al., 2016). During this task, they were presented with a stream of pictures of the objects that they encountered in the city. Objects were presented for 2000 ms, with a jittered inter-trial interval (2500, 4000, or 5500 ms). They were presented in random order for each participant, but the order was the same for all three RSA-blocks within a participant. To ensure participants would pay attention to all the objects, we implemented an oddball-paradigm. Here, an object that was never encountered in the city (a bathtub), was presented at various points in the stream of objects. Participants had to press a button every time an object appeared, but one button at this oddball object, and another button at every other object. These buttons were randomised across participants. Each object was repeated 20 times, and the oddball appeared after 20% of the trials. The PVT was programmed in Presentation®.

Santa Barbara Sense of Direction Scale. The SBSOD (Hegarty et al., 2002) is a questionnaire consisting of fifteen questions. It is a self-report measure and assesses some general navigational or spatial abilities and sense of direction. The score can range from 1 to 7, and a higher score would mean higher general navigational abilities. This questionnaire was programmed in Presentation®.

T-maze task. The T-maze task was adapted from a highly similar task used by Astur et al. (2016), to indicate use of an allocentric or egocentric (or map-based or route-based) navigation strategy. It took place in virtual room, developed using Unreal Development Kit (Unreal Engine 3, Epic Games, Inc.). In this room, a T-shaped platform was located, and a few landmarks were placed throughout the room (supplementary Fig. S9 for screenshots of the virtual room). Participants started on the platform at the bottom of the T. At the end of both arms of the T, a box was placed, and only one of these boxes contained a reward. The reward box was on the same arm throughout the whole task. Participants were instructed to find this reward box. They could only walk on the platform. When they arrived at the box, they received positive feedback (a smiling face) when it was the reward box, and negative feedback (a sad face) when it was the box without the reward. Then they started over from the bottom of the T. This was repeated for ten trials. Two of those ten trials were probe trials. The first was on trial 4, 6, or 8, and the second on trial 10. During these probe trials, the T-platform was rotated 180°, while the reward box remained on the same location in the room. Participants received positive feedback in both arms during the probe trials. Walking to the reward box during these probe trials would indicate use of an allocentric (spatial) navigation strategy or use of place memory. Taking the same (left or right) turn as in non-probe trials would indicate an egocentric (response) strategy or use of stimulus-response memory. The location of the reward box was randomised across participants, as well as the trial number (4, 6, or 8) of the first probe trial.

Distance Estimation task. After learning the locations of the objects and the shortest routes in the Object Location task, participants had to estimate the distance between each object pair. They first estimated the Euclidean distance, and then the length of the shortest route (including roadblocks). Here, the distance between the two objects that were furthest apart in space was set to 100 (arbitrary units), and a distance of 0 would mean objects are on the same location. The estimation was therefore a number between 0 and 100. Participants also performed this task after the Route Change task, where the path distance was based on the new roadblock locations. The order in which the object pairs were presented was random and randomised across participants. The task was programmed in Presentation®. The estimated distances were later also used to create behaviourally informed

prediction matrices of the distances between objects for the searchlight analysis.

Object Placement task. Next to estimating distances between objects, participants performed an Object Placement task. Here, they were presented with an empty map of the city, so without buildings, only the streets (supplementary Fig. S10). They had to mark the locations of the learned objects in this empty map, as they remember them. Higher accuracy in placement of the object would indicate that the participant uses a more allocentric or map-based navigation. This was a paper-pencil task. The empty map was overlaid with a grid (supplementary Fig. S10), which allowed us to calculate the distance of the location marked by the participant to the correct location. The mean error across objects was considered the score of the participant.

MRI image acquisition

MRI images were acquired on a Siemens PrismaFit scanner (3T; Siemens, Erlangen, Germany) for most participants (21), and for one on a Siemens Prisma. There are no technical issues that would cause any confounds due to scanning on two scanners. Both sessions within each participant were scanned on the same scanner.

For the functional scans, a multiband sequence was used (TR = 1500 ms, TE = 28 ms, multiband acceleration factor 4, 84 slices, voxel size = 2.0 × 2.0 × 2.0 mm^3, field of view (FOV) = 210 × 210 × 168 mm, flip angle = 65°). Functional images for the RSA$_{pre}$-block were acquired on day 1 of the experiment, and for the the RSA$_{post}$-block on day 2 (Fig. 2). During the fMRI sessions for the RSA-blocks, stimulus onsets in the PVT were fixed to volume onsets in the multiband sequence. Furthermore, a structural scan (T1) was obtained for each participant (TR = 2300 ms, TE = 3.03 ms, 192 slices, voxel size = 1.0 × 1.0 × 1.0 mm^3, field of view (FOV) = 256 × 256 × 192 mm, flip angle = 8°). This was the case for most participants on day 1 (21), and for one participant on day 2 due to time issues. In addition, for most participants, a gradient fieldmap was obtained on both days (for two participants not on day 1, and for two not on day 2), using a gradient echo sequence (TR = 1020 ms, TE1 = 10 ms, 64 slices, voxel size = 3.5 × 3.5 × 2.0 mm^3, FOV = 224 × 224 × 128 mm, flip angle = 45°).

fMRI preprocessing

Functional MRI images were preprocessed using FSL (http://fsl.fmrib.ox.ac.uk/fsl/fslwiki/). The brain was extracted from the structural scan, using the FSL brain extraction toolbox. The structural scan was then downsampled from 1.0 mm isotropic voxel size to 2.0 mm isotropic voxel size. Images were further preprocessed in FSL FEAT. No spatial smoothing was applied. For the functional runs and participants of whom a fieldmap scan was acquired, the functional scans from both fMRI sessions underwent distortion correction. Motion correction was applied using MCFLIRT (three rotation and three translation estimated parameters), and images also underwent high-pass temporal filtering. The structural scan was segmented into white matter, grey matter, and cerebrospinal fluid. Functional scans were registered to the downsampled structural scan. Participants whose movement exceeded twice the voxel size (2 × 2.0 mm) in the functional run of one or more of the RSA-blocks were excluded for further analysis.

Representational similarity analysis

Data from the fMRI sessions during the RSA-blocks were analysed using RSA (Kriegeskorte et al., 2008) for multivariate pattern analysis. By subtracting results from the RSA$_{pre}$-block from RSA$_{post}$-block (pre-post design; Fig. 3), this analysis yielded a change in neural pattern similarity between each object pair. This change presumably arose due to learning the locations of the objects and the routes between them during the Object Location task.

For each functional MRI run, a general linear model (GLM) analysis was performed. All presentations (the onset and duration) of each object during the PVT were entered as a regressor, as well as six motion parameters derived from the motion correction during preprocessing. These regressors were predictors for the voxel time-series, for each object. The data was modelled by convolving the regressors with the canonical haemodynamic response function (HRF). A pseudo-contrast of 1 against 0 was used. The GLM yielded β-values for each object in each voxel, for both RSA-blocks. It resulted in eight GLMs per RSA-block for each participant.

Prediction matrices. To test whether neural representations of distances between objects (locations) were Euclidean or path distances,

predictions about the change in neural similarity were made. Besides the objective distances, we also used the behaviourally informed distances (those estimated by the participant) as predictions. Before the navigation tasks, we assumed there was no association between the objects, so the neural similarity should be random and low. After the navigation tasks, so after learning the locations and the routes, the associations were assumed to be changed according to the distances between the object pairs. Therefore, the distances were predictions of how the neural similarity will change. These distances were stored in so-called prediction matrices (8×8), with all objects on the rows and columns (Fig. 3). These matrices were symmetrical, so we only used the upper half of the matrix (above the diagonal) for analyses. There were four prediction matrices (objective Euclidean and path distances, and behaviourally informed Euclidean and path distances), so four conditions for which the neural data was further analysed. The behaviourally informed prediction matrices were obtained for each participant, using data from the Distance Estimation task.

Searchlight analysis. For within-subject searchlight analysis, a sphere with a radius of 6 voxels was formed around each voxel (centre voxel), for which only grey matter voxels were considered (Deuker et al., 2016). Only spheres with 30 or more surviving voxels were analysed. The β-values from the GLM were first registered to the T1-space of the participant. Within each searchlight, using RSA, the GLM data was correlated between each object pair, yielding the neural pattern similarity for each object pair, for both the RSA_{pre} and RSA_{post}-block. Then, this neural similarity in the RSA_{pre}-block was subtracted from the RSA_{post}-block. This yielded the change in neural similarity in that searchlight, for each object pair, from RSA_{pre} to RSA_{post}. This change in neural similarity between the objects formed an 8×8 similarity matrix (Fig. 3). Since this was a symmetric matrix, only the upper half (above the diagonal) was used for further analysis.

The similarity matrix of the searchlight was then correlated with each of the four prediction matrices (four conditions). This gave a correlation value for this searchlight with each prediction matrix. These correlation values were read back into the centre voxel of the searchlight. This analysis was done for a searchlight of each grey matter voxel (when its sphere had a minimum of 30 grey matter voxels). In this way, a correlation value was assigned to each of those voxels, for each condition. The whole

searchlight analysis thus yielded four images per participant, one for each condition, and within one image, a correlation value assigned to each searchlight centre voxel. All of the images were registered to standard MNI space.

Second-level analyses

Second-level analyses were performed on the searchlight data, to analyse, across all participants, in which voxels the correlation with the prediction matrices were significantly different from zero. For each condition, the images containing searchlight data (correlation values for each voxel) from all participants were merged into one 4D image. A whole-brain mask was created that only contained grey matter voxels shared by all participants. In addition, masks were created for regions of interest (ROIs): the left, right, and whole hippocampus, and the frontal pole. Then, for whole-brain and the ROIs, a permutation test was performed using FSL, to test whether the correlation of each voxel with each prediction matrix was significantly different from zero across all participants. The p-values were FWE-corrected for multiple comparisons; whole-brain for the whole brain mask, and small-volume corrected for the ROIs. In addition to this voxel-wise correction, a Threshold-Free Cluster Enhancement (TFCE) analysis was performed. Peak voxels were extracted with a threshold $p < .001$ (uncorrected), using FSL randomise.

Behavioural data analysis

All analyses of behavioural data were performed in Matlab. All correlations were Pearson's correlations.

Navigation tasks. Behavioural data from both the Training and the Object Location tasks were analysed to check whether participants indeed learned the locations and shortest routes between them. First of all, learning curves were calculated. We could track the paths that participants navigated, using checkpoints that were regularly placed on the streets in the virtual city. The checkpoints were invisible to the participants. For every trial, we knew which checkpoints belonged to the current shortest path, and which ones did not. We could thus calculate the proportion of passed checkpoints that did not belong to the shortest path compared to the total amount of passed checkpoints. The learning curve was then computed by calculating this

proportion for each trial, up until that trial. Learning curves were generated for both the Training and the Object Location tasks. Furthermore, from the test phases of the Training task, we calculated what the maximum amount of correctly-placed boxes was, as a percentage of the total of eight boxes.

Santa Barbara Sense of Direction Scale. The SBSOD questionnaire was scored according to the guidelines of its developers (Hegarty et al., 2002). For each question, an answer was given which corresponded to a score ranging from 1 to 7. Some of the questions had to be reverse scored. In this way, each question received a score ranging from 1 to 7, in which a higher score indicates higher ability. The total score of all 15 questions was divided by the number of questions, to calculate the final score (also ranging from 1 to 7). The higher the final score, the higher the self-report of general navigational abilities.

T-maze task. From behavioural data of the T-maze task, it was assessed whether participants used a spatial or a response strategy during the probe trials, and how consistent they were on using one or the other strategy across probe trials (Astur et al., 2016). When participants walked to the correct reward box on both probe trials, they were considered as having a spatial strategy. When they took the same turn on both probe trials as on non-probe trials, they were considered as having a response strategy. Participants who had a different response during probe trials, had a mixed response. Participants were then divided into three groups: those who use a spatial strategy, those who use a response strategy, and a mixed response group. The Spatial and Response strategy groups were used for later analyses, to investigate whether these can also be distinguished in the other spatial behavioural and fMRI measurements.

Distance Estimation task. The estimations of the Euclidean and path distances between each object pair were correlated with the objective distances. These correlation values were considered the performance on this task. Performance was furthermore compared between short and long distances (median split of objective distances), using a 2-sample t-test. Results from the latter can be found in the appendix.

Object Placement task. For the Object Placement task, we analysed how accurate participants marked the locations of the objects in the empty city map. The empty map was overlaid with a grid, so each marked location had an x- and y-coordinate on this grid. Using these coordinates, the distance between the location of each object marked by the participants and its correct location was calculated. This distance was considered the error for that object, and the mean error across all eight objects was calculated for each participant.

Correlation between behavioural spatial tasks. Data from the different additional behavioural spatial tasks were correlated with each other. The SBSOD scores of all participants were correlated with performance on the Distance Estimation task (for Euclidean and path distance), and with errors on the Object Placement task. Distance Estimation performances were also correlated with errors on the Object Placement task. Furthermore, for these three tasks, data was compared for the Spatial strategy and Response strategy group from the T-maze task, and tested whether they were significantly different using a 2-sample t-test.

Linking behavioural data to neural data

As post-hoc analyses, the neural data were linked to the behavioural data. For each condition, the peak voxel was extracted for each brain mask (left, right, and whole hippocampus, frontal pole, and whole brain). For all these peak voxels, the correlation value from the searchlight analysis was obtained, for all participant. These correlation values were then correlated to the scores of all participants for the SBSOD and Object Placement task. In addition, the peak voxel correlation values were compared between the Spatial and Response strategy group from the T-maze task, and tested whether they were significantly different using a 2-sample t-test.

The Effect of Passive Whole-Body Translation on Corticospinal Excitability for Hand Selection

Béla S. Roesink[1]

Supervisors: Pieter Medendorp[1], Leonie Oostwoud Wijdenes[1], Luc Selen[1]

[1]*Radboud University Nijmegen, Donders Institute for Brain, Cognition and Behaviour, The Netherlands*

Decisions of hand choice for an action depends on whether the body is stationary or in motion. Recently, it has been shown that during lateral sinusoidal motion of the body, there is a bias to choose the right hand for leftward acceleration, which reverses to the left hand for rightward acceleration. Furthermore, this bias disappears at zero acceleration, when the body moves at maximum velocity. The neural correlates underlying these observations have not yet been studied. Here, using single-pulse transcranial magnetic stimulation, we investigated the excitability of the left primary motor cortex (M1) during a hand selection task under passive whole-body translations, imposed by a sled. Given these preferences for hand choices during motion, we expected that the excitability of the left M1 would be increased for leftward accelerations, decreased for rightward accelerations, and unchanged at maximum velocity. We measured the peak-to-peak amplitude of the motor evoked potential (MEP) from the lateral triceps of the right arm using surface electromyography (EMG) at eight equally-spaced phases of the sinusoidal whole-body translation. Results showed that MEP amplitude modulates with the whole-body motion, with the highest MEP amplitude when the body was at increasing leftward acceleration (phase 45º). A sinusoidal relationship between MEP amplitude and phase of motion outperformed a phase-independent relationship. In summary, our data suggest that passive whole-body acceleration affects corticospinal excitability, thereby biasing upcoming hand choices in an acceleration dependent manner.

Keywords: decision making; hand choice; self-motion; vestibular system; transcranial magnetic stimulation; motor-evoked potentials; primary motor cortex

---
Corresponding author: Béla S. Roesink ; **E-mail:** bela_roesink@hotmail.com

The human body is equipped with various effector systems to interact with the environment. How does its controller, the brain, decide which effector to use in a particular task? Consider a reaching movement to a cup that can be performed with either the left or right hand. In reaching tasks, several studies found that we tend to use the right hand when objects are located to the right from the body midline, and we tend to use the left hand for objects to the left (Bryden, Pryde, & Roy, 2000; Gabbard, Tapia, & Helbig, 2003; Schweighofer et al., 2015), while for objects positioned around the body midline people tend to use their dominant hand more often (Coelho, Przbyla, Yadav, & Sainburg, 2013; Oliveira, Diedrichsen, Verstynen, & Ivry, 2010; Przybyla, Coelho, Akpinar, Kirazci, & Sainburg, 2013). Also, we choose our dominant hand for challenging tasks, such as when we have to grasp an object (Gabbard et al., 2003; Mamolo, Roy, Rohr, & Bryden, 2006).

The hand selection process preceding the actual hand movement is also influenced by other factors than handedness and target location, such as the expected rewards associated with using either the left or the right hand. For instance, people make more use of their nondominant hand if either the associated expected reward related to this hand increases, or if the expected reward for the dominant hand decreases (Stoloff, Taylor, Xu, Ridderikhoff, & Ivry, 2011). Another factor is that hand choice depends on the expected biomechanical costs associated with using either the left or the right hand (Cisek, 2012). If people are free to choose between two potential reaching movements with one hand, they tend to choose the biomechanically cheaper option in terms of path distance, movement energy and stability (Cos, Bélanger, & Cisek, 2011). This suggests that the biomechanical costs of a movement are predicted before movement initiation and are used to make a calculated decision concerning hand choice (Cos, Duque, & Cisek, 2014).

The decisions in these studies are made while participants are seated with their trunk stationary in space. But in fact, this is a special, simple case of hand selection. In everyday life, our body is nonstationary and translates through space, like when we actively walk or passively sit in the train. How are hand choices affected by these real-life situations, i.e., while the body is in motion?

When we are moving passively, the vestibular system detects linear accelerations via otoliths and via pressure sensors in the skin (Angelaki & Cullen, 2008). A recent study reported that passive whole-body motion modulates hand choice (Bakker, Weijer,

Beers, Selen, & Medendorp, 2017). Right-handed participants were sinusoidally translated along the inter-aural axis using a sled, with peak accelerations at the turning points of the sled and peak velocities at the center of the sled motion (leftward and rightward). Participants were asked to perform reaching movements to body-fixed targets at eight phases of the motion. Hand choices were affected by the whole-body acceleration, resulting in a higher preference of using the right hand for leftward accelerations and a lower preference of using the right hand for rightward accelerations, but no effect of peak velocity on hand choice. Their findings were interpreted as if the brain takes on the instantaneous acceleration signal at target onset, derived from the otoliths, when deciding on hand choice in motion (Bakker et al., 2017). To date, however, the neural correlates of hand selection during passive whole-body motion have not been studied.

From a neural perspective, it has been suggested that several processes, such as action selection and movement planning, are operating in parallel and are continuously updated to bias the competition towards a movement execution (Bestmann & Duque, 2016; Cisek, 2007; Cisek & Kalaska, 2010). Evidence for this dynamic competition is found in neuronal firing of the dorsal premotor cortex in primates (Cisek & Kalaska, 2005). In humans, changes in activity from both posterior parietal cortex and dorsal premotor cortex were examined when participants were either informed or uninformed before target onset about which hand to use for the reach (Bernier, Cieslak, & Grafton, 2012). They found that the contralateral activity of these regions increased for the chosen hand only after target onset, suggesting that a hand has to be selected first before a movement plan is to be made (Bernier et al., 2012).

Others have examined the primary motor cortex (M1) in hand selection tasks by using single-pulse transcranial magnetic stimulation (spTMS; for reviews, see: Hallett, 2007; Kobayashi & Pascual-Leone, 2003; Merabet & Pascual-Leone, 2009; Sandrini, Umilta, & Rusconi, 2011). SpTMS on the scalp induces a small electrical current in the underlying cortical tissue. As a result, muscles on the body side contralateral to the stimulation site will exhibit motor evoked potentials (MEPs) in surface electromyography (EMG). By measuring the peak-to-peak amplitude of these MEPs, one can quantify the level of corticospinal excitability, which is assumed to be the current neural state of the M1 associated with the selection of movements (Barker, Jalinous, & Freeston, 1985; Bestmann & Krakauer, 2015; Leocani, Cohen, Wassermann, Ikoma, & Hallett,

2000). Several studies concerning hand selection describe a gradual increase in MEP amplitude for the selected hand 100 ms prior to execution in the contralateral M1 (Leocani et al., 2000; Cos et al., 2014), whereas a continuous suppression in MEP amplitude was found for the nonselected hand, even during movement execution (Duque et al., 2005).

Here, we investigated the corticospinal excitability of the left M1 for hand selection during passive whole-body motion in an adapted version of the paradigm used by Bakker et al. (2017). We applied spTMS to the left M1 at eight equally spaced phases of the motion while participants performed a hand choice task. Peak-to-peak MEP amplitudes from the lateral triceps of the right arm were measured as an indicator of corticospinal excitability. We expected that the left M1 would be more excitable for leftward accelerations (Leocani et al., 2000), i.e., at phases where the preference of using the right hand is higher, and that it would be less excitable for rightward accelerations (Duque et al., 2005), i.e., at phases where the preference of using the right hand is lower, with no effect of velocity on the corticospinal excitability for hand selection.

Methods

Participants

Eight participants (five females, aged 18-42) completed the intake and the Transcranial magnetic stimulation (TMS) experiment (2 sessions on separate days) except for one participant who completed only one session. All participants had normal or corrected-to-normal vision, no known sensory, perceptual or motor deficits and no history of psychiatric or neurological illness. Participants were right-handed according to the Edinburgh Handedness Inventory (mean laterality quotient = 84, SD = 16; Oldfield, 1971), except for one participant who was left-handed (laterality quotient = 22). Participants gave written informed consent and received course credits or payment proportional to their participation. The study was approved by the local medical ethical committee (Commissie Mensgebonden Onderzoek region Arnhem-Nijmegen, The Netherlands) and conformed to the Declaration of Helsinki. In addition to these eight participants, we tested another five participants during the intake session. These participants were not included in the main experiment, because their resting motor threshold for the lateral triceps was above 80% of the maximum machine output.

Furthermore, of the remaining eight participants, one complete dataset was excluded due to substandard behavioural characterization. The following behavioural and reaction time analyses are based on seven participants. Also, one complete MEP dataset was excluded, for in the first session MEP amplitudes were not obtained consistently, and in the second session MEP amplitudes were obtained at 113% instead of 120% of maximum machine output. As a result, the following MEP analyses are based on six participants.

Experimental Setup

Participants performed a hand selection task in a dimly lit room while being translated side-to-side by a custom-built sled (see Fig. 1A) that was powered by a linear motor (TB15N, Technotion, Almelo, The Netherlands) and controlled by a Kollmorgen s700 drive (Danaher, Washington, DC). The sled performed continuous sinusoidal motion with an amplitude of 0.15 m and a period of 1.6 s, resulting in a peak velocity of 0.59 m/s and peak acceleration of 2.3 m/s² (Bakker et al., 2017). The participant's body was restrained with a five-point seat belt and the head was fixed to the sled by a personalized facemask (Posicast).

During the intake, a Posicast thermoplastic mask was created to prevent the participant's head to move during the experiment (see Fig. 1A). In this procedure, the mask was placed in a water bath of 70 ºC for 1 minute. It was pulled out from the water bath and excess water was removed. While seated on the sled, the mask was placed over the participant's face and the investigator formed the thermoplastic around the nasion, chin and ears. After it hardened for 10 minutes, it was taken from the participant's face and was left for further hardening for another 24 hours. Holes for the eyes and mouth were cut out.

During the experimental sessions, an MC-B65-HO figure-of-8 coil (MagVenture, Farum, Denmark) was fixed to the left side of the sled (see Fig. 1A) and was connected to a Magpro-X-100 magnetic stimulator (MagVenture, Farum, Denmark). Participants could stop the motion of the sled at any time by pressing one or both emergency buttons located on either side of the chair. The experimenter observed the participant by a camera and an intercom system.

Reach targets were presented on a 27" touch screen (ProLite, Iiyama, Iiyama Corporation, Tokyo, Japan) that had full HD 1080p resolution (1920x1080, see Fig. 1B). The screen was mounted horizontally on a

table frame in front of the participants at about the level of their diaphragm. A photodiode registered the exact phase of the sled motion at the time of target presentation. Presentation delays were well accounted for and targets appeared within 5° of the desired phase of the sinusoidal motion. Participants could rest their elbows on supporting frames attached to the same table frame. The position of the sled, the tips of the left and right index finger, and the tip of the nose were recorded at 500 Hz using an Optotrak Certus system (NDI, Northern Digital Instruments, Waterloo, Canada).

EMG activity was recorded from six right arm muscles: first dorsal interosseous, brachioradialis, biceps long head, biceps short head, triceps lateral head (TLAT), and triceps long head. EMG data were recorded using a Trigno™ EMG system (Delsys, Inc., Boston, Massachusetts). EMG data were collected using wireless surface electrodes that were band-passed filtered (30-450 Hz), amplified (1000x) and sampled at 1111 Hz.

The TMS coil was placed tightly on the scalp over the left M1 with the handle pointing towards the back of the head, tilted 45° to the left (see Fig. 1C). The marker on the tip of the nose was taken as a proxy residual movement between the head and the coil. This resulted in sinusoidal motions that were negligible (X = 3.65 mm, SD = 1.62, Y = 5.05 mm, SD = 2.13, Z = 3.95 mm, SD = 2.21; Tarapore et al., 2014). During the intake and the experimental sessions, we used single pulses to identify the optimal location for producing MEPs in the TLAT. The resting motor threshold (rMT) is the minimum intensity needed to produce an MEP in the TLAT in 5 of 10 consecutive trials (Schutter & van Honk, 2006). The ascending staircase method was used, starting at 30% of maximum machine output while increasing the percentage in small steps until rMT was found (~5%, Schutter & van Honk, 2006). The mean rMT for each session was 61.8% (SD = 10.3) and 66.2% (SD = 13.2) of maximum machine output, respectively. We chose to increase the intensity for the experimental sessions to 120% of rMT per participant, so that the MEPs were visible on each trial.

During the intake, participants were familiarized with the setup, task, and the TMS procedure and they received the personalized facemask. The two experimental sessions were scheduled at least one day apart and were performed at the same time of day. In one experimental session, targets were displayed at the peaks of sled acceleration (phases 90° and 270°, at the turning points, see Figs. 1C and 1D) and at the peaks of sled velocity (phases 0° and 180°, at the center of the motion). In the other experimental session, targets were displayed at phases 45°, 135°, 225°, and 315° that are in between the peaks of the velocity and acceleration. Visual stimuli, TMS pulses and sled motion were controlled using custom written software in Python 2.7 (Kivy extension, version 1.9.0).

Task

Start positions, red discs of 3.5 cm in diameter, were presented on the touch screen at a distance of approximately 30 cm from the participants' sternum and 8 cm on either side of the body midline. Targets, yellow discs of 3.5 cm in diameter, appeared on a semicircle with a radius of 30 cm from the point midway at 35 possible directions: -40°, -35°, -30°, -28°, -26°, -24°, -22°, -20°, -18°, -16°, -14°, -12°, -10°, -8°, -6°, -4°, -2°, 0°, 2°, 4°, 6°, 8°, 10°, 12°, 14°, 16°, 18°, 20°, 22°, 24°, 26°, 28°, 30°, 35°, and 40°. A 2.5 cm x 2.5 cm green fixation cross was placed on the body midline, 12 cm further away than the two start positions.

Participants were instructed to look at the fixation cross and touch both start positions with their left and right index finger to initiate a trial. There were three types of trials: single target, catch, and TMS. When a single target was presented, participants were instructed to touch the target as quickly and accurately as possible with either their left or right index finger. To avoid predetermined hand choices for participants that select one hand prior to the target, ~8% of behavioural trials acted as catch trials where two targets were presented, and the participant had to touch both targets using both index fingers. In case of a TMS trial, no targets appeared, and no reach had to be made. Instead, participants received a short magnetic pulse (~1 ms) to their left M1 at one of eight phases of the sled motion. Participants were explicitly instructed that after a TMS pulse the start positions would automatically turn red, and they had to initiate the next trial by pressing the start positions again. A time interval of 3 s was implemented after the TMS trials, avoiding influences of the pulse on choice behaviour and reaction times of the preceding trial. Participants could not predict the upcoming trial type, because trials were randomized under the restriction that after a TMS or catch trial no repeat occurred in four subsequent trials.

A Bayesian adaptive approach adjusted the target direction for the single target trials based on the hand choice of all previous trials (ψ-procedure, Kontsevich & Tyler, 1999; Prins, 2013). This method
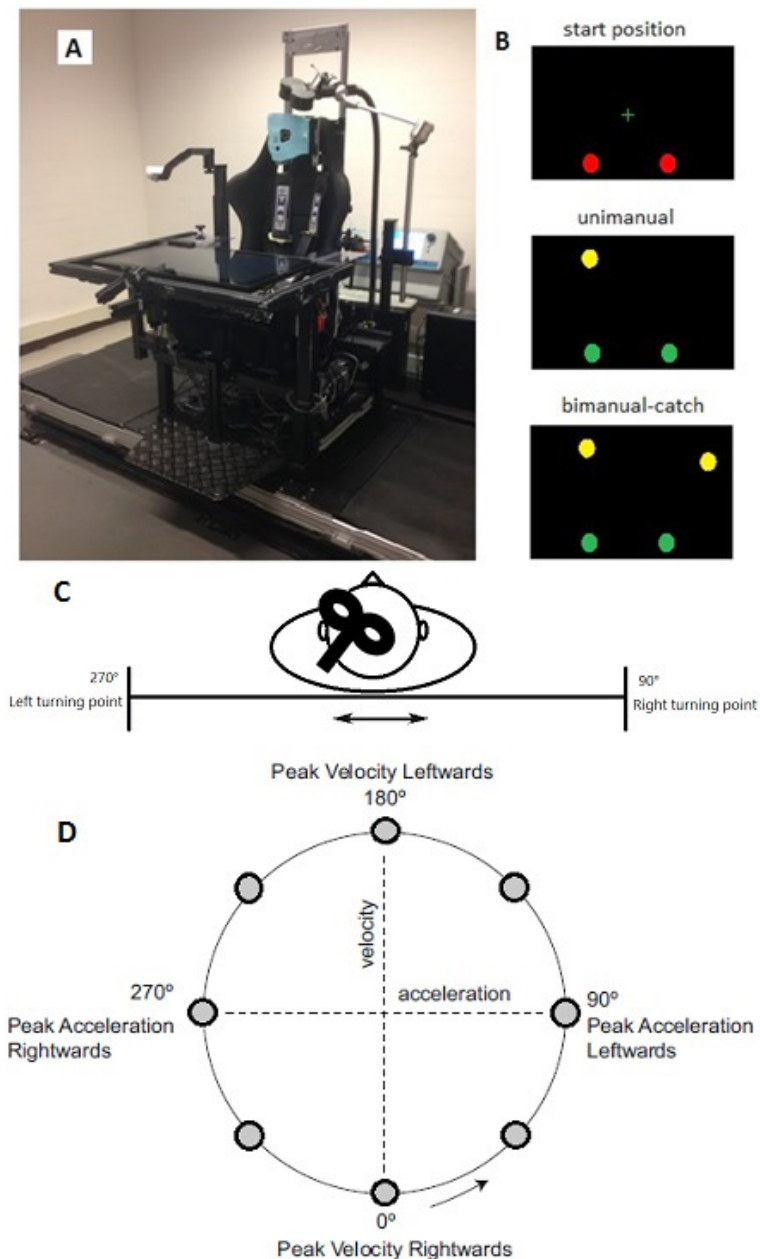
Fig. 1. Setup and stimuli. **A.** Picture of the sled with the touch screen, head mask and TMS coil. **B.** Illustration of possible screen configurations for the start positions (top), a single target trial (middle) and a catch trial (bottom). **C.** Sinusoidal motion with TMS coil. D. Acceleration-velocity phase plot. Targets were displayed at 8 phases of the sinusoidal motion (grey circles).

computes the expected information to be gained for every next possible target, based on the information from the previous hand choices, i.e., the posterior probabilities, and selects the target with the most optimal expected information. In one-fourth of all single target trials a peripheral target was presented, which was not determined by the ψ-procedure. Note that these trials were still used to compute the optimal location of the next stimulus by the ψ-procedure. This adaptive procedure to select the target direction was run for each sled phase independently.

Inter-trial intervals (ITI) were randomized

ranging from 1.6 s to 2.8 s. However, ITI could be extended by at least 1.6 s (one motion cycle) if the participant did not return their index fingers back to the start position in time (600 ms before the upcoming trial).

Participants performed six blocks of 120 trials for each session. Sessions were counterbalanced across participants. One block lasted for ~6 minutes and consisted of 96 single target trials, 16 TMS trials and 8 catch trials. After each block there was a short break (~1 minute) in which the lights were switched on and the sled was halted. Each session took ~75

minutes, where the task lasted ~50 minutes with a total of 720 trials for each session.

Data Analysis

Choice Behaviour Analysis

Hand choice was determined as the hand that first reached 30 cm/s away from a start location, as determined by the Optotrak data. Missing Optotrak data were interpolated with the function *interp1* in MATLAB. Trials were excluded when more than 10% of the first 500 ms of a trial consisted of missing data. This was the case for 14% of all trials with a range of 3%-39% for each participant. If Optotrak data were missing, hand choice was determined by the first hand leaving the touch screen. Hand choice data were fitted for each phase by a cumulative Gaussian distribution using a maximum likelihood approach including a lapse rate parameter (Wichmann & Hill, 2001):

$$(1) \quad P(x) = \lambda + (1 - 2\lambda)\frac{1}{\sigma\sqrt{2\pi}} \int_{-\infty}^{x} e^{\frac{-(y-\mu)^2}{2\sigma^2}} dy$$

Target direction is represented by x. Parameter μ indicates the target direction for which participants were equally likely to use their left and right hand: the point of subjective equality (PSE). A negative PSE demonstrates a shift towards right hand choices. Parameter σ represents the standard deviation of the curve or the participant's variability in responses, whereas parameter λ represents the lapses produced by the participant.

We investigated hand choice by comparing the PSEs for the four peak phases of the sled motion with Wilcoxon rank sum tests (α = .05), since the data were not normally distributed. By comparing PSEs at phases with equal velocity but opposing accelerations, we investigated the influence of acceleration on hand choice (phases 90° and 270°). Moreover, by comparing the PSEs at phases with equal acceleration but opposing velocities, we investigated the influence of velocity on hand choice (phases 0° and 180°).

We examined the relation between PSE and the actual size of the acceleration and velocity amplitudes at each phase for each participant. We calculated the Fisher *z*-transformed correlation coefficients for each participant and tested the mean correlation against zero with a *t*-test.

Finally, we investigated whether the modulation between hand choice and acceleration was sinusoidal (Bakker et al., 2017), with a higher preference of using

the right hand for leftward accelerations and a lower preference of using the right hand for rightward accelerations. We fitted a sinusoidal psychometric function to the hand choice data for all phases and for each participant, while assuming for μ:

$$(2) \quad \text{PSE}(phase) = A \sin(phase - phase0) + B$$

Here, *A* is the amplitude of the sinusoid, *B* is the vertical offset or handedness, and *phase0* is the phase or horizontal shift according to the sled motion. Moreover, we assumed a fixed σ that reflects the variability of hand choices, and λ for the eight phases (Bakker et al., 2017). For each session, we first normalized the PSEs by subtracting the mean PSE for all phases of a session from the separate phases of that session. The sinusoidal model contained five parameters *(A, B, phase0, σ, λ)* for each participant. In addition, we fitted another psychometric model that assumes no modulation of the motion on PSE, where μ:

$$(3) \quad \text{PSE}(phase) = constant$$

We assumed a fixed σ and λ for the eight phases. The constant model contained three parameters *(A, B, phase0)* for each participant. We used the Akaike Information Criterion (AIC) to compare the likelihoods of these models (Burnham & Anderson, 2002). The AIC estimates the quality of a model based on the goodness-of-fit and penalizes for an increase in number of parameters:

$$(4) \quad AIC = -2\log L + 2k$$

The total likelihood of the data given the model is represented by *L* and the number of parameters is captured by *k*. The model that describes the data best on the individual and group level has the lowest score relative to the other model. Because AIC is silent about the absolute quality of the model, it can only support the conclusion in combination with other results in this study.

Reaction Time Analysis

We investigated whether sled motion affected the reaction times concerning hand choices. Reaction times were computed as follows. A low-pass filter using a fifth order, bi-directional Butterworth filter with a cutoff frequency of 10 Hz was applied to the position data (Bakker et al., 2017). By subtracting the position of the sled from the markers, data were converted into a body-centered reference frame.

Speed was computed as the magnitude of the time derivative of the finger position in three dimensions. Reaction time (RT) was defined as the first moment after target onset at which the hand speed exceeded 7.5 cm/s in a range between 150 ms and 500 ms (Bakker et al., 2017) after target onset. Using the latter criterion, another 3% of trials were excluded.

People typically choose the hand ipsilateral to the target. If competition increases between hands for reach execution, for example for targets around the PSE, one would expect RTs to increase. We investigated the effect of this competition by comparing RTs for the two targets around the PSE for each participant with RT to peripheral targets more than 10 degrees to the left or right. A two-way repeated measures ANOVA was performed, with the factors hand (left, right) and target direction (PSE, periphery). Because this competition could change according to the phase of the motion, we also performed a two-way repeated measures ANOVA, with the factors hand (left, right) and phase (8 different phases).

Corticospinal Excitability Analysis

As a measure of corticospinal excitability, we focused on the MEPs from the lateral triceps, which is an extensor muscle to be recruited first when reaching in the present task. To analyse the peak-to-peak MEP amplitudes, we first excluded trials that had a background EMG activity of 100 µV or higher in a time window of 200 ms preceding the TMS pulse (4 trials; Duque et al., 2005). Subsequently, for each trial we calculated the peak-to-peak amplitude of the MEP by subtracting the minimum value from the maximum value within a time interval of 0-60 ms after the TMS pulse. Within sessions, these MEP amplitudes were transformed into z-scores by subtracting the mean and dividing them by the standard deviation and were then grouped by phase. Finally, to account for outliers, z-transformed MEP values with 2 standard deviations of the mean or higher were excluded from the analyses (4% of all trials), leaving at least 21 MEP values for each phase for every participant (Wilhelm, Quoilin, Petitjean, & Duque, 2016). By z-scoring, we accounted for corticospinal excitability differences between the two sessions.

We performed a repeated measures ANOVA on MEP amplitude with factor phase (8 different phases) to verify whether there is an effect of passive whole-body motion on the left M1 corticospinal excitability. Also, we compared the MEP amplitudes for the four peak phases of the sled motion with

Wilcoxon rank sum tests ($\alpha = .05$), since the data were not normally distributed. Analogous to the hand choice analyses, we compared the MEP amplitude at phases with equal velocity but opposing accelerations to investigate the influence of acceleration on corticospinal excitability (phases 90° and 270°). Moreover, by comparing the MEP amplitude at phases with equal acceleration but opposing velocities, we investigated the influence of velocity on corticospinal excitability (phases 0° and 180°).

We investigated the relation between MEP magnitude and the associated acceleration and velocity at each phase for each participant. We calculated the Fisher z-transformed correlation coefficients for each participant and tested the mean correlation against zero with a t-test.

Finally, we investigated whether the modulation between MEP and acceleration is sinusoidal, and analogous to the behavioural observations. We fitted a sinusoidal function to the MEP data for all phases for each participant, where :

$$(5) \qquad \text{MEP}(phase) = A \sin(phase - phase0) + B$$

Here, A is the amplitude of the sinusoid, B is the vertical offset, and $phase0$ is the phase or horizontal shift according to the sled motion. This sinusoidal MEP model contained three parameters (A, B, $phase0$) for each participant. An alternative model was also tested for which the MEP is unrelated to phase, where :

$$(6) \qquad \text{MEP}(phase) = constant$$

The constant model contained only one parameter (*constant*) for each participant. We used the least squares AIC to compare the sinusoid and the constant model:

$$(7) \qquad \text{AIC} = 2k + n^* \log(SSE)$$

Here, k is the number of parameters, n is number of data points, and SSE is the sum of squared errors.

Control Study

We performed a control experiment with one participant to test whether we probed a task-dependent effect as opposed to a default task-independent modulation of whole-body motion on the corticospinal excitability of the M1. Features of the experiment were kept the same, except for the following: (1) No hand choice task had to be

performed during the experiment; (2) all eight phases were probed with TMS in one session; (3) Phases were randomized in such a way that pulses were given in between 3.2 s and 6.4 s (2-4 cycles of the motion) after the participant pressed the start positions again. This guaranteed that there were at least 3 s in between pulses and that pulses came fairly unexpected. The rMT was comparable with previous mentioned values (57%). The data preparation was comparable, with six trials excluded for having a background EMG activity of 100 µV or higher in a time window of 200 ms preceding the TMS pulse. Six z-scored MEPs with two standard deviations from the mean or higher were excluded, leaving at least 22 MEPs for each phase to be analysed.

Results

Choice Behaviour

We studied the effect of passive whole-body translation on hand choice by presenting targets at different body-centric locations. Targets were probed at eight different phases of sled motion with adaptive procedures. We measured the PSE; the target direction for which participants were equally likely to reach with their left and right hand.

Figure 2A and 2B show the psychometric curves fitted to the proportion of right hand responses for each target of one representative participant, with circle size representing the number of trials for each target direction. Hand choice was consistent for peripheral targets such as –40° (always left hand choice) and 40° (always right hand choice). Negative PSEs demonstrate an overall preference of using the right hand for this participant. Figure 2A shows that when the participant is at the right turning point and accelerated to the left (blue circles, blue fitted curve), the preference of using the right hand increases (PSE = -7.0°). Moreover, when the participant is at the left turning point and accelerated to the right (red circles, red fitted curve), the preference of using the left hand increases, although the right hand is still chosen more often (PSE = -3.9°). This suggests that this participant's hand choice depends on the direction of acceleration. Figure 2B shows that hand choice is similar at the peaks of leftward and rightward velocity, when acceleration was zero (PSE = -5.3° and -5.5°). This implies that this participant's hand choice does not depend on the direction of velocity. All PSEs as a function of phase are depicted in Figure 4A for this participant.

In general, all participants exhibited this individual effect. A Wilcoxon signed-rank test showed a significant difference between PSEs for opposite directions of peak acceleration (z = -2.37, p = .018), with a preference of using the right hand for the leftward acceleration (PSE = -4.9°, SD = 6.6) and a preference of using the left hand for the rightward acceleration, although the right hand is still chosen more often (PSE = -1.4°, SD = 5.6). This suggests that hand choice depends on the direction of acceleration. Also, a Wilcoxon signed-rank test showed no significant difference (z = -1.52, p = .128) between PSEs for opposite directions of peak velocity (PSE = -1.9°, SD = 5.7 and PSE = -3.6°, SD = 7.3). This implies that hand choice does not depend on the direction of velocity. All PSEs (with SEs) as a function of phase for all participants are depicted in Figure 4B.

To understand the relation between PSE and the corresponding size of the acceleration for each phase, we calculated individual correlation coefficients. All participants showed a positive correlation between PSE and acceleration size, with the mean significantly different from zero (Fisher's r to z transform, r = .71, $t(6)$ = 3.13, p = .020). Figure 2C illustrates the linear relation between PSE and acceleration. We also calculated the correlation between PSE and velocity in the same way for each participant, resulting in four positive and three negative correlations, and a nonsignificant mean correlation (r = .18, $t(6)$ = 0.06, p = .955, see Fig. 2D). These results suggest that there is a relation between PSE and the size of acceleration, but not for velocity.

Finally, we tested whether the effect of acceleration on hand choice modulates sinusoidally with phase. We first verified the assumption that from the fitted psychometric curves did not differ across the eight phases for all participants with a repeated measures ANOVA ($F(2.10, 71.59)$= 0.46, p = 0.653). We fitted a psychometric sinusoidal model and a constant model to the hand choice data for all phases and for each participant. Lower AIC values indicate a better fit for the sinusoidal model (1017.6; see Table 1) compared to the constant model (1025.6).

Figure 4A shows the sinusoidal fit to the data of the representative participant. Table 2 lists the best-fit parameters for each participant for the sinusoidal model ($A, B, phase0, \sigma, \lambda$). We verified that the amplitude, parameter A, was significantly different from zero ($t(6)$ = 4.56, p = .004). This suggests that the choice bias varies with phase. The participants' best-fit parameters were averaged, and the resulting mean curve is overlaid on the mean

Table 1.

Akaike Information Criteria (AIC). Lower AIC values are expressed in bold.

Participant	PSE=sin	PSE=B	Difference in model PSE	MEP=sin	MEP=B	Difference in model MEP
1	957.4	966.8	9.4	-3.46	-1.28	2.18
2	1077.2	1082.3	5.1	0.58	5.94	5.36
3	1099.8	1099.3	0.5	-17.75	-19.65	1.9
4	970.5	993.1	22.6	-	-	-
5	1012.6	1031.5	18.9	3.14	5.53	2.39
6	1441.5	1444.6	3.1	-4.27	-0.44	3.83
7	564.3	561.8	2.5	-14.01	-8.25	5.76
Mean	1017.6 (SD=258.6)	1025.6 (SD=259.4)		-5.96 (SD=8.23)	-0.28 (SD=10.21)	

Table 2.

Fitted parameters for the sinusoidal model.

Participant	Acceleration					MEP		
	A	B	Phase 0	σ	λ	A	B	Phase 0
1	1.1	-4.1	164.9	5.0	0	0.299	-0.178	315.8
2	1.8	-4.4	225.1	10.4	0.041	0.531	-0.0758	300.0
3	1.1	-4.1	261.4	10.4	0.034	0.062	-0.0906	8.1
4	1.5	-.02	203.6	4.4	0.012	-	-	-
5	2.8	3.1	191.5	9.1	0.019	0.462	-0.105	284.4
6	4.1	-14.6	182.0	28.9	0	0.339	-0.129	347.5
7	1.3	0.0	178.5	11.9	0.020	0.077	-0.185	86.5
Mean	1.96	-3.46	201 (SD= 8.19)	11.44	0.018 (SD= 0.016)	0.30 (SD= 0.19)	-0.13 (SD= 0.05)	103.7 (SD= 54.39)

PSE as a function of phase with shaded error bars of the mean sinusoid in Figure 4B. As shown, the phase modulation is biased by the peak acceleration, not peak velocity, with a higher preference of using the right hand for leftward accelerations and a lower preference of using the right hand for rightward accelerations.

Reaction Time

We investigated whether an effect of competition between hands for reach execution could be discerned based on RTs for targets around the PSE compared to peripheral targets. A repeated measures ANOVA with factors hand (left, right) and target direction (PSE, periphery) on all RTs (phases combined) showed that movements to targets around the PSE were initiated slower ($M = 327$ ms, $SD = 10.8$) than movements to targets in the periphery ($M = 309$ ms, $SD = 5.9$), supporting a competition process
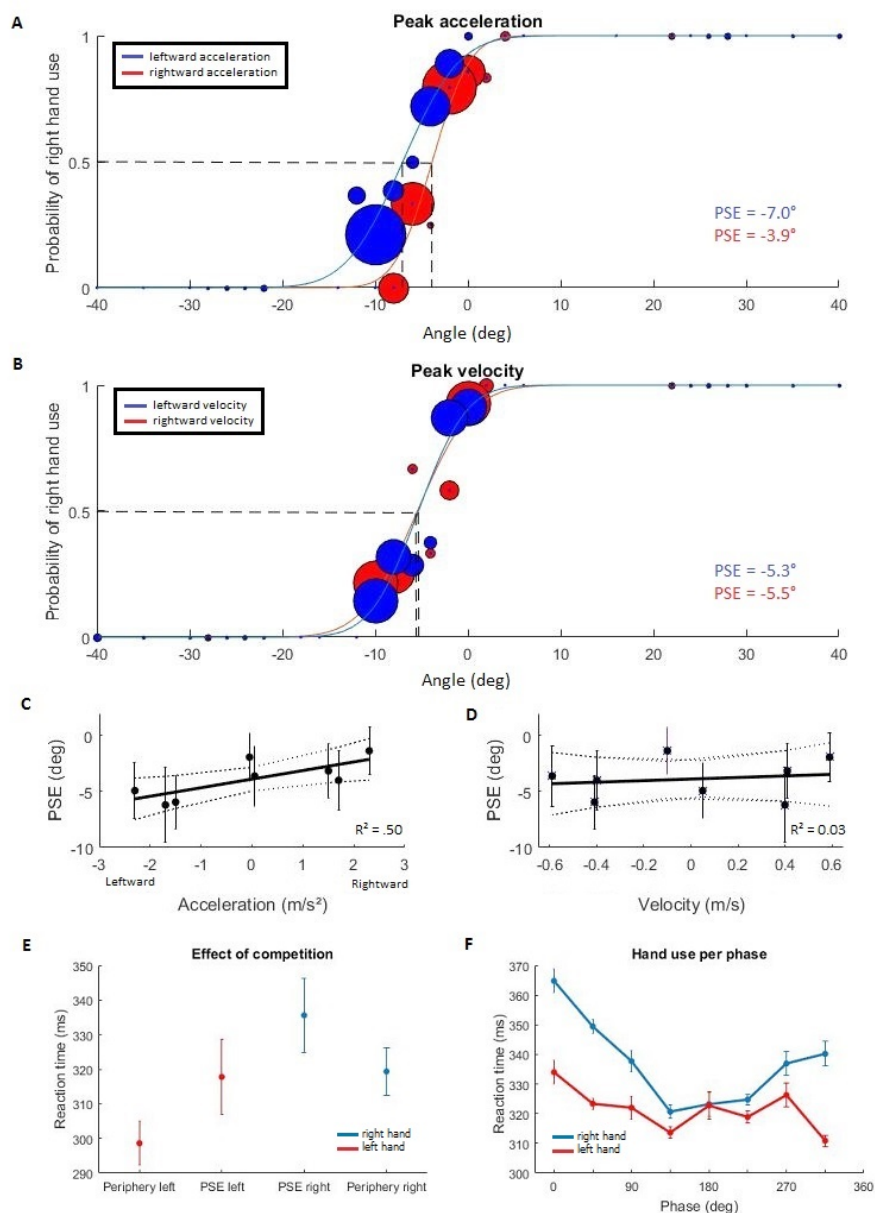
Fig. 2. PSE plots for a single participant. The probability of a right-hand choice for each target direction is shown, optimally fitted with the psychometric curve. Circle size represents the number of trials for each target direction. **A.** Hand choice for leftward and rightward peak acceleration. **B.** Hand choice for leftward and rightward peak velocity. **C.** Mean PSEs (with error bars indicating SEs) are plotted as a function of acceleration, accompanied by the 95% confidence interval (dotted lines) around the regression line. **D.** Mean PSEs (with SEs) are plotted as a function of velocity, accompanied by 95% confidence interval (dotted lines) around the regression line. **E.** Mean left (red) and right hand (blue) reaction times (with SEs) for targets around PSE (center) and periphery (exterior). **F.** Mean left (red) and right hand (blue) reaction times (with SEs) for each phase.

($F(1,6) = 7.12$, $p = .037$; Bakker et al., 2017). This effect is shown in Figure 2E. Participants responded generally faster with their left hand ($M = 308$ ms, $SD = 8.2$) than their right hand ($M = 327$ ms, $SD = 8.2$; $F(1,6) = 34.85$, $p = .001$). There was no interaction effect.

To investigate the relation between phase and RT, we conducted another repeated measures ANOVA with factors hand (left, right) and phase (8 different phases) on RT. This demonstrated a main effect of phase on RT ($F(3.92, 19.58) = 3.92$, $p = .017$; Huynh-Feldt). Also, a main effect of hand on RT showed that participants responded faster with their left ($M = 321$ ms, $SD = 6.7$) than their right hand ($M = 337$ ms, $SD = 6.7$; $F(1,5) = 9.05$, $p = .030$). An interaction effect between hand and phase was found that was in line with the competition analysis ($F(4.26, 21.28) = 4.54$, p = .008; Huynh-Feldt).
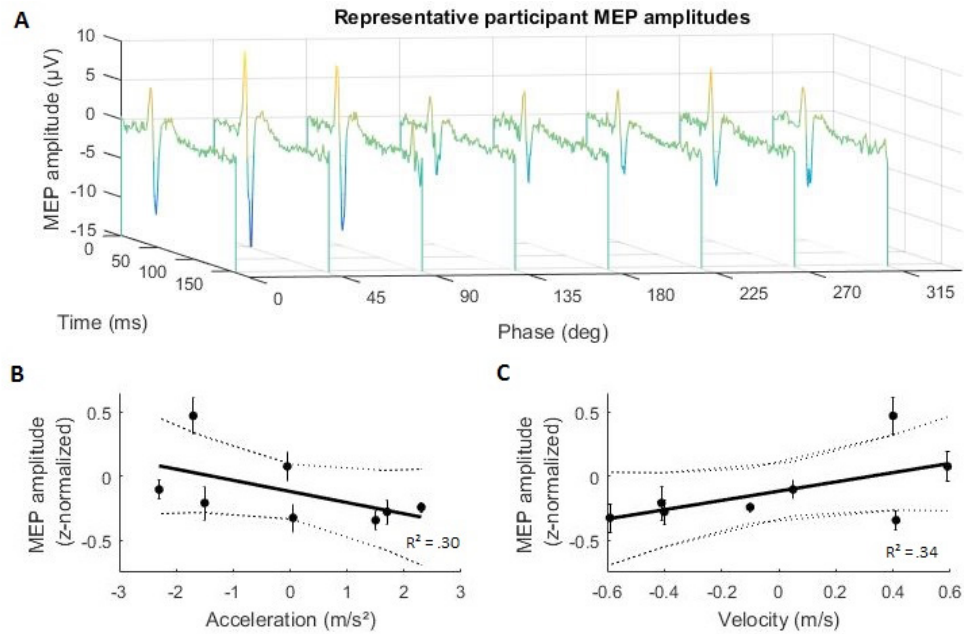
Fig. 3A. Evolution of MEP amplitudes over time plotted as a function of phase for one representative participant. **B.** Mean *z*-normalized MEP amplitude as a function of acceleration, fitted regression slope and 95% confidence interval around the regression line (dotted lines). **C.** Mean *z*-normalized MEP amplitude as a function of velocity, fitted regression slope and 95% confidence interval around the regression line (dotted lines).

Figure 2F shows the relation between phase and RT, implying that the choice bias with phase changes according to RT in both hands.

Corticospinal Excitability

The main objective of this study was to examine the effect of passive sinusoidal whole-body translations on corticospinal excitability in the left M1 for hand selection and to see whether this excitability can be associated with the behavioural findings. We measured the peak-to-peak MEP amplitude of the right TLAT while pulses were applied at eight different phases of sled motion.

If acceleration modulates the MEP amplitudes, we expect a difference between MEPs measured at peak acceleration. However, if velocity modulates the MEP amplitudes, we expect a difference between MEPs measured at peak velocity. Figure 3A shows the averaged MEP amplitudes for each phase over time for the representative participant. Here, the peak-to-peak MEP amplitude for the first leftward acceleration (phase 45°) is largest compared to all other phases. Figure 4C shows the *z*-scored MEP values with accompanied error bars indicating SEs as a function of phase for the representative participant, where the MEP value is highest for the first leftward acceleration (phase 45°) compared to all other phases.

A repeated measures ANOVA verified this effect across participants ($F(7, 28) = 6.57$, $p<.001$), suggesting that whole-body translation does affect the left M1 corticospinal excitability for hand selection (see Figure 4D). A Wilcoxon signed-rank test showed no significant difference ($z = -1.36$, $p = .173$) between MEP amplitudes for leftward peak acceleration ($M = -0.10$, $SD = 0.19$) and rightward peak acceleration ($M = -0.24$, $SD = 0.09$). A Wilcoxon signed-rank test between MEP amplitudes for opposite directions of peak velocity ($M = 0.08$, $SD = 0.28$ and $M = -0.32$, $SD = 0.27$) showed no significant difference ($z = -1.57$, $p = .116$). These results suggest that whole-body translation does not affect the left M1 corticospinal excitability for hand selection at the peaks (leftward and rightward) of acceleration and velocity.

We next correlated the MEP values with the corresponding size of the acceleration. All participants showed a negative correlation between MEP value and acceleration size. This correlation was significantly different from zero (Fisher's *r* to *z* transform, $r = -0.55$, $t(5) = 3.45$, $p = .018$). Figure 3B illustrates the linear relation between MEP and acceleration. We also calculated the correlation between MEP magnitude and velocity in the same way for each participant, resulting in four positive and two negative correlations, and a nonsignificant mean correlation ($r = 0.58$, $t(5) = 0.86$, $p = .432$,
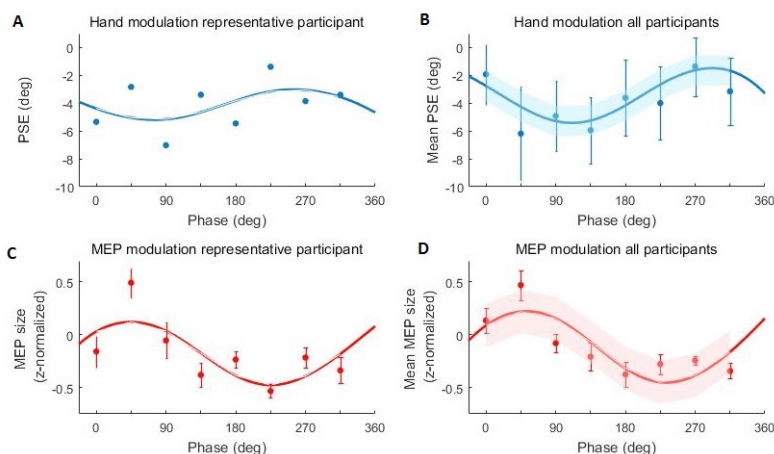
Fig. 4. Sinusoidal fits to the PSE and MEP modulations. Left panels, data from the representative participant; right panels, data from all participants; upper panels, PSE as a function of phase; lower panels, MEP amplitude as a function of phase. All panels are accompanied by the sinusoidal model fit (error bars are used when appropriate; the standard error for the sinusoid is indicated by the shaded area).

Fig. 3C). These results suggest that there is a relation between MEP amplitude and the size of acceleration, but not for velocity.

Finally, we tested whether the effect of acceleration on MEP amplitude modulates sinusoidally with phase. We fitted a sinusoidal model and a constant model to the MEP amplitudes for all phases and for each participant. Lower AIC values indicate a better fit for the sinusoidal model (-5.96; see Table 1) compared to the constant model (-0.28).

Figure 4C shows the best-fitted sinusoid for the representative participant. Table 2 lists the best-fit parameters for each participant (*A, B, phase0*). We verified that the amplitude, parameter *A*, was significantly different from zero ($t(5) = 3.73$, $p = .014$). This suggests that the MEP amplitude modulates sinusoidally with phase. The participants' best-fit parameters were averaged, yielding a best-fit

curve that is overlaid on the mean MEP amplitude as a function of phase with shaded error bars of the mean sinusoid in Figure 4D. The model shows that the phase modulation is biased by the increasing leftward acceleration (phase 45°) and the increasing rightward acceleration (phase 225°), but is not biased by peak velocity. Higher MEP amplitudes are only observed for the increasing leftward acceleration (phase 45°), but no changes in MEP amplitude for rightward accelerations.

Control Study

To understand whether the MEP modulation was caused by the hand choice task or simply reflects a default task-independent modulation of whole-body motion on the corticospinal excitability of the M1, we performed a control experiment with one
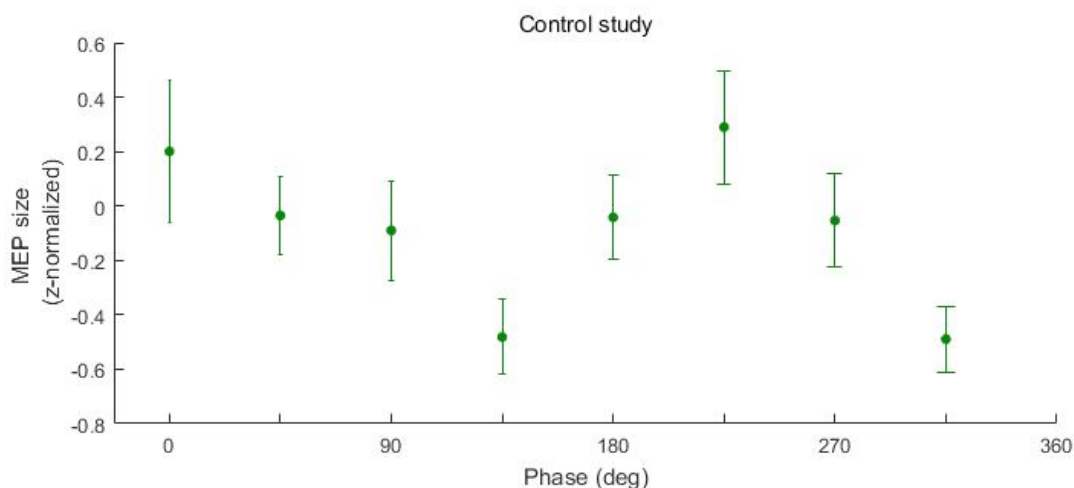

Fig. 5. Control study in a single participant. MEP amplitude as a function of phase (with SEs).

participant. In Figure 5, one can observe the MEP amplitude as a function of phase, which is different from when a hand selection task is involved. There was no significant correlation between MEP amplitude and the associated acceleration ($r = .18$, $p = .667$) or velocity ($r = .008$, $p = .986$). This single participant control study proposes that we have successfully explored a task-dependent effect of passive whole-body motion on hand selection.

Discussion

This is the first study to investigate the corticospinal excitability of the left primary motor cortex (M1) for hand selection during passive whole-body motion. We applied single-pulse transcranial magnetic stimulation (spTMS) to the left M1 at eight equally-spaced phases of the motion while participants performed a hand choice task. Motor evoked potential (MEP) amplitudes were measured from the lateral triceps of the right arm as an indicator of corticospinal excitability. Our results show that passive whole-body motion affects the left M1 corticospinal excitability for hand selection. We found that MEP amplitudes were dependent on the phase of the motion, with the highest amplitude for the increasing leftward acceleration (phase 45°) of the sinusoidal sled motion. We verified that there is no effect of velocity on the left M1 corticospinal excitability for hand selection.

We replicated the main behavioural findings by Bakker et al. (2017). Hand choices were affected by the whole-body acceleration, resulting in a higher preference for using the right hand for leftward accelerations and a lower preference for using the right hand for rightward accelerations, but no effect of peak velocity on hand choice. Our RT results showed that we successfully probed a competition process for hand selection, with longer RTs for reaches to targets around the PSE compared to targets from the periphery. Overall, participants responded faster with their left hand than their right hand.

We showed that the sinusoidal model described the data better than a phase-independent model (i.e. no influence of passive whole-body motion on cortical excitability). Figure 4D shows that the sinusoid increases for leftward accelerations and decreases for rightward accelerations. However, results are not pure symmetrical, with a strong increase in MEP amplitude for the increasing leftward acceleration (phase 45°) but no decrease in MEP amplitude for the increasing rightward acceleration (phase 225°).

One explanation for this could be that the arm has to compensate for the inertia corresponding to the direction of the sled acceleration. In body-centered coordinates, during leftward acceleration, inertia drives both hands to the right, while during rightward acceleration, inertia drives both hands to the left. Because we are reading out the state of the left M1 for the right lateral triceps, we only see an increase in MEP amplitude for leftward accelerations, while for rightward accelerations this effect is much smaller. This suggests that biomechanical costs of possible reaching movements with the right hand are calculated before movement initiation during passive whole-body motion (Cos et al., 2014).

Although our control study is severely limited by testing only a single participant, the result may suggest that we successfully explored a task-dependent effect of passive whole-body motion on hand selection. The control data show that the modulation of excitability was different than when participants were translated and performed a hand choice task. Still, the results of the control study cannot rule out the biomechanical cost explanation, because there were neither hand choices nor biomechanical costs to calculate during the control study. To test the biomechanical cost explanation, one could perform the same experiment, but instead of making reaching movements, participants would have to move the index finger while MEPs of the first dorsal interosseous of the selected hand are measured (Duque et al., 2005). We expect that the influence of inertial forces of the acceleration on the index finger is negligible. This would remove the biomechanical cost calculation of the reaching movement, making it possible to discern whether the difference in cortical excitability that we found is related to calculating these costs or is related to selecting which hand to use.

Initially, we assumed a symmetrical, i.e. sinusoidal modulation of corticospinal excitability for the lateral triceps, similar to the sinusoidal choice modulation of the arms. We expected that the left M1 would be more excitable at phases where the right hand was preferred (leftward accelerations), and that the left M1 would be less excitable at phases where the left hand was preferred (rightward accelerations). Contrary to our expectations, no decrease in MEP amplitude for the left M1 was observed for rightward accelerations, but rather a constant level of cortical excitability was found. One explanation is that we only probed a facilitating process for the right lateral triceps in the left M1. Several studies have described that during 'Go' signals with a predefined hand, only a gradual increase in MEP amplitude is

probed for that hand 100 ms prior to execution in the contralateral M1, whereas the unchosen hand is often not explicitly suppressed (Bestmann & Duque, 2016; Leocani et al., 2000). This differs considerably from a competition resolution concerning which hand to use, where the nonselected hand is suppressed. Perhaps the passive whole-body motion only facilitates the selection in favor of one arm, in our case, the right arm. It would be interesting to verify if the right M1 works in a similar way for the left arm.

One reservation of our study is that we had a limited number of participants. A reason for this is that we had to exclude five participants, because their rMTs for the lateral triceps were above 80% of the maximum machine output. We experienced that the brachioradialis and bicep were easier to target with spTMS. If the data of these muscles resembles the effects found in this study, one could adopt one of these muscles for recruitment.

Conclusion

Our study shows that the corticospinal excitability of the left M1 for hand selection is affected by whole-body translation and as such may be a readout of a bias modulation for hand selection. However, further studies are needed to understand how the brain exactly incorporates whole-body motion for hand selection.

References

Angelaki, D. E., & Cullen, K. E. (2008). Vestibular system: The many facets of a multimodal sense. *Annual Review of Neuroscience, 31*, 125–150.

Bakker, R. S., Weijer, R. H. A., van Beers, R. J., Selen, L. P. J., & Medendorp, W. P. (2017). Decisions in motion: Passive body acceleration modulates hand choice. *Journal of Neurophysiology, 117,* 2250–2261.

Barker, A. T., Jalinous, R., & Freeston, I. L. (1985). Non-invasive magnetic stimulation of human motor cortex. *Lancet, 1,* 1106–1107.

Bernier, P. -M., Cieslak, M., & Grafton, S. T. (2012). Effector selection precedes reach planning in the dorsal parietofrontal cortex. *Journal of Neurophysiology, 108,* 57–68.

Bestmann, S., & Duque, J. (2016). Transcranial magnetic stimulation: Decomposing the processes underlying action preparation. *The Neuroscientist, 22,* 392–405.

Bestmann, S., & Krakauer, J. W. (2015). The uses and interpretations of the motor-evoked potential for understanding behaviour. *Experimental Brain Research*, 1–11.

Bryden, P. J., Pryde, K. M., & Roy, E. A. (2000). A performance measure of the degree of hand preference. *Brain and Cognition*, *44*, 402–414.

Burnham, K. P., & Anderson, D. R ., (2002) Model selection and multimodel inference: a practical information-theoretic approach, 2nd edition. Springer-Verlag, New York.

Cisek, P. (2007). Cortical mechanisms of action selection: The affordance competition hypothesis. *Philosophical Transactions of The Royal Society B*, *362,* 1585–1599.

Cisek, P. (2012). Making decisions through a distributed consensus. *Current Opinion in Neurobiology, 22,* 927–936.

Cisek, P., & Kalaska, J. F. (2005). Neural correlates of reaching decisions in dorsal premotor cortex: Specification of multiple direction choices and final selection of action. *Neuron, 45,* 801–814.

Cisek, P., & Kalaska, J. F. (2010). Neural mechanisms for interacting with a world full of action choices. *Annual Review of Neuroscience, 33,* 269–298.

Coelho, C. J., Przybyla, A., Yadav., & Sainburg, R. L. (2013). Hemispheric differences in the control of limb dynamics: A link between arm performance asymmetries and arm selection patterns. *Journal of Neurophysiology, 109,* 825–838.

Cos, I., Bélanger, N., & Cisek, P. (2011). The influence of predicted arm biomechanics on decision making. *Journal of Neurophysiology, 105*, 3022–3033. .

Cos, I., Duque, J., & Cisek, P. (2014). Rapid prediction of biomechanical costs during action decisions. *Journal of Neurophysiology, 112*, 1256–1266..

Duque, J., Mazzocchio, R., Dambrosia, J., Murase, N., Olivier, E., & Cohen, L. G. (2005). Kinematically specific interhemispheric inhibition operating in the process of generation of a voluntary movement. *Cerebral Cortex, 15,* 588–593. .

Gabbard, C., Tapia, M., & Helbig, C. R. (2003). Task complexity and limb selection in reaching. *International Journal of Neuroscience, 113*, 143–152. doi:10.1080/00207450390161994.

Hallet, M. (2007). Transcranial magnetic stimulation: A primer. *Neuron, 55,* 187–199. .

Kobayashi, M., & Pascual-Leone, A. (2003). Transcranial magnetic stimulation in neurology. *Lancet Neurology, 2*.

Kontsevich, L. L., & Tyler, C. W. (1999). Bayesian adaptive estimation of psychometric slope and threshold. *Vision Research, 39*, 2729–2737.

Leocani, L., Cohen, L. G., Wassermann, E. M., Ikoma, K., & Hallett, M. (2000). Human corticospinal excitability evaluated with transcranial magnetic stimulation during different reaction time paradigms. *Brain, 123*, 1161–1173. .

Mamolo, C. M., Roy, E. A., Rohr, L. E., & Bryden, P. J. (2006). Reaching patterns across working space: The effects of handedness, task demands, and comfort levels. *Laterality: Asymmetries of Body, Brain and Cognition, 11*, 465–492.

Merabet, L. B., & Pascual-Leone, A. (2009). Transcranial Magnetic Stimulation. 1055–1062.

Oldfield, R. C. (1971). The assessment and analysis of handedness: The Edinburgh inventory.

Neurophsychologia, 9, 97–113.

Oliveira, F. T. P., Diedrichsen, J., Verstynen, T., Duque, J., & Ivry, R. B. (2010). Transcranial magnetic stimulation of posterior parietal cortex affects decisions of hand choice. *PNAS, 107,* 17751–17756.

Prins, N. (2013). The psi-marginal adaptive method: How to give nuisance parameters the attention they deserve (no more, no less). *Journal of Vision, 13*, 1–17.

Przybyla, A., Coelho, C. J., Akpinar, S., Kirazci, S., & Sainburg, R. L. (2013). Sensorimotor performance asymmetries predict hand selection. *Neuroscience, 228*, 349–360.

Sandrini, M., Umiltà, C., & Rusconi, E. (2010). The use of transcranial magnetic stimulation in cognitive neuroscience: A new synthesis of methodological issues. *Neuroscience and Biobehavioral Reviews, 35*, 516–536.

Schutter, D. J. L. G., & van Honk, J. (2006). A standardized motor threshold estimation procedure for transcranial magnetic stimulation research. *Journal ECT, 22*, 176–178.

Schweighofer, N., Xiao, Y., Kim, S., Yoshioka, T., Gordon, J., & Osu, R. (2015). Effort, success, and nonuse determine arm choice. *Journal of Neurophysiology, 114,* 551–559.

Stoloff, R. H., Taylor, J. A., Xu, J., Ridderikhoff, A., & Ivry, R. B. (2011). Effect of reinforcement history on hand choice in an unconstrained reaching task. *Frontiers in Neuroscience, 5*, 1–14.

Tarapore, P. E., Tate, M. C., Findlay, A. M., Honma, S. M., Mizuiri, D., Berger, M. S., & Nagarajan, S. S. (2012). Preoperative multimodal motor mapping: a comparison of magnetoencephalography imaging, navigated transcranial magnetic stimulation, and direct cortical stimulation. *Journal of Neurosurgery, 117*, 354–362.

Wichmann, F. A., & Hill, N. J. (2001). The psychometric function: I. Fitting, sampling and goodness of fit. *Perceptual Psychophysiology, 63*, 1293–1313.

Wilhelm, E., Quoilin, C., Petitjean, C., & Duque, J. (2016). A double-coil TMS method to assess corticospinal excitability changes at a near-simultaneous time in the two hands during movement preparation. *Frontiers in Human Neuroscience, 10*, 1–11.

World Medical Association. (2013). *WMA declaration of Helsinki: Ethical principles for medical research involving human subjects*. Retrieved from http://www.wma.net/en/30publications/10policies/b3/

Children's Integration of Action Gestures and Verbs During Online Language Comprehension: An Event-Related Potentials Study

Christina Schoechl[1]
Supervisor: Prof. Dr. Asli Özyürek[1,2,3]

[1]*Radboud University Nijmegen, Donders Institute for Brain, Cognition and Behaviour, The Netherlands*
[2]*Centre for Language Studies, Radboud University, Nijmegen, The Netherlands*
[3]*Max-Planck-Institute for Psycholinguistics, Nijmegen, The Netherlands*

Behavioural measures show that five-year-olds can integrate iconic gestures that co-occur with speech. Both behavioural and neuroscientific studies show that adults integrate gestures (e.g. a C-shaped hand depicting a glass while moving it towards the mouth to indicate drinking) with simultaneous speech. However, no study has investigated the underlying neural activity of online multimodal semantic integration processes in seven-year-old children. We used electroencephalography (EEG) to record Dutch speaking children's brain activity while they watched videos of simultaneously presented speech-gesture combinations of action gestures and action verbs in matching and mismatching conditions. We observed an N400 effect with larger amplitude to mismatching speech-gesture combinations compared to matching speech-gesture pairs, reflecting semantic integration of gestural information to the spoken word. Our findings suggest that seven-year-old children display adult-like online neural integration strategies of iconic gestures co-occurring with speech.

Corresponding author: Christina Schoechl ; **E-mail:** christina.schoechl@gmail.com

As human beings, we interact and communicate with others by using language. Language, however, does not only refer to the auditory modality of spoken language. Rather, we communicate in a multimodal way: we gesture while we speak. Speech and gesture form an integrated system that combines auditory and visual information to create a unified message (Kelly, Özyürek, & Maris, 2010; McNeill, 1992). Iconic co-speech gestures are specific hand movements made during speaking (McNeill, 1992). These gestures represent movements and actions of people or depict concrete objects and events in space, such as a C-shaped hand depicting a glass while moving it towards the mouth to indicate drinking (McNeill, 1992). In adults, gestures are not only integrated during linguistic production (Kita & Özyürek, 2003), but also during linguistic comprehension (Kelly, Barr, Church, & Lynch, 1999). Neuroscientific studies investigating adults' ability to integrate gesture to speech have further confirmed that auditory and visual input are processed simultaneously rather than sequentially, suggesting the presence of an integrated system both during production and comprehension (Drijvers & Özyürek, submitted; Habets, Kita, Shao, Özyürek, & Hagoort, 2011; Wu & Coulson, 2007).

Despite the speech-gesture integration found on cognitive, behavioural and neural levels in adults, we know little about such processes in children. Some studies show that children's ability to integrate iconic gestures to speech during language comprehension emerges between the ages of three and five (McNeil, Alibali, & Evans, 2000; Sekine, Sowden, & Kita, 2015; Stanfield, Williamson, & Özçalışkan, 2013). However, these findings are based on offline measures of behavioural experiments and provide only limited information about the development of an integrated system in children. Behavioural results about children's integration abilities in language comprehension are scarce, and neuroscientific findings about the underlying cognitive processes of gesture-speech integration especially regarding online measures are practically non-existent. We do not know at what age children develop the ability to combine and integrate gestures to speech. Therefore, the current study aimed, as a first step, to expand upon previous behavioural results. We investigated whether seven-year-old children can integrate information communicated through gestures to the auditory information from speech during language comprehension by recording children's brain activity.

Developmental trajectory of gesture

Children gesture before they speak (Bates, Benigni, Bretherton, Camaioni, & Volterra, 1979; Carpenter, Nagell, Tomasello, Butterworth, & Moore, 1998). Twelve-month-old infants are able to extend their index finger to point to draw an individual's attention to a specific object (declarative pointing) or to request that object (imperative pointing) before they are able to communicate verbally (Behne, Liszkowski, Carpenter, & Tomasello, 2012; Carpenter et al., 1998). Such deictic (pointing) gestures are among the first signs of a child's desire to communicate with his or her caregiver, and gestures therefore appear to serve as the building block of language development and human communication (Kita, 2003; McNeill, 1992). In addition to deictic gestures, infants around 12-13 months of age begin to produce words to refer to objects and events in their environment (Sheehan, Namy, & Mills, 2007). Not only do children produce single words, but they often do so in combination with a pointing gesture, which may be a further sign of the infant's wish to communicate intentionally (Bates et al., 1979). A speech-gesture combination can be produced to communicate redundant information, such as naming an object with a single word while pointing at it, or may be used to add semantic meaning to the single spoken word, such as pointing to an object while referring to the person who owns it (Greenfield & Smith, 1976). In a recent study, Igualada and colleagues were able to confirm a predictive relationship between 12-month-old infants' use of speech-gesture combination and their expressive language development at 18 months of age (Igualada, Bosch, & Prieto, 2015). One-year-old infants preferred to communicate by using pointing-speech combinations rather than a pointing gesture only, suggesting that children use this strategy to reinforce the information they want to communicate (Igualada, Bosch, & Prieto, 2015; Liszkowski, Albrecht, Carpenter, & Tomasello, 2008). This reinforcement strategy may relate to the advancement of communicative strategies and therefore influence expressive language use around 18 months. This transitional period of a language learner to explore additional means of communication may reflect cognitive change in advancing from one-word speech to two-word speech. Speech-gesture combinations therefore seem to be predictive of the age a child will produce two-word combinations (Goldin-Meadow & Butcher, 2003; Iverson & Goldin-Meadow, 2005; Özçaliskan & Goldin-Meadow, 2005, 2009). The

development of gesture and early speech appear to be tightly connected, and gesture-speech integration in production may start to emerge during the one-word period (Butcher & Goldin-Meadow, 2000).

Although young children are able to produce deictic gestures and speech-gesture combinations around their first birthday, Schulze and Tomasello (2015) suggest that comprehending the communicative intention of others' deictic gestures may not become robust until around 18 months of age. The use of speech-gesture combinations at the one-word stage in infants suggests their intention to communicate, but applying a communicative meaning to another person's gesture requires the infant to have developed an understanding of the other as an intentional agent who also wants to communicate information (Behne, Carpenter, & Tomasello, 2005; Carpenter et al., 1998). During the second year of life, young children are beginning to understand the importance of a caregiver's communicative cues as they learn to establish a meaningful connection between a word and its referent (Kita, 2003).

While one-year-old children frequently use deictic gestures, iconic gestures may emerge as the result of having acquired a spoken language, as children only produce them after they have learned their first verbs (Özçalışkan & Goldin-Meadow, 2011). In comparison to deictic gestures that appear to serve as a building block for, and precede spoken language, children start producing iconic gestures around their second birthday when they develop a sensitivity to iconicity (the resemblance between a symbol and its referent) of hand movements (Hrabic, Williamson, & Özçalışkan, 2014; Namy, Campbell, & Tomasello, 2004; Özçalışkan & Goldin-Meadow, 2005, 2011). Establishing a connection between an iconic gesture and a referent (gestured object or action) seems to be more complex and cognitively demanding for children than establishing a relation between a pointing gesture and a referent (Özçalışkan & Goldin-Meadow, 2011). Nevertheless, Furman, Küntay and Özyürek (2014) show that in languages where verbs are acquired early, iconic gestures might also emerge earlier than two years of age.

Young children seem to start producing gestures describing a specific action (representational gestures) earlier than they produce iconic gestures describing an object (e.g., forming a cupped hand to represent a round circle; Hrabic et al., 2014; Namy et al., 2004; Özçalışkan & Goldin-Meadow, 2011). During comprehension, children may understand nonverbal symbols, such as gestures, as either representational, iconic or arbitrary (Namy et al., 2004), but the interpretation of a gesture as either form may follow a different developmental trajectory. While 18-month-old infants showed a robust mapping of both iconic and arbitrary gestures to their referents, 26-month-old infants failed to map arbitrary gestures to their referents (Namy & Waxman, 1998). It appears as if children interpret the iconicity of gestures as a relevant source of information from a young age, when they are developing sensitivity to both the auditory and the visual modality of communication. Arbitrary gestures, however, may not seem as communicatively informative as iconic gestures during this period of focused attention to spoken language development and may be interpreted differently than representational or iconic gestures.

As children acquire a larger spoken vocabulary, more resources may be allocated to the development of spoken language as children learn to speak (Namy et al., 2004). In turn, four-year-old children are more competent language users than young infants, and have developed an enhanced understanding of the communicative intentions of others. Such an understanding of language may allow for a more flexible processing of unconventional symbols such as arbitrary gestures (Namy et al., 2004). Four-year-old children, just like 18-month-olds, display a robust mapping of arbitrary gestures to their referent. The U-shaped development of the sensitivity to arbitrary gestures may be related to children's 'zooming in' to the most informative modality to learn more spoken words (Namy et al., 2004; Namy & Waxman, 1998). The maturation of language and an increase in understanding the communicative intentions of both speech and gestures may provide an important leeway for understanding and processing speech-gesture combinations.

Can children comprehend a gesture in combination with speech ?

The processing of information communicated simultaneously through two modalities is cognitively challenging, but children seem to get better at understanding the importance of visual input and learn to combine it with the auditory information as they get older (Sekine et al., 2015; Stanfield et al., 2013). In a previous study (Stanfield et al., 2013), an experimenter sitting across from a two-, a three- or a four-year-old child said 'I am eating' while simultaneously producing an iconic action gesture depicting an object (e.g., moving the hands to the mouth as if eating a sandwich). This speech-gesture combination was produced twice before the child was given two different pictures, one of which always

matched the object depicted by the iconic gesture. The child then had to select the picture that best matched what the experimenter had communicated. Three- and four-year-old children, but not two-year-olds, were able to reliably select the correct picture. The ability to understand speech-gesture combinations with iconic action gestures depicting information about an object therefore appears to develop around age three.

Speech-gesture combinations with iconic gestures conveying action information about motion may, however, be more difficult to process. Motion can be communicated by depicting the manner and path of a particular event, such as gesturing running (manner) up a hill (path; Talmy, 2000) and children as young as three years are able to produce such iconic action gestures (Özyürek et al., 2008). However, when three- and four-year-old children were asked to distinguish between manner and path of an iconic action gesture about motion in speech-gesture combinations, three-year-olds failed to comprehend the action information of the iconic gesture (Hrabic et al., 2014). In Hrabic et al.'s (2014) study, children watched video clips with speech-gesture combinations in three different conditions. The gesture either conveyed both manner and path, only manner, or only path of a particular motion. Children were then asked to select one animation out of two that best matched the video clip they had watched. Only the animation displaying a character depicting the same manner and path information as presented via the iconic gesture in the video clip was the correct choice. The other animation displayed either manner only or path only. Although three-year-old children can produce iconic gestures conveying motion information, only four-year-old children selected the correct animations reliably during a comprehension task (Hrabic et al., 2014). These findings suggest that comprehending gestures conveying information about motion follows the production of iconic gestures depicting object information.

Are gestures integrated to speech during comprehension on a behavioural level?

From the presented literature we can see that producing and understanding iconic gestures in speech-gesture combinations develops within the first few years of life. However, iconic gestures do not always only convey additional information that is not apparent in speech, but gestures and speech may also mutually constrain each other. Speech and gesture may convey information that is different, yet, when combined, present useful information for comprehending a message. During comprehension, people automatically try to establish a semantic relation between both the visual and the auditory modalities and adults are able to integrate multimodal information without effort (Habets et al., 2011; Kelly et al., 2010). For children, however, interpreting information from two modalities that mutually constrain each other is more challenging. Sekine et al. (2015) presented three- and five-year-old children with short video clips of an actress performing an iconic action gesture (e.g. eating with a fork) while she said, 'One is eating'. The videos were presented in three different conditions. In the first condition, children only heard the sound of the videos (verbal only, VO). In the second condition children only saw the video, but did not hear the sound (gesture only, GO), whereas in the third condition children both saw the video and heard the sound (verbal and gesture combined, VG). After each video, children had to select one picture of four that best matched the information from the video. As in previous studies, only one picture was the correct choice that corresponded to the VG condition. A second picture represented only the verbal modality, so that the picture matched the action (eating) but the shape of the gesture did not (eating an apple instead of using a fork). A third picture was only a match for the gesture condition, in that the gesture matched the iconic action gesture (eating with a fork) but the meaning of the gesture represented brushing teeth. The fourth picture was an unrelated distractor, such as a person taking a photograph. Only five-year-old children reliably selected the picture that matched the display of both the speech and the gesture. The findings of Stanfield et al. (2013) and Hrabic et al. (2014) suggest that children between the ages of three and five are learning to comprehend information conveyed through gesture to co-occurring speech. Moreover, Sekine et al.'s findings show that, behaviourally, children may start to integrate information from gestures to speech conveying different, but semantically related, information around the age of five.

There is behavioural evidence to confirm the existence of a unified system that automatically allows for the integration of both modalities during production and comprehension in adults (Kelly et al., 1999, 2010; Kelly, Healey, Özyürek, & Holler, 2015). Although there is one neuroscientific study (based on functional magnetic resonance imaging, fMRI) showing that eight-year-old childrens' brains

appear to be sensitive to the meaning of hand movements (Dick, Goldin-Meadow, Solodkin, & Small, 2012), there is only one study showing that younger children may also be able to integrate two modalities during language comprehension on a behavioural level (Sekine et al., 2015). These results are, however, only based on offline behavioural measures, which neither allow us to assume a direct relationship between neural mechanisms that process speech and gesture, nor do these behavioural results confirm an integrated neural system in children. In turn, neuroscientific measures, such as electroencephalography (EEG) or fMRI (as in Dick et al., 2012), can provide information about the underlying neural correlates of multimodal integration processes.

Neural integration of speech and gesture in adults

The N400, a negative deflection measured between 300 and 500 ms after stimulus onset using EEG, is a good measure for neurocognitive processing of semantic information of pictures, words, or sentences during language comprehension (Kutas & Hillyard, 1980, 1984). The amplitude of the N400 varies as a function of the semantic fit between the meaning of a word and its context (a word, a sentence or a discourse; Hagoort & Van Berkum, 2007), and indexes the ease of semantic processing in language. The N400 amplitude is larger in response to semantically mismatching information in comparison to matching information (Kutas & Federmeier, 2011). The N400 congruency effect is observed as the difference of the brain activity of mismatching information compared to the brain activity of matching information.

In addition to semantically mismatching speech, gestures have been found to evoke similar effects (Wu & Coulson, 2007). When participants were presented with gestures that followed words unrelated to the gesture, a larger N400 effect was observed when compared to words that related to the previously produced gesture (Wu & Coulson, 2007). The integration processes of semantically related or unrelated information from two modalities can, therefore, also be investigated using event-related potentials (ERPs) such as the N400. This method presents advantages over other neuroimaging techniques since it is easier to carry out with young children when compared to, for example, fMRI. The EEG technique is non-invasive and pain free, and this practicality allows us to get valid measures

of children's brain activity underlying multimodal integration processes. Moreover, it allows us to investigate such processes with a high temporal resolution.

In a study (Özyürek, Willems, Kita, & Hagoort, 2007), adults' ERPs were recorded while they watched video clips of a person creating speech-gesture combinations in a sentence. When a particular gesture mismatched the information from the preceding sentence, a stronger N400 effect was observed than when the gesture semantically matched the context of the sentence (Kelly, Kravitz, & Hopkins, 2004; Wu & Coulson, 2007; Özyürek et al., 2007). Similar results were found in studies investigating speech-gesture combinations with single action verbs (Drijvers & Özyürek, submitted; Habets et al., 2011). In Drijvers and Özyürek (submitted), adults watched a video clip of an actress saying 'to drink' while she gestured 'to type'. The mismatching information from the visual modality elicited a stronger N400 effect than when adults saw a matching speech-gesture combination (Drijvers & Özyürek, submitted). When information that is presented via two different modalities is a semantic mismatch, adults appear to have a difficult time processing the contrasting information, and the N400 effect indicates processes of semantic integration. The findings of these studies investigating neural/neurocognitive processes of multimodal integration add value to the behavioural results from speech-gesture integration studies. Moreover, such findings provide strong evidence for the presence of an integrated system that automatically processes and combines speech and gesture (Kelly et al., 2010).

Neural measures of speech and gesture in children

Literature about children's ability to process and integrate multimodal information during language comprehension is scarce and has only reported on offline measures in behavioural tasks. Studies, such as Sheehan and colleagues, have reported on neuroscientific evidence of infant's sensitivity to gestures (Sheehan et al., 2007). In their study, the authors recorded ERPs from 18- and 26-month-old infants in a priming task that included both words and gestures. Infants watched a video clip of a person either naming an object or using an action gesture to depict an object while the children's brain activity was recorded. The order of presentation of the stimuli was sequential, as the video was followed by a picture of an object that either matched or

mismatched the preceding word or gesture. The resulting ERPs from both conditions (word or gesture) in response to a matching or a mismatching picture were compared, and an N400 effect was observed to pictures preceded by a word in both age groups. However, only 18-month-old infants showed a significant N400 effect for pictures preceded by a gesture. These findings suggest that younger infants, who have a limited spoken vocabulary, may place similar semantic and communicative expectations to words and gestures (Sheehan et al., 2007). These findings align with Namy et al.'s (2004) behavioural data of 18-month-old but not 26-month-old infants' sensitivity to arbitrary gestures. Even though 26-month-olds showed a behavioural sensitivity to iconic gestures, the fact that such sensitivity is absent in online neural measures may further point to a U-shaped development of gesture sensitivity. As children get older, and they learn to appreciate the conventional role of words, they may rely less on the visual modality in communication as can be seen in both behavioural and neuroscientific investigations. Despite young children's sensitivity to gesture, it is still unclear how gesture is integrated with co-occurring speech.

In addition to the ERP results of sequential processing of gesture, there is neuroscientific evidence showing that children are sensitive to auditory semantic linguistic integration during speech comprehension (Atchley et al., 2006; Benau, Morris, & Couperus, 2011; Holcomb, Coffey, & Neville, 1992). Most of the studies investigating semantic integration have focused on children around the age of seven and older, except Holcomb et al., 1992, who included five-year-olds in their study (Atchley et al., 2006; Benau et al., 2011). All of these authors have reported an N400 effect to semantically mismatching words at the end of auditory sentences that is similar to the effect observed in adults (Atchley et al., 2006; Benau et al., 2011; Holcomb et al., 1992). In adults, the N400 effect can be observed in the posterior regions, but the topography for the N400 in children appears not to be localized (Holcomb et al., 1992). Nevertheless, one recent study investigating semantic processing in preschool-aged children reported on an effect distributed around the posterior regions (Pijnacker et al., 2017). The authors presented auditory sentences ending with either a matching or a mismatching word to children between the ages of four and six while recording the children's brain activity. The results of the ERPs are in line with previous research, showing a robust N400 effect to mismatching words compared to matching words. Although the posteriorly observed N400 in this age

group is similarly distributed as the effect observed in adults, it is important to mention that ERPs of children and adults may not be comparable, since children's brains are not fully developed and differences in neural density or myelination may affect the brain activity in different ways (DeBoer, Scott, & Nelson, 2005).

Despite the sensitivity to gestures observed in 18-month-old infants, five-year-olds' ability to integrate speech-gesture combinations on a behavioural level, and the evidence of semantic integration in the spoken modality in five- to seven-year-old children, it is not clear whether seven-year-old children integrate gesture to speech on a neural level. To fill this gap and learn more about children's integration abilities we tested seven-year-old children in a match-mismatch paradigm with simultaneous speech-gesture word combinations.

The present study

The present study aimed to investigate whether seven-year-old children were able to integrate visual information communicated through gesture to auditory information from speech. To test this, we used EEG to measure children's brain activity while they watched video clips of a woman producing either matching or mismatching speech-gesture combinations of single action verbs/gestures. As in Drijvers and Özyürek (submitted), we hypothesized that mismatching speech-gesture pairs would elicit a larger N400 effect than matching pairs. We did not make specific predictions about the amplitude, the latency or the distribution of the effect, given the limited literature reporting on N400 effects in children. We chose to focus on the N400 because it is a robust effect that allows for a detailed investigation of the brain activity for semantic integration processes. To our knowledge, this is the first study to use ERPs to investigate multimodal integration in children during language comprehension. EEG research with young children presents challenges and requires participants to sit still and stay attentive. Since no research has been carried out in this area, we decided, as a first step, to select an age group in which we can predict an N400 effect to be present based on behavioural results. The added value of using EEG instead of behavioural measures with seven-year-old children is that such online measures allowed us to learn more about the time course of speech-gesture integration. Moreover, we could test whether the N400 effect would be more distributed over the scalp in children than it is in

adults, predicted based on the findings by Holcomb et al. (1992) and Dick et al. (2012). Additionally, we recorded children's reaction times and error rates in a behavioural task, during which children had to respond 'yes' to a question when they heard a verb in a previous trial, and had to respond with 'no' when the verb they heard did not match the previous trial. This task served two purposes. First, by presenting a question to which the children had to respond to we were able to check whether children stayed attentive during the experiment. Second, this task allowed us to investigate how the congruency of the video clips would influence children's behavioural responses and may suggest how children process integration on a behavioural level.

We expected to see faster responses and fewer errors to verbs that matched the previous trial. We further predicted that children would be faster and more accurate in responding to a question following a matching speech-gesture video. Based on the behavioural studies and the findings about auditory semantic processing, we expected to observe a stronger N400 effect to mismatching videos when compared to matching videos, which would suggest that a fully developed integrated system exists in children around seven years old. Since the presence of an integrated system in adults has been confirmed by several studies, we believe it to be important to investigate the development of such a system in children. In addition, ERPs can provide information about topographical processing differences and differences in the time-course of speech-gesture integration processes in children and adults.

Method

Participants

Our final sample consisted of 17 native Dutch speaking children with a mean age of 7.37 (SD = 0.46, 11 female). Some children reported to have some knowledge of English (3), Frisian (1) or Russian (2; through school or family). All children were right handed and reported no developmental issues such as autism or attention deficit hyperactivity disorder (ADHD). We recruited participants by contacting local schools, sports centres and libraries, and handed out flyers to individuals in the city centre of Nijmegen, The Netherlands.[1]

Materials

Verb list. The list of Dutch action verbs used in the present study was based on a list created by Drijvers & Özyürek (2016). The original list consisted of 240 verbs out of which we selected 170, based on the criteria that 80% of five- and six-year-old children in the Netherlands are familiar with these verbs (Bacchini, Boland, Hulsbeek, Pot, & Smits, 2005; Schaerlaekens, Kohnstamm, Lejaegere, & Vries, 1999). We created a list with verb-gesture combinations in two conditions: 1) verb-gesture match and 2) verb-gesture mismatch. We carefully controlled the items in the mismatch condition so that a verb and its mismatching gesture were neither semantically nor phonetically related. For example, the verb *'koken'* (*'to cook'*) was combined with a mismatching gesture *'slaan'* (*'to hit'*). This verb-gesture combination had no semantic or phonetic relation. See Appendix A for all verb-gesture combinations.

Video stimuli. For each verb on the list a female native Dutch speaker produced a gesture with simultaneous speech in both conditions. The actress, wearing neutral coloured clothing, was standing in front of a neutral-coloured background (see Figure 1) facing the camera placed in front of her, while producing speech-gesture combinations. We instructed the actress to create the gestures spontaneously, but made sure the gestures were iconic and representative of the action the verbs described (e.g., typing gesture resembling fingers typing on a keyboard for the verb 'to type'). We further told the actress to speak in a child-directed voice and have a neutral, but friendly, facial expression. In the mismatch condition the actress combined a verb with a mismatching gesture. The videos displayed the actress from head to knees, her hands hanging casually to the side of her body, and were recorded using the camera Canon XF205. Each video clip was edited with ELAN (Version 4.6.1, Lausberg & Sloetjes, 2009) to be 2300 ms long. In each video the preparation of the gesture started at 120 ms and the gesture lasted until the end of the video clip. The average onset of speech was around 660 ms (SD = 0.1) after the start of the video (Figure 1).

Pre-test for stimuli selection. To ensure that seven-year-old children can understand the selected gestures and can relate them to the relevant verbs,
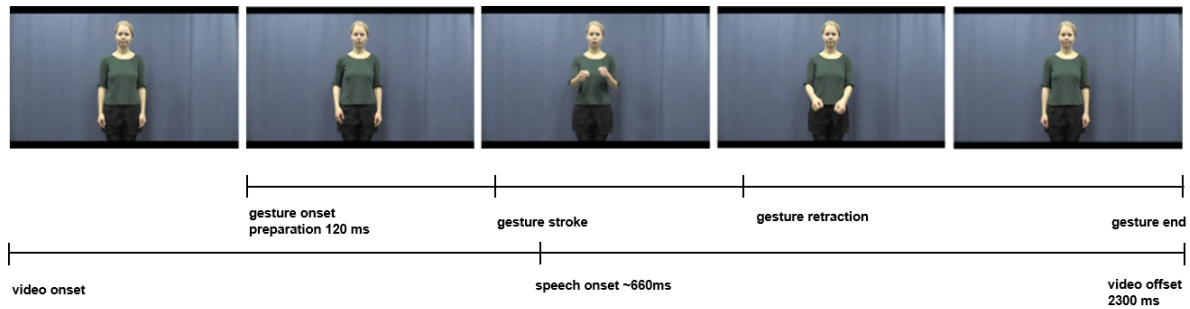
Fig. 1. Time-line of the video clip. The speech-gesture combination in this example is 'boksen' ('to box'). The gesture started 120 ms after onset of the video. The stroke (i.e., the meaningful part of the gesture) occurred before the speech onset (on average at 660 ms after video onset). Gesture retraction occurred before both the speech and the gesture ended at video offset at 2300 ms.

we conducted a pre-test at two elementary schools in the Netherlands. To this end, we tested 104 children (M_{age} = 6.74, SD = 0.64) in 8 different groups with 8 different lists, containing 43/44 items each (half match, half mismatch). Those children did not participate in the ERP experiment. The lists were carefully constructed so that no speech-gesture pair occurred twice. After children were split into smaller groups (N ranging from 11 to 14), we introduced them to our actress in the videos as 'Lore, the girl who had lost her voice'. We explained that Lore was trying to communicate particular words by using her hands only. We told the children to pay close attention to her gestures, because they would have to decide if Lore's gestures looked like a word they knew or not. In the context of this story, children were asked to watch the short video clips, presented with PowerPoint, during which Lore would perform a hand movement that was indicative of a certain verb. We presented the video clips without sound to make sure that children focused on the gesture only. After playing the video clip twice, we asked the children "Hoe erg vind je deze beweging lijken op *'boksen'*?" ("Does this gesture look like *'to box'*?"). Children had to allocate stars to Lore's performance on a scale from 1 star (not at all) to 5 stars (very much) to indicate how much the gesture represented the verb we asked the children about (see Appendix B for questionnaire). Each group had four practice items before the actual ratings to make sure children understood the rating procedure. Based on these ratings, we selected 120 verbs that fulfilled the following criteria: 1) The mean rating of match items was 3 or above (SD ± 1), and 2) the mean rating of mismatch items was of 2.6 or below (SD ± 1). To obtain a total of 120 words we had to include seven items that had larger standard deviations; These items were marked as critical to be removed from analysis if we would observe an item effect on these verbs. We

excluded four children from the final analysis due to lack of attention or their non-native language status.

Multimodal Task

EEG stimuli. The final verb list for the EEG trials consisted of 120 items selected based on the pre-test ratings, suggesting that these are the speech-gesture combinations best understood by 6 to 8-year-old children. Sixty verbs were presented in the matching condition, whereas the other 60 items were a mismatching speech-gesture combination. Each of the 120 video clips was presented only once and all combinations were counter-balanced to ensure that no gesture would occur twice (either in a match or a mismatch condition). Each trial started with a fixation-cross (500 ms), followed by a grey transition screen (500 ms, for baseline measure). The video clip was played (2300 ms), and after a short delay period (1000 ms), a fixation-cross appeared again on the screen. Each child received six practice trials (see Figure 2A).

Behavioural trials. We added 40 behavioural trials (20 match, 20 mismatch) that were presented randomly after the videos throughout the 120 video stimuli. We presented the question "Hoorde je *'boksen'*?" ("Did you hear *'to box'*?") 1000 ms after the video clip ended, and children had to respond by pressing a button. Children pressed a green button *'Ja'* (*'Yes'*) if *'boksen'* matched the verb of the EEG trial. Children pressed a red button *'Nee'* (*'No'*) if *'boksen'* mismatched the verb of the EEG trial. The mismatching target verb did not occur in the video stimuli list. If children failed to respond to the question, the following trial started after a 5000 ms delay during which a grey transition screen was presented (see Figure 2B). We selected one third of the total number of trials to have a behavioural trial. This allowed us to present the trials at randomized
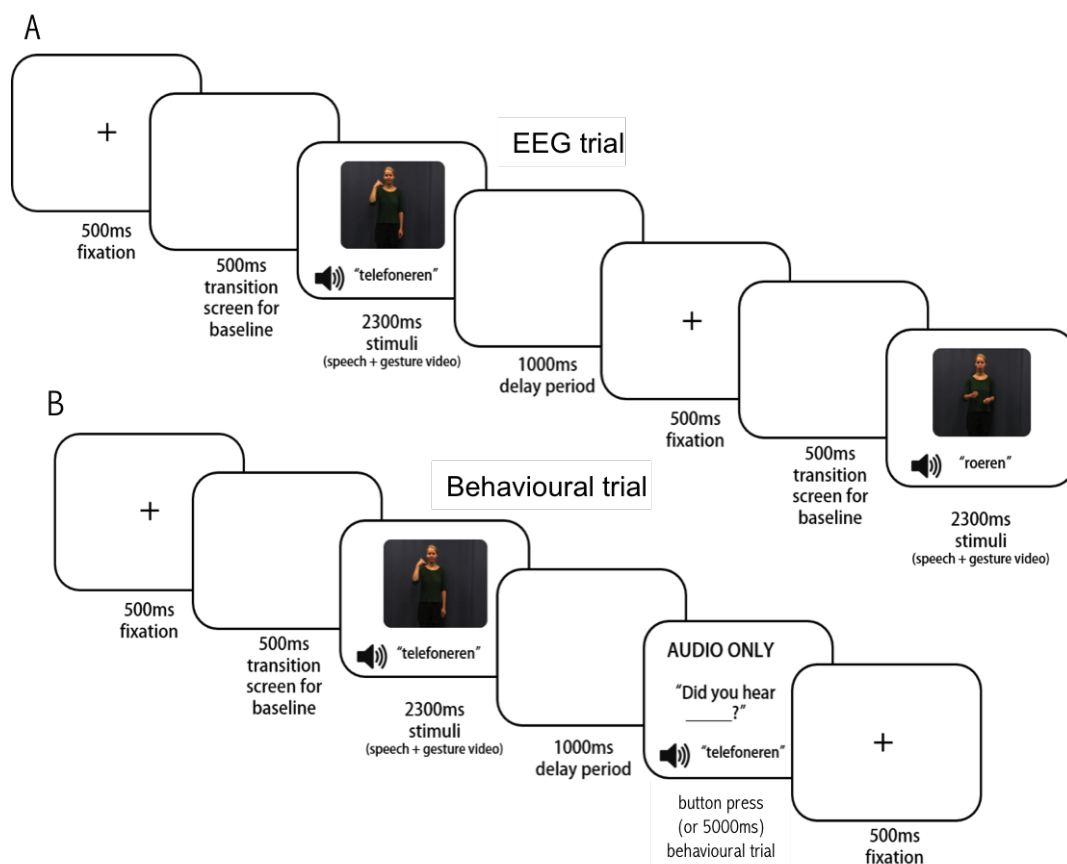
Fig. 2. Figure A shows the structure of an EEG trial. Figure B shows the structure of an EEG trial with a behavioural trial that followed 1000 ms after a video clip was played. There were no visual stimuli present when children heard a question. We measured ERPs from speech onset (~660 ms after video onset).

positions throughout the experiment without building up an expectation of a question following every (or every second) video. A further reason for 40 behavioural trials was to collect enough responses to analyse reaction times and error rates. A lower number of trials would not have been sufficient for a reliable statistical analysis. Before the start of the experiment, we presented three behavioural practice trials to make sure children understood the procedure.

Procedure

Upon arrival, we asked the participants' parents to fill out a consent from. We also asked the parents to fill out The Edinburgh Inventory of Handedness (Oldfield, 1971) and a general demographics information sheet. The child sat in front of a mirror, so s/he could see him-/herself while we fitted him/her with the EEG cap (actiCap). We prepared the cap for children before they arrived by putting the electrodes in the corresponding holes. We allowed the child to touch the electrode cap to make him/her feel comfortable, while a student assistant gave

the child a detailed step-by-step explanation of the procedure. While we put the EEG cap on the child's head and filled the electrodes with gel, the child colored lightbulbs on a sheet of paper when the electrode light switched from red to green. After the impedance check, we walked the child into an electrically and acoustically shielded room to sit in front of a computer monitor (distance between the child and the monitor was 60 cm). We asked the child to hold the two-button box like a game-controller, so the child would press the button with their left and their right thumb. Before the experiment started, we showed the child his/her brain waves on the computer monitor and demonstrated how sensitive the brain waves are to movement, blinking and chewing. Afterwards, the student assistant explained to the participant that s/he would watch short video clips of a girl uttering verbs. We instructed the participant to attentively watch and listen to the video clips and to sit as still as possible. We also explained that sometimes they would hear a question, which they would have to answer with either yes or no by pressing the corresponding button on the button box.

We presented the video stimuli on a monitor using the Presentation software (Version 19.0, Neurobehavioural Systems, inc.). Behavioural trials were presented randomly throughout the experiment and occurred after the video clip was played. Participants heard "Hoorde je *'boksen'*?" ("Did you hear *'to box'*?") and had to press a button as fast as possible (see Figure 2B). The order of the video and behavioural trials was pseudo-randomized and presented in four blocks of 40 trials, lasting around 4 minutes per block. Each block consisted of 30 video clips (15 in each condition) and 10 behavioural trials (five yes- and five no-responses). After each block, a student assistant entered the room to make sure the child would take a break. During the break, the child completed a simple maze to disengage him/her from the computer monitor. After completing the maze, the child put a stamp on a map to visualize the progress of the experiment. This allowed the child to see how many blocks were left and it encouraged him/her to stay engaged during the task. To make sure the child kept his/her eyes on the screen and watched the videos (instead of only listening to the speech), we told the child that one video might be presented in black and white. After each block, we asked the child whether s/he had spotted a black and white video. The EEG recording procedure, including the breaks, lasted around 40 minutes. After completion of the experiment, children received stickers and a certificate of participation. Parents and their children could choose their compensation. We offered €20, €10 and a children's book, or two books.

Behavioural data analysis

We analysed the behavioural data with RStudio (RStudio Team, 2015). We included only the 17 children who were also included in the EEG analyses. First, we inspected the accuracy scores of all children to remove those participants with low accuracy scores (no participants were excluded, mean accuracy 98.66%, range 92.31% - 100.00%). We removed null responses (when children failed to press a button) from the dataset. We calculated outliers from all the reaction times (RTs) and removed those data points that fell above or below two and a half standard deviations from the grand mean. This resulted in a dataset of 656 data points for the accuracy analysis. We only analysed RTs of correct responses (measured at word onset). This resulted in a dataset of 649 data points.

Because our reaction time data was not normally distributed, we log-transformed the reaction times to attenuate the non-normality. We analysed our normalized RT data with linear mixed effects models with *participants* and *items* as cross-random effects. For the analyses we considered the following factorial predictors: congruency of the speech-gesture video (*speech-gesture congruency*; 2 levels: match or mismatch), congruency of the behavioural trial (*audio congruency*; 2 levels: match or mismatch). We also considered random slopes for *audio congruency* by item. We performed a stepwise variable selection procedure to obtain the best fitting model. We added one predictor at a time and evaluated whether the model would be improved by including a certain predictor (i.e., when a predictor was not part of the model our current model assumed to have a lower AIC). The final model contained the following predictors: *Trial, speech-gesture congruency, audio congruency* and a random slope for *audio congruency* by item.

EEG data acquisition and analysis

We recorded the EEG continuously throughout the experiment from 32 Ag/AgCl electrodes. Twenty-seven electrodes were mounted in a cap according to the 10-20 international system, four electrodes were used for bipolar horizontal and vertical electrooculograms (EOG) and one electrode was placed on the right mastoid. The reference electrode was placed on the left mastoid and re-referenced offline to the average of the left and right mastoid electrodes. Electrode impedance was kept below 5 KΩ. The EEG was filtered through a 0.02 – 100 Hz band-pass filter and digitized on-line with a sampling frequency of 500 Hz (BrainVision Recorder, Brain Products, Gilching, Germany).

We pre-processed the EEG data with BrainVision Analyzer (Version 2.1.1, Brain Products, Gilching, Germany). First, we re-referenced the EEG data offline to the average of the left and right mastoid and filtered the data with a high-pass filter at 0.01 Hz and a low-pass filter at 35 Hz. We further segmented the data into epochs from 200 ms before to 1000 ms after the onset of the videos. After a semi-automatic artifact rejection routine removing only muscle-related artifacts, we rejected eye-movement artifacts using an ocular independent component analysis (ICA). The mean number of analysable trials was 34 ($SD = 7.44$) for matching trials and 34 ($SD = 8.55$) for mismatching trials. On average, we excluded 41% of the trials for each participant (49/120). We excluded four participants from analyses due to an insufficient sum of artefact-free trials and one

participant due to hardware malfunction.

We calculated the time-locked average (time-locked to speech onset) for each condition of the remaining trials for each participant to obtain the ERPs in the time window 0 to 1000 ms. To evaluate the differences between the matching and the mismatching condition we used a non-parametric cluster-based permutation test (Maris & Oostenveld, 2007) and analysed our data using the Fieldtrip toolbox (Oostenveld, Fries, Maris, & Schoffelen, 2011) running under MATLAB (Mathworks, Natick, MA).

In the cluster-based permutation test, t-values for every data point of each condition were calculated to determine which data points exceeded the pre-set threshold of 0.05. All adjacent data points exceeding this threshold were considered and grouped into clusters. The t-values in each cluster were summed to calculate the cluster-level statistics. Further, the significance probability was calculated by means of the Monte-Carlo permutation. To calculate this, a participant's time-locked average is randomly assigned (5000 times) to one of the two conditions to calculate the largest cluster-level statistic for every permutation. The highest cluster-level statistic from each randomized calculation was entered into the Monte-Carlo permutation distribution and cluster-level statistics were calculated for the data. The statistics were then compared against this permutation distribution. Only those clusters that fell into the highest or lowest 2.5th percentile of the distribution were considered significant (see Maris & Oostenveld, 2007).

Results

Behavioural results

The children in our study showed accuracy means ranging from 92% to 100% (Table 1), suggesting that children performed at ceiling. Because there was no variation in our data with respect to accuracy, the linear mixed effects model could not be fitted (due to convergence errors), and we used a two-way repeated measure analysis of variance (ANOVA). We did not observe a significant main effect in the accuracy scores (*speech-gesture congruency* $F(1,16)$ = 1.247, p = .28; *audio congruency* $F(1,16)$ = 0.146, p = .71) and no significant interaction (*speech-gesture congruency * audio congruency* $F(1,16)$ = 0.128, p = .72).

In contrast to what had been hypothesized, we observed a main effect of RTs in *audio congruency* (Table 2). These results show that children were significantly faster in responding to words that matched the speech of the previous video clip. However, there was no significant interaction between *audio congruency* and *speech-gesture congruency* (this interaction was removed from the final model), indicating that children in our study were able to allocate their attention to one modality when asked to do so. The final model of RTs revealed a significant effect of *Trial*, showing that children's RTs became faster during the experiment. In addition, the model suggested that items showed a different sensitivity in response to *audio congruency*. We report the relevant statistics and corresponding coefficients of the final model in Table 3.

Table 1.

Mean accuracy scores and standard errors in parentheses.

		Audio congruency (behavioural trials)	
		Match	Mismatch
Speech-gesture congruency	Match	0.988 (0.009)	0.982 (0.010)
	Mismatch	0.993 (0.006)	0.994 (0.006)

Table 2.

Mean RT scores and standard errors in parentheses.

		Audio congruency (behavioural trials)	
		Match	Mismatch
Speech-gesture congruency	Match	1237.09 (24.82)	1423.37 (26.31)
	Mismatch	1253.73 (23)	1411.21 (27.77)

Table 3.

Summary of the model predicting RTs. Note. $t < -1.96$ and $t > 1.96$ is significant, printed in bold. For speech-gesture congruency we used congruent as the reference in the intercept; for audio congruency we put congruent in the intercept.

Predictor	β	Standard error	t
Intercept	7.060	0.033	**216.47**
Trial	-0.084	0.012	**-7.11**
Speech-gesture congruency	0.001	0.017	0.08
Audio congruency	0.138	0.018	**7.64**
Random effects	**Var.**	**Standard deviation**	
Item (intercept)	0.011	0.102	
Item (Audio congruency)	0.005	0.074	
Participant (intercept)	0.013	0.116	
Residual	0.036	0.190	

EEG results

We included the entire time window (0 ms at speech onset to 1000 ms) for the EEG data analysis. The ERPs of both conditions were time-locked to the speech onset and we compared the data of both conditions of all 17 participants. The cluster-based permutation test revealed two significant clusters in the time windows from 80 ms to 300 ms and from 326 ms to 562 ms after speech onset and showed a significant difference between the matching and the mismatching conditions ($p<.05$). However, these clusters only reached significance in a two-tailed test ($\alpha = 0.05$). As a second step, we selected a pre-defined time window for the N400 analysis based on previous work in semantic integration research (Holcomb et al., 1992). This time window was chosen based on visual inspection and previous research on speech-gesture integration in adults investigating the N400 effect (Drijvers & Özyürek, submitted; Habets et al., 2011).When we selected the time window from 300 ms to 600 ms after speech onset, a one-
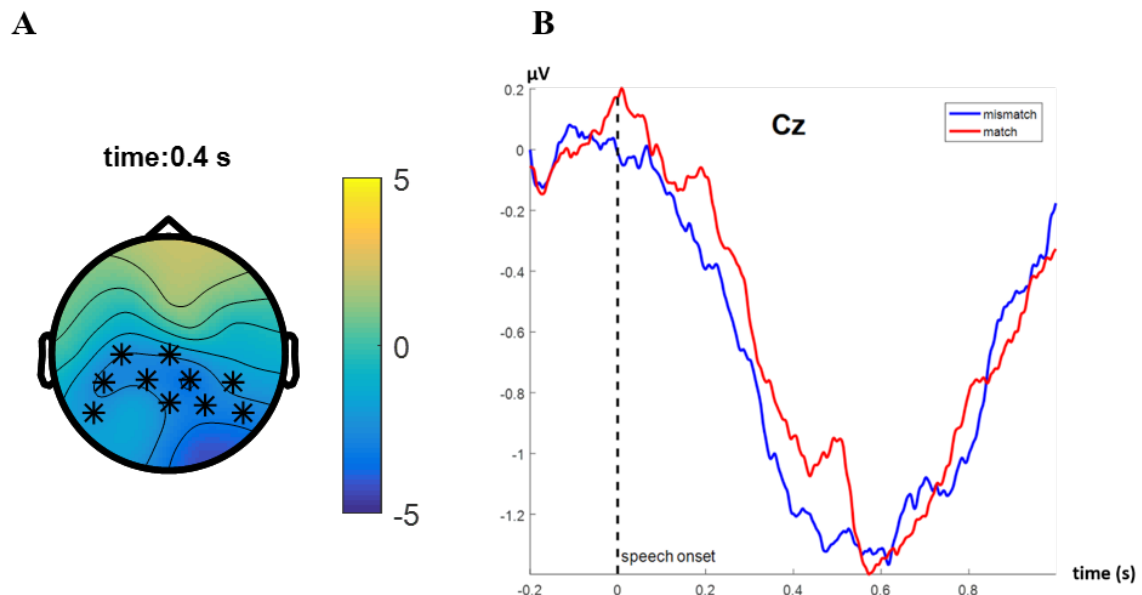

Fig. 3. Figure A shows the topoplot of the significant effect at 400 ms after speech onset. The significant electrodes at this time-point were C3, Cz, CP5, CP1, CP2, CP6, P7, Pz, P4 and P8. Figure B shows the grand average waveforms for ERPs elicited in the match (red) and mismatch (blue) condition at electrode Cz. Negativity is plotted downward. Waveforms are time-locked to 200 ms before speech onset (baseline).

tailed test revealed one significant cluster between 326 ms and 562 ms after speech onset ($p<.025$). The plots in Figure 3A show that the N400 effect was larger for the mismatching videos compared to the matching videos and was more pronounced over central-parietal electrodes. The electrodes showing significance based on the cluster-based permutation test in the time window 300-600 ms were Cz (plotted in Figure 3B), C3, CP5, CP1, CP2, CP6, P7, Pz, P4 and P8 (see Figure 3A).

Discussion

The aim of our study was to investigate seven-year-old children's ability to integrate iconic gestures that co-occur with speech during online language comprehension. Offline behavioural measures about speech-gesture integration allow us to assume that five-year-old children are able to process multimodal information. There is evidence of five to seven-year-old children's ability to semantically integrate linguistic information, as indicated by an N400 effect to linguistic information of a sentence that mismatches its preceding context. Despite these behavioural findings, and Dick et al.'s (2012) report on the neural sensitivity to co-speech gestures in eight-year-old children, it remains unclear as to how seven-year-old children process gestures that simultaneously occur with speech on a neural level. In the present study, we therefore investigated the brain activity underlying speech-gesture integration processes in seven-year-old children. To this end, we examined the amplitude of children's brain activity in response to gestures that either matched or mismatched simultaneous speech presented in short video clips. We were specifically interested in the N400 component, which we expected to have increased amplitude in response to mismatching videos, and would suggest semantic integration of multimodal information.

We observed a significant congruency effect of gestures mismatching simultaneous speech 300-600 ms after speech onset (see Figure 3) during an analysis with a pre-defined time window. If, however, we consider the entire time window in our analysis, we observe two significant clusters only when using a two-sided test. It may be possible that the N400 effect starts very early (at speech onset), if participants were able to predict the upcoming word based on meaningful information in the gesture that preceded speech. However, given that we do not see such an early effect in adults (Drijvers & Özyürek, submitted), the effect observed in our data may

have had a different cause. This early effect could be driven by the choice of our baseline window, which was selected to be 200 ms before the speech onset (instead of before video onset). However, during this period children are already exposed to hand movements on the video clips, as the gesture preparation starts before the speech onset. Future analysis should consider a baseline window before the video onset, where no movement occurs and a potential influence of such movements on brain activity could be dismissed.

Nevertheless, if we choose the time window based on previous literature to investigate our data in the pre-defined time window of 300-600 ms after speech onset, our findings are in line with previous research investigating gesture integration with single action verbs in adults, where a more negative amplitude for gestures that mismatched the co-occurring verb was observed (Drijvers & Özyürek, submitted; Habets et al., 2011). Our findings further extend to findings investigating congruency effects in a sentence context (Kelly et al., 2004; Özyürek et al., 2007; Wu & Coulson, 2007). We show that the auditory and visual information communicated through two modalities is processed and integrated simultaneously with speech in children similarly to adults. The effect we observed at the centro-parietal electrodes is similar in topography and time-course to the N400 observed in Drijvers and Özyürek (submitted), suggesting that integration processes in children may be similar to those observed in adults. Moreover, the N400 effect observed in response to words or pictures that mismatch the preceding context in linguistic priming tasks also mirrors our findings during unimodal semantic integration (Atchley et al., 2006; Benau et al., 2011; Holcomb et al., 1992). However, our findings go beyond unimodal integration and we were able to show that semantic integration difficulties do not only occur during information processing of the auditory modality, but are apparent when information is communicated via two modalities. As the N400 effect we observe to speech-gesture integration in children is apparent in the same time window as in linguistic semantic priming studies, we believe that linguistic semantic integration and multimodal (speech-gesture) integration are strongly related processes.

Although we cannot provide an explanation for the significant divergence of matching vs. mismatching brain activity occurring at speech onset, we can speculate that the gestures contained meaningful information that allowed the children to guess the upcoming words, which may have led

to an early N400 effect. Additionally, the gestures in our study were both observational (e.g., *'groeien'* - *'to grow'*) and action (e.g. *'kloppen'* - *'to knock'*). It may be that gestures that are performed by the children themselves are understood more easily and processed faster than observational gestures. This may have led to early processing of specific gestures and may relate to the early effect we observed at speech onset. Moreover, regarding speech, the initial phoneme or the first syllable of individual words may have played a role. In some cases, it may be easier to decide which word was heard based on the first few phonemes (e.g. *'drinken'* – *'to drink'*), whereas other words that had either two or three syllables or an affix (e.g. *'afwassen'* – *'to do the dishes'*) may have required more phonemes or syllables to be recognizable. This effect may share some similarity with the P2 component assumed to reflect phonological processing of speech information (Dorman, 1974). It is, however, unclear why we observe this early effect. Nevertheless, we are not the first to observe this early effect of divergence at the speech onset (Kelly et al., 2004).

Our findings are novel because no study has investigated the time course of neural processes underlying speech-gesture integration in children and we are able to show strong neural evidence for a tight link between gesture and speech integration during children's language comprehension. Our results further support the integrated systems hypothesis and expand the theory to include children (Kelly et al., 2010). The tight link between speech and gesture in language production is already apparent in young infants, as they rely on speech-gesture combinations to communicate. Although we are not sure when the integration of speech-gesture combination during language comprehension develops, we provide evidence that a mismatching gesture appears to be disruptive for language processing on a neural level in seven-year-old children and that integration of speech and gesture has already developed. Seven-year-old children display adult-like activities in how their brain processes and integrates gestures to speech, and it may be interesting to investigate at what age we cannot observe neuroscientific evidence of online processing abilities.

The observed effect in our study shows that our brains are sensitive to semantically mismatching information at a relatively early age. Although the behavioural task in our study biased children's attention to the speech, children cannot help but consider both the visual and auditory modalities when processing a multimodal message online, as indicated by the N400 effect. Children were, however, able to focus their attention to only the spoken modality when specifically instructed to do so. Our behavioural results suggest that children were able to 'ignore' the visual mode when we asked them to give a behavioural response on whether they had heard a word, and the ERPs still showed an integration effect of gesture. Seven-year-old children were particularly accurate in making offline choices about our stimuli, and they appear to be capable of giving an accurate response. Although children quickly learned how to respond to a question during our experiment, they still had to stay attentive, as not every video was followed by a question. The fact that children performed at ceiling and were able to stay focused until the end of the experiment suggests advanced cognitive development in seven-year-olds. It seems that our behavioural task was easy for children, and a measure for cognitive control may have revealed children's executive function and self-regulation abilities. Future studies should also include tasks that allow for investigations of children's working memory, mental flexibility and cognitive control abilities. Such measures could have provided more insight about children's ability to consciously keep and allocate their attention in our study.

With our study we are able to provide ecologically valid results of neural activity showing that semantic integration of gestures takes place immediately and simultaneously in relation to speech in children. Additionally, we are able to present evidence that seven-year-old children may process speech and gesture in a similar way to adults. Although we are not able to draw inferences about when the ability to integrate iconic co-speech gestures develops, we are able to show that seven-year-old children can automatically integrate information that is presented via two different modalities. An advantage of ERPs is the detailed temporal information about the unfolding of speech-gesture integration processes, both in adults and in children. The temporal synchrony of multimodal processing may suggest that gestures not only aid our comprehension of a message, but also puts forward that gestures are strongly integrated into our understanding of a message. Iconic gestures are processed semantically and neural processes of speech-gesture combinations rely on overlapping resources in the brain similar to those involved in semantic processing of speech (Drivers & Özyürek, submitted; Kelly et al., 2010; Özyürek et al., 2007). Therefore, our brain processes and interprets iconic gestures to be an equally relevant communicative component of language comprehension. Gestures appear to affect and improve the conceptual understanding of a message.

Given that the integration of gestures to speech is apparent in seven-year-old children, multimodal communication may be a powerful tool to enhance comprehension in educational settings. We can use this knowledge and build on the fact that co-speech gestures in natural conversation start simultaneously with co-expressive words (Goldin-Meadow, 2003; Hostetter, Bieda, Alibali, Nathan, & Knuth, 2006; Kelly, Kravitz, & Hopkins, 2004; Kendon, 2004; Kita & Özyürek, 2003; McNeill, 1992).

Future research could utilize the neuroscientific results we are presenting and investigate how children with language disorders may process simultaneous speech-gesture combinations. Co-speech gestures are an inevitable part of human communication, and we may be able to use this naturally occurring phenomenon to improve communication with children with language disorders or other developmental challenges.

Conclusion

Children develop an understanding of gestures as a communicative function from an early age and integrating both gesture and spoken language is a necessary aspect for simultaneous processing of multimodal communication. Our study provides important methodological implications for the investigation of children's ability to comprehend multimodal communications. Based on our findings, we can conclude that the ability to process iconic gestures co-occurring with speech is a skill that has fully developed in seven-year-old children. The simultaneous presentation of audiovisual language may closely relate to real-world language use and may aid the development of strategies to improve communication with children in educational settings. Our findings further support the claim that human language is complex and multimodal, and that gestures have the potential to greatly contribute to language comprehension not only in adults, but also in children.

Acknowledgements

References

Atchley, R. A., Rice, M. L., Betz, S. K., Kwasny, K. M., Sereno, J. A., & Jongman, A. (2006). A comparison of semantic and syntactic event related potentials generated by children and adults. *Brain and Language*, *99*(3), 236–246.

Bacchini, S., Boland, T., Hulsbeek, M., Pot, H., & Smits, M. (2005). *Een gefundeerde woordenlijst gefaseerd naar verwerving Duizend-en-een-woorden.*

Bates, E., Benigni, L., Bretherton, I., Camaioni, L., & Volterra, V. (1979). Relationships between cognition, communication, and quality of attachment. In *The emergence of symbols: Cognition and communication in infancy* (pp. 223–269).

Behne, T., Carpenter, M., & Tomasello, M. (2005). One-year-olds comprehend the communicative intentions behind gestures in a hiding game. *Developmental Science*, *8*(6), 492–499.

Behne, T., Liszkowski, U., Carpenter, M., & Tomasello, M. (2012). Twelve-month-olds' comprehension and production of pointing. *British Journal of Developmental Psychology*, *30*, 359–375.

Benau, E. M., Morris, J., & Couperus, J. W. (2011). Semantic processing in children and adults: Incongruity and the N400. *Journal of Psycholinguistic Research*, *40*, 225–239.

Brain Products. (n.d.). BrainVision. Gilching, Germany.

Butcher, C., & Goldin-Meadow, S. (2000). Gesture and the transition from one- to two-word speech: When hand and mouth come together. In D. McNeill (Ed.), *Language and Gesture* (pp. 235–258). Cambridge: Cambridge University Press.

Carpenter, M., Nagell, K., Tomasello, M., Butterworth, G., & Moore, C. (1998). Social cognition, joint attention, and communicative competence from 9 to 15 months of age. *Source: Monographs of the Society for Research in Child Development*, *63*(4), 1–174.

DeBoer, T., Scott, L. S., & Nelson, C. A. (2005). Event-related potentials in developmental populations. In Handy Todd. (Ed.), *Methodological handbook for research using event-related-potentials.* (pp. 263–297). Cambridge, MA: TheMIT Press.

Dick, A. S., Goldin-Meadow, S., Solodkin, A., & Small, S. L. (2012). Gesture in the developing brain. *Developmental Science*, *15*(2), 165–180.

Drijvers, L., & Özyürek, A. (2016). Visual context enhanced: The joint contribution of iconic gestures and visible speech to degraded speech comprehension. *Journal of Speech, Language and Hearing Research*, *60*(1), 212–222.

Furman, R., Küntay, A. C., & Özyürek, A. (2014). Early language-specificity of children's event encoding in speech and gesture: Evidence from caused motion in Turkish. *Language, Cognition and Neuroscience*, *29*(5), 620–634.

Goldin-Meadow, S. (2003). *Hearing gesture: How our hands help us think*. Belknap Press of Harvard University Press.

Goldin-Meadow, S., & Butcher, C. (2003). Pointing toward two-word speech in children. In K. Sotaro (Ed.), *Pointing: Where language, culture, and cognition meet* (p. 339).

Greenfield, P. M., & Smith, J. H. (1976). *The structure of communication in early language development*. Academic Press.

Habets, B., Kita, S., Shao, Z., Özyurek, A., & Hagoort, P. (2011). The role of synchrony and ambiguity in speech–gesture integration during comprehension. *Journal of Cognitive Neurscience*, *23*(8), 1845–1854.

Hagoort, P., & Van Berkum, J. (2007). Beyond the sentence given. *Philosophical Transactions of the Royal Society*, (362), 801–811.

Holcomb, P. J., Coffey, S. A., & Neville, H. J. (1992). Visual and auditory sentence processing: A developmental analysis using event-related brain potentials. *Developmental Neuropsychology*, *8*(2–3), 203–241.

Hostetter, A. B., Bieda, K., Alibali, M. W., Nathan, M. J., & Knuth, E. J. (2006). Don't just tell them, show them! Teachers can intentionally alter their instructional gestures. *Proceedings of the Annual Meeting of the Cognitive Science Society, 28*.

Hrabic, M. L., Williamson, R. A., & Özçalışkan, Ş. (2014). How early do children understand iconic co-speech gestures conveying action? *Proceedings Supplement for 38th Boston University Conference on Language Development*.

Igualada, A., Bosch, L., & Prieto, P. (2015). Language development at 18 months is related to multimodal communicative strategies at 12 months. *Infant Behaviour and Development*, *39*, 42–52.

Iverson, J. M., & Goldin-Meadow, S. (n.d.). Gesture paves the way for language development.

Kelly, S. D., Barr, D. J., Church, R. B., & Lynch, K. (1999). Offering a hand to pragmatic understanding: The role of speech and gesture in comprehension and memory. *Journal of Memory and Language*, *40*, 577–592.

Kelly, S. D., Kravitz, C., & Hopkins, M. (2004). Neural correlates of bimodal speech and gesture comprehension. *Brain and Language*, *89*, 253–260.

Kelly, S. D., Özyürek, A., & Maris, E. (2010). Two sides of the same coin: Speech and gesture mutually interact to enhance comprehension. *Psychological Science*, *21*(2), 260–267.

Kelly, S., Healey, M., Özyürek, A., & Holler, J. (2015). The processing of speech, gesture, and action during language comprehension. *Psychon Bull Rev*, *22*(22), 517–523.

Kendon, A. (2004). *Gesture: vVisible action as utterance*. Cambridge University Press.

Kita, S. (2003). Pointing: A foundational building block of human communication. In *Pointing: Where Language, Culture, and Cognition Meet* (pp. 1–9).

Kita, S., & Özyürek, A. (2003). What does cross-linguistic variation in semantic coordination of speech and gesture reveal?: Evidence for an interface representation of spatial thinking and speaking. *Journal of Memory and Language*, *48*, 16–32.

Kutas, M., & Federmeier, K. D. (2011). Thirty years and counting: Finding meaning in the N400 component of the event-related brain potential (ERP). *Annual Review of Psychology*, *62*(1), 621–647.

Kutas, M., & Hillyard, S. A. (1980). Reading between the lines: Event-related brain potentials during natural sentence processing. *Brain and Language*, *11*(2), 354–373.

Kutas, M., & Hillyard, S. A. (1984). Brain potentials during reading reflect word expectancy and semantic association. *Nature*, *307*(5947), 161–163.

Lausberg, H., & Sloetjes, H. (2009). Coding gestural behaviour with the NEUROGES-ELAN system. *Behaviour Research Methods*, *4*(3), 841–849. Retrieved from http://tla.mpi.nl/tools/tla-tools/elan/

Liszkowski, U., Albrecht, K., Carpenter, M., & Tomasello, M. (2008). Infants' visual and auditory communication when a partner is or is not visually attending. *Infant Behaviour and Development*, *31*(2), 157–167.

Maris, E., & Oostenveld, R. (2007). Nonparametric statistical testing of EEG- and MEG-data. *Journal of Neuroscience Methods*, *164*(1), 177–190.

Mathworks. (n.d.). Natick, MA.

McNeil, N. M., Alibali, M. W., & Evans, J. L. (2000). The role of gesture in children's comprehension of spoken language: Now they need it, now they don't. *Journal of Nonverbal Behaviour*, *24*(2).

McNeill, D. (1992). *Hand and Mind: What Gestures Reveal about Thought*. University of Chicago Press.

Namy, L. L., Campbell, A. L., & Tomasello, M. (2004). The changing role of iconicity in non-verbal symbol learning: A U-shaped trajectory in the acquisition of arbitrary gestures. *Journal of Cognition and Development*, *5*(1), 37–57.

Namy, L. L., & Waxman, S. R. (1998). Words and gestures: Infants' interpretations of different forms of symbolic reference. *Child Development*, *69*(2), 295–308.

Olfield, R. C. (1971). The assessment and analysis of handedness: The Edinburgh Inventory. *Neuropsychologia*, *9*, 97–113.

Oostenveld, R., Fries, P., Maris, E., & Schoffelen, J.-M. (2011). FieldTrip: Open source software for advanced analysis of MEG, EEG, and invasive electrophysiological data. *Computational Intelligence and Neuroscience*, *2011*, 156869.

Özçaliskan, S., & Goldin-Meadow, S. (2005). Do parents lead their children by the hand? *Journal of Child*

Language, *32*(3), 481.

Ozçalışkan, S., & Goldin-Meadow, S. (2009). When gesture-speech combinations do and do not index linguistic change. *Language and Cognitive Processes*, *24*(2), 190.

Özçalışkan, Ş., & Goldin-Meadow, S. (2005). Gesture is at the cutting edge of early language development. *Cognition*, *96*, B101–B113.

Özçalışkan, Ş., & Goldin-Meadow, S. (2011). Integrating Gestures: The interdisciplinary nature of gesture. In G. Stam & M. Ishino (Eds.), *Integrating Gestures: The Interdisciplinary Nature of Gesture* (pp. 163–174). Amsterdam/Philadelphia: John Benjamins Publishing Company.

Özyürek, A., Kita, S., Allen, S., Brown, A., Furman, R., & Ishizuka, T. (2008). Development of cross-linguistic variation in speech and gesture: Motion events in English and Turkish. *Developmental Psychology*, *44*(4), 1040–1054.

Özyürek, A., Willems, R. M., Kita, S., & Hagoort, P. (2007). On-line integration of semantic information from speech and gesture: Insights from event-related brain potentials. *Journal of Cognitive Neurscience*, *19*(4), 605–616.

Pijnacker, J., Davids, N., Van Weerdenburg, M., Verhoeven, L., Knoors, H., & Van Alphen, P. (2017). Semantic processing of sentences in preschoolers with specific language impairment: Evidence from the N400 effect. *Journal of Speech, Language and Hearing Research*, *60*(3), 627–639.

RStudio Team. (2015). RSudio: Integrated Development for R. Boston, MA: RStudio, Inc. Retrieved from http://www.rstudio.com

Schaerlaekens, A. M., Kohnstamm, G. A., Lejaegere, M., & Vries, A. K. (1999). *Streeflijst woordenschat voor zesjarigen: Gebaseerd op nieuw onderzoek in Nederland en België*. Swets & Zeitlinger.

Sekine, K., Sowden, H., & Kita, S. (2015). The development of the ability to semantically integrate information in speech and iconic gesture in comprehension. *Cognitive Science*, *39*, 1855–1880.

Sheehan, E. A., Namy, L. L., & Mills, D. L. (2007). Developmental changes in neural activity to familiar words and gestures. *Brain and Language*, *101*, 246–259.

Stanfield, C., Williamson, R., & Özçalışkan, S. (2013). How early do children understand gesture- speech combinations with iconic gestures? *Journal of Child Language*, *41*(2), 1–10.

Talmy, L. (2000). *Toward a Cognitive Semantics* (1st ed.). United States: MIT Press.

Wu, Y. C., & Coulson, S. (2007). How iconic gestures enhance communication: An ERP study. *Brain and Language*, *101*, 234–245.

Predictive Processing in Adolescents with Autism Spectrum Disorder

Ricarda Florine Weiland[1]
Supervisors: Sabine Hunnius[1], Harold Bekkering[1], Jan K. Buitelaar[2,3]
Additional supervisors: Emma Ward[1], Ricarda Braukmann[1]

[1]*Donders Institute for Brain, Cognition and Behaviour, Radboud University Nijmegen, P.O. Box 9104, 6500 HE Nijmegen, The Netherlands*
[2]*Department of Cognitive Neuroscience, Donders Institute for Brain, Cognition and Behaviour, Radboud University Medical Centre, Nijmegen, The Netherlands*
[3]*Karakter Child and Adolescent Psychiatry University Centre, Nijmegen, The Netherlands*

The present study investigated a recently proposed theory of Autism Spectrum Disorder (ASD) in a previously untested age range. The theory puts ASD in a predictive processing framework, posing that individuals with ASD show impairments in predictive processing. Namely, individuals with ASD rely less on prior expectations and more on immediate sensory input, resulting in a more veridical perception. This theory was tested in an adolescent population with ASD and typically developing controls using two tasks: an adaptation task aimed at assessing differences in perception biased by expectation, using a behavioural eye gaze classification task. And secondly, an action prediction task aimed at assessing the ability to make predictions about others' everyday actions, using neurophysiological and eye tracking data. Results of the adaptation task clearly show a more veridical perception in the ASD compared to the control group. Some eye tracking results from the action prediction task also speak for differences in the ability to make predictions but neurophysiological results did not show such a difference. Although some serious limitations were identified, these findings provide valuable evidence for the predictive processing accounts of ASD by extending the previously tested age range.

Keywords: autism spectrum disorder, EEG, predictive processing, adolescents

---

Corresponding author: Ricarda Florine Weiland**;** **E-mail:** Ricarda.weiland@gmail.com

Autism Spectrum Disorder (ASD) is a neurodevelopmental disorder with a wide range of symptoms. The most prominent impairments are in the social domain, such as difficulties in verbal and non-verbal communication. However, individuals with ASD also show symptoms in nonsocial domains, such as rigid behaviours and hypo- or hypersensitivity to sensory input (American Psychiatric Association, 2013). Classically, neurocognitive theories about ASD focused on either the social or the nonsocial aspect of ASD (eg. Boucher, 1989; Happé & Frith, 2006). As a result, no theory so far has been able to capture all symptoms. Recently, however, a promising new theory has been put forward; the Predictive Processing account of ASD (Pellicano & Burr, 2012; Van De Cruys et al., 2014). Proponents claim that this framework can explain the whole range of symptoms (Van De Cruys et al., 2014). However, although some studies have already found evidence for this theory (eg. Pellicano, Jeffery, Burr, & Rhodes, 2007; Turi et al., 2015), two important questions remain open: First, studies investigating predictive processing in ASD have found different results in children compared to adults with ASD. A reconciliation from a developmental perspective is missing. Second, predictive processing is operating on different hierarchical levels, such as low-level versus high-level visual processes. Whether there are differences in how these levels are affected in ASD has not yet been investigated. These two questions will be approached in this study, by investigating an adolescent population with ASD using two tasks of predictive processing operating on different hierarchical levels.

Predictive Processing

Predictive processing is a model unifying many different brain functions, such as perception and motor control in one framework (Friston, 2010). The key claim of predictive processing is that the brain predicts future sensory input based on knowledge in a probabilistic manner by assigning prior probabilities to expectations. Therefore, world knowledge and expectations shape perception. World knowledge is organized in generative models that are constantly being updated to match the world best (Clark, 2013). From these generative models, predictions are formed about future sensory input. This happens in a hierarchical manner: more abstract, high-level predictions lead to more concrete, low-level predictions (Clark, 2013). An example for a (visually) high-level prediction would be what your

whole house looks like, whereas the texture of your house's walls would be a (visually) low-level prediction. At first the high-level prediction (your house) is activated, this in turn leads to a top-down cascade of activations of low-level predictions (eg. texture of the walls).

The generative models are constantly updated by comparing them with the actual sensory input (Clark, 2013). When the prediction does not match the sensory input, a prediction error occurs. This prediction error can result in an updating of the generative model but should only do so if the prediction error carries relevant information about the world (Kwisthout, Bekkering, & van Rooij, 2017). Often, prediction errors are merely the result of some sensory noise (eg. you forgot your glasses and cannot see your house properly), or some random variation in the environment (eg. it is raining and your percept of the house is blurred). In this case, prediction errors are irreducible and should not lead to an updating of the generative model. In other cases, however, prediction errors reflect a systematic change in the environment (eg. your house got painted). In this case, the prediction errors are reducible by updating the generative model.

Predictive processing has been computationally formalized in a Bayesian framework, where predictions and prediction errors are operationalized by conditional probability density functions (see Fig. 1). Prior knowledge and incoming sensory information can be represented as distributions of probability. The maximum of a distribution represents the event with the highest probability, and the amount of variance represents its precision. A broad prior distribution (see Fig. 1B) reflects a very unspecific expectation. This is, for instance, the case when situations are unfamiliar, such as when entering a friend's house for the first time. One does expect a living room and a kitchen, but the location, size and other details are still unknown. However, when entering a familiar house, one has very specific and precise predictions about these details.

Predictive Processing in ASD

Multiple research groups have suggested explaining ASD with the predictive processing framework (Pellicano & Burr, 2012; Sevgi et al., 2016; Sinha et al., 2014; Van de Cruys et al., 2014). Although there are some small differences between the individual accounts, a common proposal is that individuals with ASD rely to a lesser extent on their previous knowledge and to a bigger extent on their
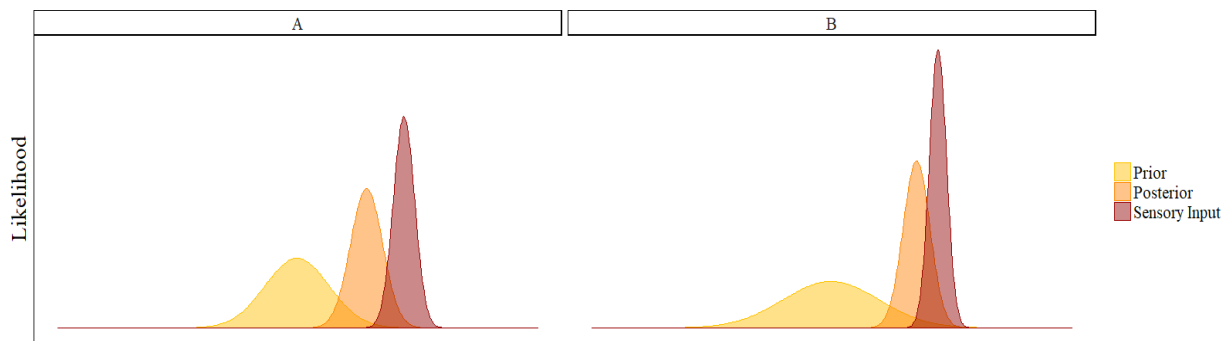
Fig. 1. Visualization of Predictive Processing Using Conditional Probability Density Functions. **A.** In typical individuals, the distribution of the sensory input is shifted towards the prior distribution of expectations. The resulting posterior distribution, or subjective percept, is therefore a weighted combination between the two distributions. **B.** In individuals with ASD the posterior distribution is closer to the distribution of the sensory input. This can be either to a flatter prior distribution, or a more precise sensory input, or both, as depicted. (Figure adapted from Brock, 2012).

immediate sensory input. As a result, perception in individuals with ASD is more veridical. Although this framework is mainly about perception in ASD, some authors argue that these changes in perception can lead to other symptoms, for example, in the social domain (Van De Cruys et al., 2014). Social situations are one of the most complex situations in everyday life. Perceptual input in social situations is particularly noisy and has to be interpreted with regard to many different contexts and background knowledge (Van de Cruys et al., 2014). However, since this knowledge is weighted less, and the (exceptionally noisy) sensory input is weighted more, individuals with ASD should (and do) show exceptional difficulties in interpreting social situations and building reliable generative models (Van de Cruys et al., 2014). This, in turn, leads to abnormal behaviour in social situations or put differently: it leads to social symptoms.

However, bridging the gap from rather simple aberrations in perception to very complex symptoms in the social domain has proven difficult. Studies investigating predictive processing in ASD have so far focused on investigating low-level perceptual processes, for example with adaptation paradigms (eg. Pellicano, Jeffery, Burr, & Rhodes, 2007; Turi et al., 2015). Only a few studies have also investigated high-order social processes, such as action prediction (Chambon et al., 2017; Falck-Ytter, 2010; Schuwerk, Sodian, & Paulus, 2016). In this study, these two tasks will be used: an adaptation task to investigate low-level perceptual processes and an action prediction paradigm to investigate high-level social processes.

Adaptation in ASD

Adaptation is the process of changing the

perception based on previous experiences and predictions. Since this influence of expectations has been hypothesised to be smaller in ASD, this makes adaptation an ideal paradigm to study differences between individuals with ASD and typically developing individuals (TDs).

In adaptation tasks, the repeated presentation of stimuli that share a specific feature (eg. faces with the same gaze direction) induces an expectation of this particular feature in stimuli. For example, when repeatedly presented with face stimuli that look to the right, one learns to expect faces with that particular gaze direction. The later perception of a deviant stimulus (eg. a face looking straight ahead) is influenced by that expectation and is biased towards the opposite gaze direction (slightly to the left, in this example). The extent to which the expectation influences perception is called the adaptation after-effect, and can be quantified by comparing a behavioural or neurophysiological response to the test stimulus with or without a previous adaptation phase (Nordt, Hoehl, & Weigelt, 2015).

Studies investigating the adaptation effect in children with ASD have repeatedly found that their adaptation after-effect is decreased in comparison to TD controls (Ewing, Pellicano, & Rhodes, 2013; Pellicano, Jeffery, Burr, & Rhodes, 2007; Turi et al., 2015). Surprisingly, studies investigating adaptation effects in adults have found no difference between adults with ASD and TDs (eg. Cook, Brewer, Shah, & Bird, 2014; Walsh, Vida, Morrisey, & Rutherford, 2015; Walsh, Vida, & Rutherford, 2014). Some have argued that the difference in perceptual processing leading to a reduced adaptation after-effect can be overcome during development (Nordt et al., 2015). This would also explain why children with ASD

show more severe symptoms than adults with ASD (Burd et al., 2002; Shattuck et al., 2007). Although this has not been investigated directly, it seems evident that perception changes in individuals with ASD throughout development. The developmental course of these changes has, however, not yet been investigated. To study this developmental course, a first logical step would be to test predictive processing abilities in adolescents with ASD.

Action Prediction in ASD

The second task that was used in this study is an action prediction task. Action understanding and prediction are essential for everyday interactions (Sebanz & Knoblich, 2009). To understand what another person is intending, and doing so before the other person has completed their action makes it possible to synchronize actions and builds the basis for interactions (Bekkering et al., 2009; Meyer, Bekkering, Paulus, & Hunnius, 2010). The neural implementation of action prediction has been shown to be the Mirror Neuron System (MNS) (Maranesi, Livi, Fogassi, Rizzolatti, & Bonini, 2014). Mirror neurons are active both during the execution and the observation of an action (Caggiano et al., 1996). They are therefore hypothesised to simulate others" actions in order to understand them (Cattaneo et al., 2007). Crucially, it has also been shown that the MNS is active before observing an action (Kilner, Vargas, Duval, Blakemore, & Sirigu, 2004) indicating that the MNS also takes a role in predicting others' actions (Kilner, Friston, & Frith, 2007).

Multiple studies have found that action prediction is impaired in individuals with ASD, using behavioural, or (neuro-)physiological measurements: A behavioural study showed that children with ASD performed worse on predicting the outcome of familiar and unfamiliar actions compared to TDs and children with mental retardation (Zalla, Labruyère, Clément, & Georgieff, 2010). This indicates that not only do children with ASD show impairments in explicit predictive processing, but also that this impairment is specific for ASD. Another way to measure action prediction is through eye movements while participants are watching an action sequence (Flanagan & Johansson, 2003). People look at the target location of an action before the action arrives there (eg. looking at the binder while the paper is still being perforated; Poljac, Dahlslätt, & Bekkering, 2013). This is achieved by high-level priors, such as the representation of the action goal, guiding eye-movements in a top-down fashion, leading

to so-called predictive eye movements (Elsner, D'Ausilio, Gredebäck, Falck-Ytter, & Fadiga, 2013). Predictive eye movements can also be observed in more complex actions. TD adults make predictive eye movements in three-step actions (Braukmann et al., 2017; Poljac et al., 2013). Interestingly, predictive eye movements became more frequent, longer and earlier in later action steps, showing that participants were able to integrate knowledge from previous steps to form better predictions about future steps. It can be assumed that individuals with ASD do not show this pattern of increasing predictive eye movements in this task since they rely to a lesser extent on previous knowledge and expectations.

Goal of this study

Although predictive processing accounts seem promising to explain symptoms in ASD, there are some gaps in the past literature. On the one hand, the developmental course of predictive processing over the lifespan is still unclear. Children with ASD seem to perform differently to adults with ASD but the ages between those two groups have not yet been investigated. On the other hand, there is a large gap between tasks measuring predictive processing on a very basic perceptual level and the complex symptoms individuals with ASD display. Action prediction paradigms could help to bridge this gap, since they require predictive processing on a relatively high level, compared to adaptation paradigms.

This study investigated the differences in predictive processing between adolescents with ASD and TDs using two paradigms: In the adaptation task, participants were adapted to gaze direction. The adaptation after-effect was measured using behavioural responses (Ewing, Pellicano, & Rhodes, 2013). In line with previous research (Pellicano et al., 2007; Pellicano, Rhodes, & Calder, 2013; Turi et al., 2015), we hypothesised that the ASD group would show smaller adaptation after-effects, namely a smaller bias in their behavioural responses. In the action prediction task, participants watched short videos of everyday three-step actions (Braukmann et al., 2017). Predictive processing was operationalised using predictive eye-movements and MNS activation (beta-desynchronisation over central brain areas). We hypothesised that the TD group shows increasing predictive eye-movements, and increasing beta-power desynchronisation over the three action steps (Braukmann et al., 2017; Poljac et al., 2013). This increase should be smaller when stimuli are

occluded, withholding crucial information. For the ASD group, we hypothesised based on recently proposed predictive processing accounts of ASD (Pellicano & Burr, 2012; Sinha et al., 2014; Van de Cruys et al., 2014), that the ASD group both shows less predictive eye-movements (i.e. fewer predictive fixations, and less predictive fixations) and beta-power desynchronisation overall, and a smaller increase of predictive eye-movements and beta-power desynchronisation over the three action steps, compared to the TD group. Additionally, we expected a smaller difference between an occluded and an un-occluded condition in the ASD group.

Methods

Participants

Participants from the ASD group were between 12 and 18 years old (mean age = 14.6 years, *SE* = 3.43; see Table 1). They were recruited through Karakter child psychiatry clinics (https://www.karakter.com/) and were all diagnosed with Autism Spectrum Disorder according to the DSM 5 (American Psychiatric Association, 2013), or with Asperger's Syndrome, Autism, or pervasive developmental disorder not otherwise specified (PDD NOS) according to the DSM 4 (American Psychiatric Associaton, 2000). To confirm the diagnosis, a researcher completed the Autism Diagnostic Interview, Revised (ADI-R) with one parent of each participant from the ASD group.

TD participants were recruited via local schools. However, this only resulted in two participants (ages 12 and 16 years old). Therefore, additional students were recruited from the university to serve as a control group (ages 21 to 27 years old). The two young controls and the student controls were put together in the TD control group. The TD participants did not report having any psychiatric disorders.

Procedure

Before the testing day, participants had received detailed information about the study and the informed consent forms by email. On the testing day, underaged participants were accompanied by at least one parent or guardian. They were first shown around the lab and encouraged to ask questions. When participants felt comfortable, they were asked to sit in the chair where the EEG-measurement took place and the EEG procedure was explained. Participants always performed the action prediction task first, followed by the adaptation task. The action prediction task took around 45 minutes, and the adaptation task took around ten minutes. At the beginning of each task, the eye tracker was calibrated using a nine-point calibration. After successful calibration, the participants were debriefed to remind them what the task was about. Additionally, the parents of participants with ASD completed the ADI-R, which was either done during the EEG and IQ measurements or on a second meeting. In total, the underaged participants spent approximately four hours, and the TD students approximately 1.5 hours in the lab.

Experimental Setup

Stimuli from the adaptation and the action prediction task were presented on a 27" BenQ XL2420Z screen with a resolution of 1920*1080 and a vertical refresh rate of 120 Hz. Participants were seated approximately 70 cm away from and centered to the screen. The experiment was performed using Presentation® software (Version 18.0, Neurobehavioral Systems, Inc., Berkeley, CA, www.neurobs.com). Behavioural responses were recorded using a Bits-to-Serial-Interface (BITSI) button box with three buttons, a custom production of the technical support group of the social sciences faculty at the Radboud University Nijmegen (http://tsgdoc.socsci.ru.nl). Eye tracking data were recorded by an SMI RED 500 eye tracker (SensoMotoricInstruments, Teltow, Germany),

Table 1.

Demographics of study population.

Variable	Total (*n* = 20)	ASD (*n* = 9)	TD (*n* = 11)
Age in years	18.4 (*SE* = 4.39)	14.63 (*SE* = 3.43)	22.3 (*SE* = 3.45)
Sex	7 female, 13 male	1 female, 8 male	6 female, 5 male

positioned directly under the screen using a sampling rate of 500 Hz. EEG data was recorded at 500 Hz using 32 active Ag/AgCl channels of the ActiCap System (Brain Products GmbH, Gilching, Germany), bandpass-filtered between .016 and 125 Hz using the program Brain Vision Recorder (Brain Products GmbH, Gilching, Germany). The electrodes were placed according to the international 10/20 system. The electrode on the left mastoid served as an online reference and the AFz electrode served as ground electrode. Impedances were kept below 20 kΩ when possible. Additionally, vertical and horizontal oculomotor activity was recorded using four passive electrodes placed at the left and right outer canthi and above and below the left eye (horizontal and vertical EOGs).

Offline, the EEG and EOG data were analyzed using Fieldtrip (Oostenveld, Fries, Maris, & Schoffelen, 2011). First, the data was demeaned and detrended and artifacts were rejected by visual inspection per trial and channel for each participant. Then, eye artifacts were removed using an independent component analysis by identifying two factors corresponding to horizontal and vertical eye movements respectively. Identification of these factors was done by investigating the correlation between the 20 biggest factors and choosing the two factors with the biggest correlation with the EOG data. Additionally, the correlations and time courses of the 20 biggest factors were plotted for visual inspection to confirm that the two factors with the biggest correlations did indeed show the typical pattern of reflecting eye movements (see Fig. 1 in the Appendix for an example). When this was not the case, factors that visually matched vertical or horizontal eye movements were taken, if they also showed a very strong correlation. Finally, excluded channels were interpolated by nearest neighboring channels. Data was then re-referenced using the average of all channels. The channel of interest (COI) for the action prediction task was Cz and the frequency of interest (FOI) was beta (16-25 Hz). This COI and FOI were chosen to measure MNS activation, according to Braukmann and colleagues (2017).

Adaptation Task

The adaptation task was adapted from the task used by Ewing and colleagues (2013). The task comprised three blocks: preadaptation, adaptation and postadaptation. Stimuli presented in these blocks were pictures of faces of 12 different individuals. From each individual, five different stimuli were available (Jenkins, Beaver, & Calder, 2006): one where the individual looked straight at the camera (0°), two where the individual looked slightly to the left/right (L5°, R5°) and two where the individual looked strongly to the left/right (L25°, R25°, see Fig. 2).

During the preadaptation block, participants saw randomised stimuli with 0°, L5° and R5° gaze. Following the procedure of Ewing et al. (2013), each stimulus was presented for 1500ms. After each stimulus, participants had to indicate in which direction the face was looking (straight, left or right) by button press. In total, each participant saw 36 different stimuli. During the adaptation block, participants viewed adaptor stimuli with either L25° or R25° gaze. Each individual stimulus was presented twice, leading to 24 trials. Here, participants were not asked to indicate the gaze direction. In the final postadaptation block, participants were presented with the same test stimuli as in the pre-adaptation phase. However, before each test stimulus, a top-up adaptor of L25° or R25° gaze was presented for 4000ms. After each test stimulus, participants were again asked to indicate gaze direction of the test stimulus.
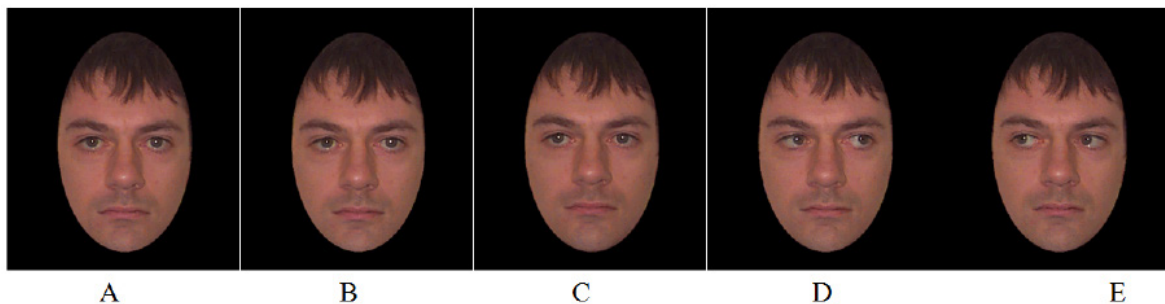

Fig. 2. Example Stimuli Items for the Adaptation Task. **A-E** show different stimuli from the same individual. **A** shows a 0° gaze, **B** shows a 5° gaze to the right, **C** shows a 5° gaze to the left. **D** and **E** show a 25° degree to the right and left respectively.

Action Prediction Task

The action prediction task was adapted from Braukmann et al. (2017). In this task, participants were asked to passively watch short video clips (approximately ten seconds) of everyday actions consisting of three action steps (see Fig 3). The videos were divided into two conditions: occluded and unoccluded. In the unoccluded condition, participants should be able to infer the action goal based on the displayed objects and on the previous action steps, and predict future action steps. In the occluded condition, gray rectangles (occluders) hid the objects in the videos by moving in front of the objects. In this occluded condition, participants should not be able to infer the action goal and form predictions, since crucial information was missing. Participants were instructed to watch the videos attentively and to keep as still as possible while EEG and eye movements were recorded. The participants performed no behavioural task. In total, 27 videos were presented, each four times, twice in the un-occluded and twice in the occluded condition, leading to 108 trials. Trials were divided into four blocks.

Results

For easier comprehension, analyses and results are hereafter presented per task.

Adaptation Task

Analysis of the behavioural data was performed in R, version 3.4.1 (R Development Core Team, 2017) using the packages *gdata* (Warnes et al., 2017), *multilevel* (Bliese, 2016), *ordinal* (Christensen, 2015) and *gmodels* (Warnes, Bolker, Lumley, & Johnson, 2015). Data visualization was done with the package *ggplot2* (Wickham, 2009). Button presses recorded during the preadaptation and post-adaptation block were analyzed. First, button presses and stimulus gaze direction were recoded from left, straight, and right to adapted, straight and unadapted, depending on adaptation direction of the participant (eg. if a participant was adapted using left-looking stimuli, all button responses indicating "left" were recoded to "adapted", button responses for "right" were recorded to "unadapted", button responses for straight always remained the same, regardless of adaptation direction).

One participant from the ASD group could not
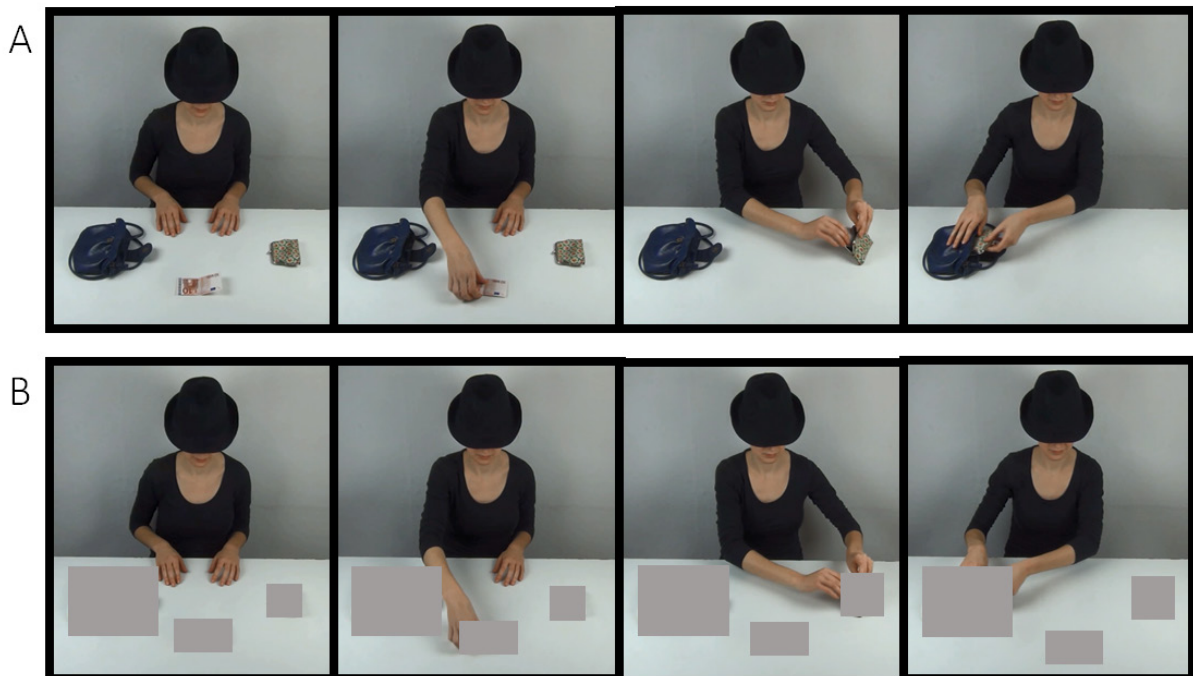
Fig. 3. Frames from Videos in the Action Prediction Task. **A.** Un-occluded condition where predictions in the form of goal representations should be possible. In a first step, the actor takes the money, in a second step she puts it into the purse, and in the third step she puts the purse into a bag. **B.** Occluded condition where predictions in the form of goal representations should be impossible because crucial information is missing. The participant is not able to infer the goal and should therefore not form predictions.

perform the task due to technical difficulties and one participant from the ASD group was excluded from further analysis because his performance in the preadaptation block was below chance level (27.7% correct responses, chance level being 33%). The overall group performance of the remaining participants was 72.1% ($SE = 10.3\%$) in the pre-adaptation block.

On the remaining data, an ordered logistic multilevel regression (Meijer & York, 2008) was performed with a random intercept and random slopes per participant. Fixed effects were the independent variables. Gaze Direction of the Stimulus (adapted, un-adapted, straight), Block (pre-adaptation, post-adaptation), Group (ASD, TD) and a Block * Group interaction and the control variable Age. Results showed significant main effects of Gaze Direction of the Stimulus ($b = 2.86$, $p < .001$), Block ($b = -1.22$, $p < .001$), and a significant interaction of Block * Group ($b = -1.00$, $p = .003$). The significant effect of Block indicates that participants classified the same stimuli differently before compared to after the adaptation. This indicates that an adaptation after-effect was induced. More crucially, the significant interaction indicates that the size of the adaptation aftereffect differed between the two groups. The other independent variables, Age and Group, were not significant (all ps > .268). A full summary of the statistics can be found in Table 2 and a visualization of button responses to the straight looking stimuli is presented in Figure 4. Figures for the adapted and unadapted stimuli can be found in the Appendix (Fig. 2 & 3).

Action Prediction Task

Eye Tracking Data Preprocessing and Analyses. The raw data files and the video files were read into SMI BeGaze 3.6.52 (SensoMotoricInstruments, Teltow, Germany). There, areas of interest (AOIs) were defined for each video, both in its un-occluded and occluded condition, following Braukmann et al. (2017). AOIs were four stationary rectangles per video, three around each object in the video and one around the lower part of the actor's face since some actions ended there. One of the four AOIs was always unused since each video only had three action steps. Fixations were defined as lasting a minimum of 50 ms. Fixations to the AOIs were then exported from SMI BeGaze and read into MATLAB 2012b (The MathWorks, Inc., Natick, Massachusetts, United States). Additionally, time windows of interest (TOI) were defined for each video and loaded into MATLAB. TOIs classified fixations as predictive (looking at the AOI after the actor's hand moved towards the AOI but before entering it), reactive (looking at the AOI after the actor's hand entered the AOI) or neither (occurring outside of TOIs). The reactive time window was always as long as the predictive time window and fixations being neither reactive nor predictive were excluded from further analysis. These fixations were then analysed using three different measures: First, predictive and reactive fixations were treated as two different outcomes and analysed using a logistic multilevel regression (*Predictive vs Reactive Fixations*). Second and third, the *Onset* and the *Duration of Predictive Fixation* were analysed using multilevel regressions. *Onset of Predictive Fixation* was coded relative to the end of the TOI. Large values therefore indicate earlier onsets and vice versa.

For the statistical analyses, I decided to analyse each of the three measures with three different multilevel regression models. In the first model, the fixed effects Group (ASD, TD), Action Step (one, two, three), Condition (un-occluded, occluded), the two-way interactions Group * Action Step,

Table 2.

Summary of the fixed effects in the ordered logistic multilevel regression for the behavioral data in the adaptation task.

Variable	b	SE	p
Group	.05	.35	.893
Gaze direction of stimulus	**2.86*****	.21	< .001
Block	**-1.22*****	.27	< .001
Block * Group interaction	**-1.00****	.34	.003
Age	.03	.03	.268

Note: ** indicates a significant result to a level < .01, *** indicates a significant result to a level < .001 Significant findings are printed in bold.
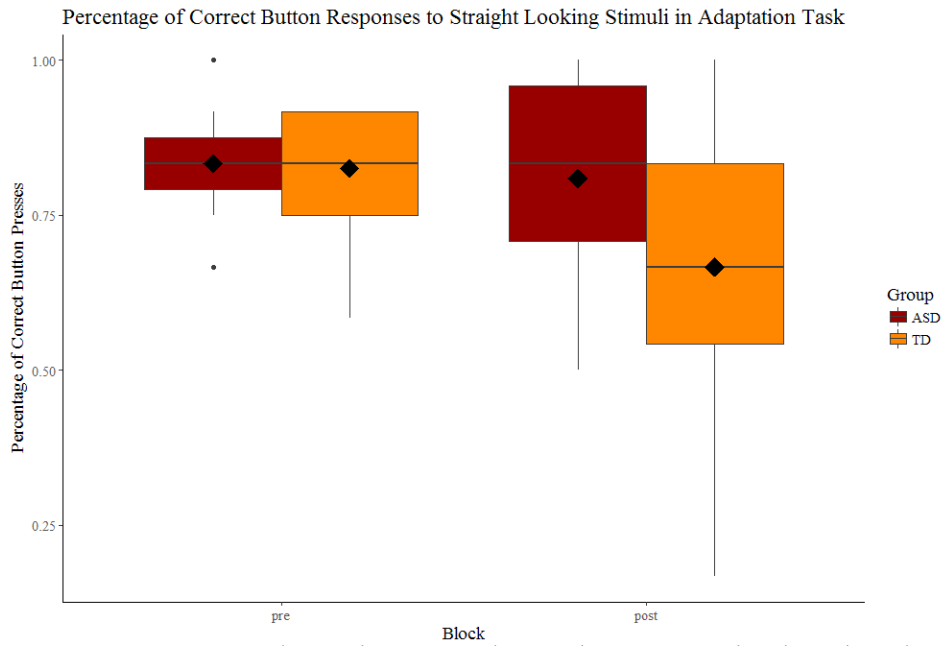
Fig. 4. Button Responses to Straight Looking Stimuli in Adaptation Task. These boxplots show parts of the behavioral results from the adaptation task. Diamonds indicate means. This graph shows that in the pre-adaptation block, both groups perform equally well in classifying straight gaze direction. In the post-adaptation block, however, performance of the TD group is influenced by the adaptation block while performance of the ASD group remains unaffected.

Group * Condition, and Action Step * Condition, and the three-way interaction Group * Action Step * Condition were included. Random effects were a random intercept and random slopes for Condition and Action Step per participant and random intercepts per stimulus. Additionally, age of the participant and DoTOI were included as fixed effects to control for their influence. To investigate potential significant three-way interactions, two additional models were planned for each measure: In these second and third models, data from each group (ASD and TD) was analysed separately, using the same model as above, except for the predictor group and its interactions.

To test whether all assumptions were met for the linear mixed models (Onset and Duration of Predictive Fixation), residuals of the models were inspected visually. If residuals seemed to deviate from normality and/or heteroscedasticity, the outcome variable was transformed (eg. using a log or square root transformation), until the assumptions were met. *P*-values for these non-binomial multilevel regressions were obtained by estimating the number of degrees of freedom using the Kenward-Roger approximation (Halekoh & Hojsgaard, 2014; Kenward & Roger, 1997).

Eye Tracking Results. Data from three participants from the ASD group was not available due to technical reasons. Furthermore, for one participant from the TD group only one fixation in total was registered. This participant was therefore also excluded. The remaining 16 participants were analyzed using the statistics program R, version 3.4.1 (R Development Core Team, 2017) with the packages *lme4* (Bates, Maechler, Bolker, & Walker, 2015), *pbkrtest* (Halekoh & Hojsgaard, 2014), *car* (Fox & Weisberg, 2011), *lattice* (Sarkar, 2008), *MuMIn* (Barton, 2016) and *gmodels* (Warnes et al., 2015). Data visualization was realized with the package *ggplot2* (Wickham, 2009).

Predictive versus Reactive Fixations. The first analysis investigated the difference between predictive and reactive fixations using a multilevel logistic regression model. Unfortunately, the planned first model with the three-way interaction did not converge with 200 million iterations. Therefore, the most parsimonious model (Condition predicts type of fixation) was used as a starting point from where consecutively predictors were added until the best model fit according to the Akaike information criterion (AIC) was achieved. The terms Age and DoTOI (both z-standardised, see Bates et al., 2015) were not included but neither resulted a significant effect when used as predictors alone (*p*s > .306). The resulting model included the main effects of Group, Action Step, Condition, and the interactions Group * Action Step, Group * Condition, and Action Step * Condition. Although adding more predictors
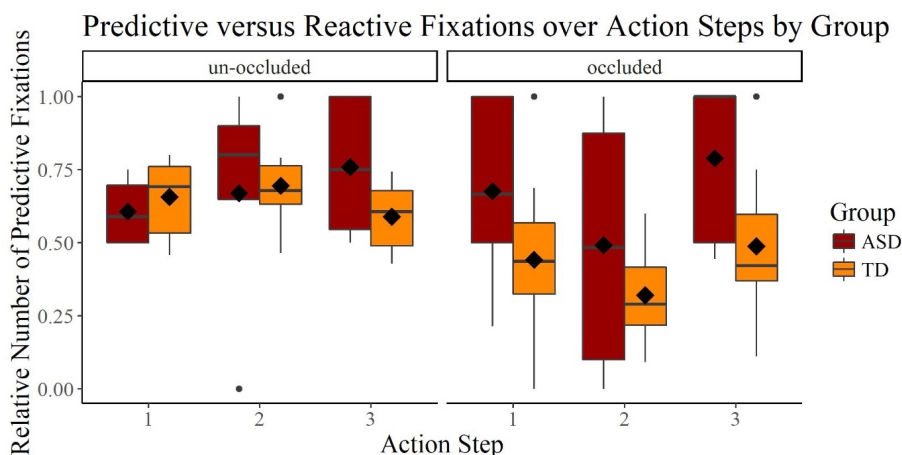
Fig. 5. Boxplots of Predictive versus Reactive Fixations from the action prediction task. These Boxplots show the ratio between Predictive and Reactive Fixations, in the un-occluded and occluded condition, over the action steps, by group. Diamonds indicate means. Results showed significantly more predictive fixations in the un-occluded condition compared to the occluded condition.

resulted in a better model fit according to the AIC, only the effect of Condition was significant ($b = 1.30$, $p = .002$, all other ps > .219).

Onset of Predictive Fixations. The second analysis investigated the Onset of Predictive Fixations. Since this variable showed a strong skewness which could not be captured by a linear model, it was first transformed. Taking its square root resulted in a better distribution compared to a log-transformation. Residuals were inspected visually and did not seem to violate the criteria of normality and homoscedasticity.

Results from the first model showed a significant effect of the interactions Group * Condition ($b = 12.11$, $p = .012$), Action Step * Condition ($b = 5.22$, $p = .011$) and Group * Action Step * Condition ($b = -5.88$, $p = .007$) and the control variable DoTOI ($b = .01$, $p < .001$). The other effects did not reach significance (all ps > .121, except Group where $p = .080$). The fixed effects combined explained 14% of the variance ($R^2 = .14$). For the full results, see Table 3 and for visualization of the data see Figure 6.

The significant three-way interaction indicates that the interaction of Action Step and Condition differentially affected the two groups. To further investigate this, two consecutive models were performed, for the ASD and TD group, respectively. In the ASD-model, no effect yielded a significant result (all ps > .121, except DoTOI, $p = .074$). In the TD-model, no effects except the control variable DoTOI ($b = .01$, $p < .001$) were significant although Condition was close to significance ($b = 4.09$, $p = .056$). All other effects did not reach significance (all ps > .652). For a full summary, see Table 5.

These results indicate that while predictive fixations from the TD group probably began earlier in the un-occluded condition compared to the occluded one, the onset of predictive fixations did not differ in the ASD group. Also, a shorter DoTOI in the TD group led to later predictive fixations, while it had barely an effect on the predictive fixations in the ASD group. Interestingly, the interaction Action Step * Condition was significant in the first model but failed to reach significance in either of the group models.

Duration of Predictive Fixations. In the third analysis the Duration of Predictive Fixations was investigated. Since the data was not normally distributed, it was first transformed. From a log-transformation and a square root transformation, the latter yielded residuals that visually seemed to better fit the assumptions of normality and homoscedasticity. Results from the first model showed that the effects of Group ($b = -6.59$, $p = .048$), Action Step ($b = -2.75$, $p = .036$), the interactions Group * Action Step ($b = 3.46$, $p = .015$), Group * Condition ($b = 8.40$, $p = .028$) and Group * Action Step * Condition ($b = -3.44$, $p = .044$), as well as the control variable DoTOI ($b = .88$, $p < .001$) were significant. The interaction Action Step * Condition just failed to reach significance with $p = .07$, and p-values for Condition and Age were > .145 (see Table 3 for a full summary and Figure 7 for boxplots of the data). The fixed effects together explained 6% of the variance.

Again, the significant three-way interaction was further investigated with two models, separately investigating the two groups. Results for the ASD-
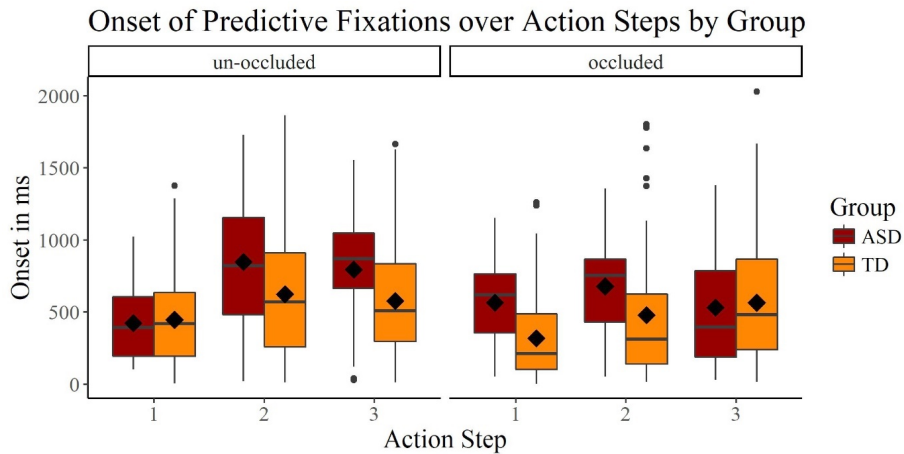
Onset of Predictive Fixations over Action Steps by Group

Fig. 6. Boxplots of Predictive Fixation Onsets in the action prediction task. These boxplots show the onset of predictive fixations relative to the endpoint of the predictive window of interest. Hence, larger numbers indicate an earlier onset. Diamonds indicate means. Results indicate earlier fixations for the TD group in the un-occluded condition compared to the occluded condition.

group did not show any significant effect (all ps > .183, except Action Step * Condition where p = .090). Results for the TD-group show a significant effect of Condition (b = 3.10, p = .027) and of DoTOI (b = 1.14, p < .001). A full summary of these results can be found in Table 6.

These results show a similar pattern to the previous measure Onset of predictive fixations: in the occluded condition, predictive fixations from the TD group were significantly shorter than for the un-occluded condition. This was not the case for the ASD group. Also, DoTOI had an influence on the duration of predictive fixations in the TD group, but not in the ASD group. In the first model, a significant interaction of Group * Action Step was observed. In both consecutive models, however, Action Step failed to reach significance. However, b-values for each group have different signs which might explain the significant interaction in the first model.

Duration of Time Window of Interest as a Predictor. The previous analyses showed that DoTOI has a significant effect in two of the three fixation measures (Duration and Onset of Predictive Fixations). This is an interesting finding because of three reasons: First of all, this effect has not been taken into consideration in previous studies (Braukmann et al., 2017; Poljac et al., 2013). Secondly, the effect of Action Step found in those previous studies could not be replicated in the TD sample in this study (Table 4 and 5). And lastly, when investigated more closely, it is revealed that both the mean and the standard deviation (SD) of the DoTOI corresponding to the first action step are smaller (mean = 992.35 ms, SD = 205.51 ms) than compared to the second (mean = 1451.75 ms, SD = 295.67 ms) and third (mean = 1433.46 ms, SD = 281.62 ms) action step. A linear model with contrasts

Duration of Predictive Fixations over Action Step by Group
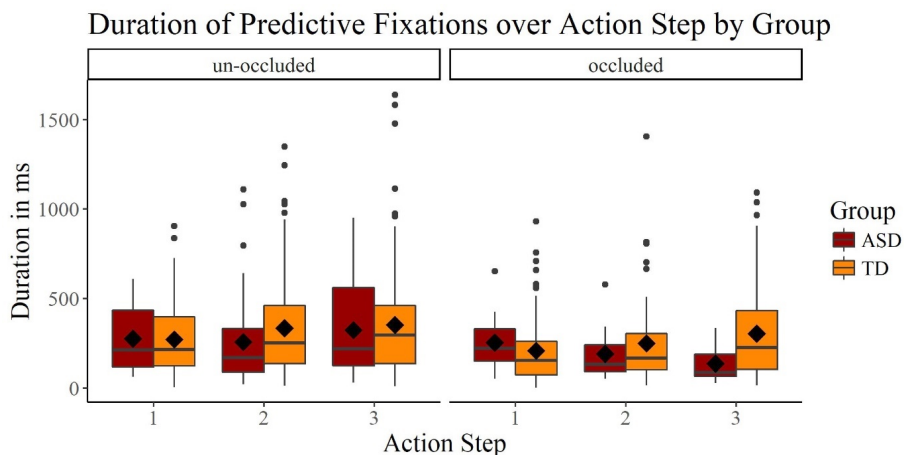

Fig. 7. Boxplots of Predictive Fixation Durations in the action prediction task. These boxplots represent the raw durations of predictive fixations in ms. Diamonds indicate means. Results show that predictive fixations were longer for the TD group in the un-occluded compared to the occluded condition.

Table 3.

Summary of the fixed effects in the first multilevel regression models including the three-way interaction for the eye tracking data in the action prediction task.

Variable	Onset of Predictive Fixation[a]					Duration of Predictive Fixation[a]				
	b	SE	t	Appr. dfs	p	b	SE	t	Appr. dfs	p
Group	-7.36	4.05	-1.82	115.60	.080	**-6.59***	3.20	-2.06	89.62	.048
Action Step	-2.13	1.72	-1.24	189.25	.220	**-2.75***	1.29	-2.12	230.27	.036
Condition	-6.99	4.40	-1.59	422.11	.122	-5.21	3.49	-1.50	409.05	.146
Group * Action Step	2.80	1.86	1.51	120.99	.139	**3.46***	1.39	2.50	148.05	.015
Group * Condition	**12.11***	4.69	2.58	374.01	.012	**8.40***	3.70	2.27	373.42	.028
Action Step * Condition	**5.22***	2.00	2.61	632.52	.011	2.92	1.56	1.87	612.67	.068
Group * Action Step * Condition	**-5.88****	2.13	-2.76	655.47	.007	**-3.44***	1.67	-2.06	652.59	.044
Age	-.24	.14	-1.69	8.72	.188	.07	.11	.63	8.90	.610
Duration of Time Window of Interest[b]	**2.42*****	.34	7.17	463.69	< .001	**.88*****	.26	3.42	417.03	< .001

Note: * indicates a significant result to a level < .05, ** indicates a significant result to a level < .01, *** indicates a significant result to a level < .001.
Significant findings to either of those levels are printed in bold.
[a] The outcome variable of this model was transformed using a square root transformation.
[b] This variable was z-standardized.
Note that the model for *Predictive versus Reactive Fixations* did not converge and is therefore not represented here.
R^2 for fixed effects:
R^2 (Onset of Predictive Fixation) = .14
R^2 (Duration of Predictive Fixation) = .06
R^2 for fixed and random effects combined:
R^2 (Onset of Predictive Fixation) = .30
R^2 (Duration of Predictive Fixation) = .20

Table 4.

Summary of the fixed effects in the group-wise logistic multilevel regression models investigating *Predictive versus Reactive Fixations* for the eye tracking data in the action prediction task.

Variable	b	SE	z	p
Group	-.49	.56	-.88	.380
Action Step	.16	.22	.71	.478
Condition	**1.30***	.43	3.04	.002
Group * Action Step	-.10	.22	-.47	.642
Group * Condition	.18	.35	.52	.603
Action Step * Condition	-.17	.14	-1.23	.219

Note: * indicates a significant result to a level < .05, ** indicates a significant result to a level < .01, *** indicates a significant result to a level < .001.
Significant findings are printed in bold.

Table 5.

Summary of the fixed effects in the second and third multilevel regression models investigating *Onset of Predictive Fixation* for the eye tracking data in the action prediction task.

Variable	ASD Group[a]					TD Group[a]				
	b	*SE*	*t*	Appr. dfs	*p*	*b*	*SE*	*t*	Appr. dfs	*p*
Action Step	4.17	1.67	2.49	3.23	.203	.35	.76	.46	106.08	.653
Condition	5.71	5.03	1.14	25.15	.418	4.09	2.07	1.97	49.69	.056
Action Step * Condition	-4.43	2.05	-2.16	40.94	.122	-.38	.88	-.43	57.39	.671
Age	-1.15	.76	-1.50	1.82	.493	-.06	.20	-.29	7.92	.778
Duration of Time Window of Interest [b]	1.67	.86	-2.16	113.07	.074	**2.23*****	.36	6.19	159.54	< .001

Note: * indicates a significant result to a level < .05, ** indicates a significant result to a level < .01, *** indicates a significant result to a level < .001.
Significant findings are printed in bold.
[a] The outcome variable of this model was transformed using a square root transformation.
[b] This variable was z-standardized.
R^2 for fixed effects:
R^2 (ASD) = .16
R^2 (TD) = .11
R^2 for fixed and random effects combined:
R^2 (ASD) = .59
R^2 (TD) = .26

Table 6.

Summary of the fixed effects in the second and third multilevel regression models investigating *Duration of Predictive Fixation* for the eye tracking data in the action prediction task.

Variable	ASD Group[a]					TD Group[a]				
	b	*SE*	*t*	Appr. dfs	*p*	*b*	*SE*	*t*	Appr. dfs	*p*
Action Step	-1.54	1.38	-1.11	13.04	.323	.46	.59	.79	38.99	.454
Condition	-6.07	3.56	-1.71	41.83	.184	**3.10***	1.33	2.33	122.76	.027
Action Step * Condition	3.43	1.56	2.20	62.55	.090	-.45	.59	-.76	688.75	.466
Age	.02	.53	.04	1.54	.985	.06	.12	.54	7.34	.666
Duration of Time Window of Interest[b]	-.58	.63	-.93	96.00	.388	**1.14*****	.28	4.14	362.31	< .001

Note: * indicates a significant result to a level < .05, ** indicates a significant result to a level < .01, *** indicates a significant result to a level < .001.
Significant findings are printed in bold.
[a] The outcome variable of this model was transformed using a square root transformation.
[b] This variable was z-standardized.
R^2 for fixed effects:
R^2 (ASD) = .05
R^2 (TD) = .06
R^2 for fixed and random effects combined:
R^2 (ASD) = .24
R^2 (TD) = .20

was used to evaluate two differences in DoTOI. First, the difference between the first action step and the other two, and second, the difference between the second and third action step. Results revealed that DoTOI for the first action step is significantly shorter than the other two ($b = 137.28$ ms, $p < .001$) and that there is no significant difference between action step two and three ($b = -17.78$ ms, $p = .626$). A full summary of the model can be found in the Appendix (Table 1). This shows that the DoTOI of the first action step is significantly shorter compared to the second and third action step. Also, there is no difference between the second and third action step.

Taking these three points into account, it is possible that in past studies (Braukmann et al., 2017; Poljac et al., 2013) the effect of DoTOI has been explained by the variable of Action Step. To explore this possibility further, the two measures *Onset of Predictive Fixations and Duration of Predictive Fixations* were analysed again in the student TD sample ($n = 9$) without DoTOI as a predictor. This data should correspond most closely to the data from Braukmann et al. (2017). Predictive versus Reactive Fixation was not analysed again since DoTOI did not reach significance (see Table 4).

Results for the *Onset of Predictive Fixations* show indeed that without DoTOI as a predictor, the factor Action Step becomes significant ($b = 2.87$, $p < .001$). Similarly, results for the *Duration of Predictive Fixations* shows that the factor Action Step becomes significant ($b = 1.87$, $p < .001$). For a full

summary of the models, see the Appendix (Table 2). This indicates that the influence of Action Step and DoTOI might overlap, making it difficult to interpret results when DoTOI is not controlled for.

Electrophysiological Analysis. The pre-processed data (see Experimental Setup) was analyzed using a fast Fourier transformation, separately for each action step, in the un-occluded and occluded condition, respectively, and the fixation in between trials. Timings for action steps were determined for each video separately. Beta-power was furthermore z-standardised using the grand mean and standard deviations and then analysed using a multilevel regression. Model residuals were inspected visually and did not seem to deviate from normality and homoscedasticity. *P*-values were again obtained by using the Kenward-Roger approximation of the number of degrees of freedom.

Electrophysiological Results. One participant had to be excluded from analysis due to technical difficulties. The remaining 19 participants were analysed using R, version 3.4.1 (R Development Core Team, 2017) with the packages *lme4* (Bates et al., 2015) and *pbkrtest* (Halekoh & Hojsgaard, 2014). Data was visualised with the package *ggplot2* (Wickham, 2009).

A multilevel regression with the fixed effects Group (ASD, TD), Action Step (one, two, three), Condition (un-occluded, occluded), the two-

Table 7.

Summary of the fixed effects in the multilevel regression for the electrophysiological data in the action prediction task.

Variable	b	SE	t	Approximated dfs	p
Group	.61	.60	1.03	36.91	.310
Action Step	-.25	.12	-1.97	89.00	.052
Condition	-.16	.38	-.41	89.00	.682
Group * Action Step	-.23	.17	-1.35	89.00	.180
Group * Condition	-.50	.52	-.96	89.00	.342
Action Step * Condition	.05	.18	.28	89.00	.782
Group * Action Step * Condition	.28	.24	1.13	89.00	.260
Age	-.08	.68	-1.94	16.00	.070

Note: * indicates a significant result to a level < .05
Significant findings are printed in bold.
R² for fixed effects:
R² = .21
R² for fixed and random effects combined:
R² = .81

way interactions Group * Action Step, Group * Condition and Action Step * Condition, and a three-way interaction Group * Action Step * Condition, plus the control variable Age, along with a random intercept and slope per participant was performed. A summary of the fixed effects can be found in Table 7.

Results reveal a nearly significant negative effect of Action Step ($t = 1.97$, $p = .052$), indicating a beta-power desynchronisation over the action steps. All other effects did not reach significance (all ps > .070).

To further investigate the effect of Action Step, I performed a second multilevel regression with the contrasts Action Step 1-2 and Action Step 2-3. The results show a smaller effect of the first contrast ($t = .63$) than the second ($t = -1.31$). However, both effects are rather small, indicating that the marginal significance of the factor in the first model was mainly driven by the difference between Action Step one and three. Boxplots for the data can be found in Figure 8.

Discussion

In this study, I used two different tasks to examine predictive processing in adolescents with ASD and TD controls. These tasks shed light on a previously untested age group with ASD. This is also the first study to examine predictive processing mechanisms operating on different hierarchical levels in ASD. However, results must be interpreted with utmost caution since the control group was not matched for either age or IQ.

Adaptation Task

Results from the adaptation task show that adolescents with ASD show a smaller adaptation after-effect compared to TDs. This indicates that their perception relies more on immediate sensory input and less on previous experiences (see Fig. 1). This is in line with the predictive processing account of ASD (eg. Pellicano & Burr, 2012; Van De Cruys et al., 2014) proposing an imbalance between the weighting of priors and sensory information in the perceptual process. This result is particularly interesting in the light of the developmental changes in individuals with ASD. Previous studies in children showed a bigger adaptation after-effect for TD compared to ASD (eg. Ewing et al., 2013; Pellicano, Rhodes, & Calder, 2013; Turi et al., 2015), whereas studies with adult participants did not show such a difference (Cook et al., 2014; Walsh et al., 2015). The present study is the first attempt to investigate the age between childhood and adulthood. Interestingly, the effect is still present during adolescence. Previous studies have argued that the reduced adaptation after-effect in ASD is only observable during a limited time window in development and not representative for ASD in general (Cook et al., 2014; Nordt et al., 2015).

The present results, however, showed that the reduced adaptation after-effect is present in a much bigger age range than previously assumed. This raises the question when and, most importantly, why this effect vanishes in individuals with ASD at some point after adolescence. An important factor might be brain maturation. The adolescent brain is subjected to major changes, such as white matter
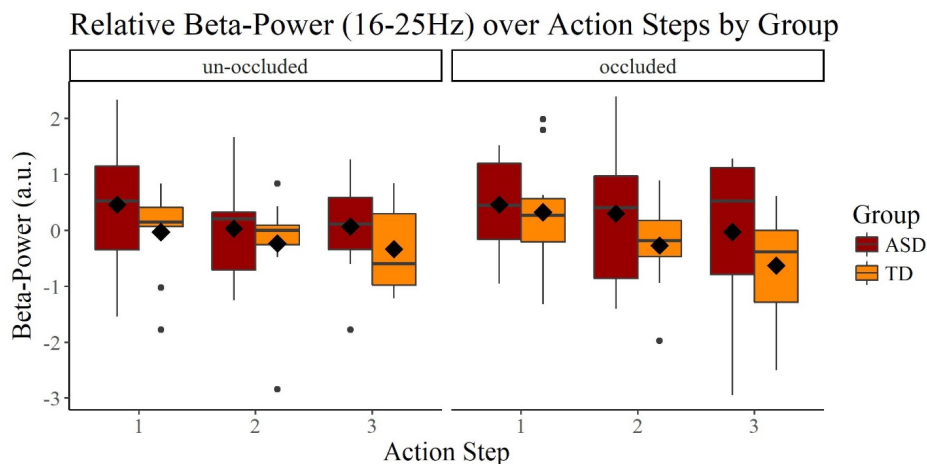

Fig. 8. Boxplots of the beta-power (16-25Hz) per action step per group. Although the analyses did not show an interaction between Group * Action Step, the plot here shows a slight trend: whereas beta-power for the TD seems to decrease over the action steps, this does not seem to be the case for the ASD group.

increase and grey matter decrease and changes in the neurotransmitter systems (Arain et al., 2013; Blakemore & Choudhury, 2006; Wahlstrom, Collins, White, & Luciana, 2010). These developments have extensively been interpreted in the light of changes in behaviour and higher cognitive functions in TDs (Kilford, Garrett, & Blakemore, 2016; Knoll, Magis-Weinberg, Speekenbrink, & Blakemore, 2015; Pfeifer & Blakemore, 2012), but no evidence seems to point to a change in more basic perceptual processes in TDs, such as adaptation. However, individuals with ASD might show some delayed developments. Indeed, one study showed that visual processing of complex stimuli still develops during adolescence in individuals with ASD, especially stimuli processed in temporal lobes (O'Hearn et al., 2014; O'Hearn, Schroer, Minshew, & Luna, 2010). Gaze direction is indeed processed in temporal areas (Hooker et al., 2003). Performance in categorising gaze direction is comparable in adolescents with and without ASD (Webster & Potter, 2008), indicating that the adaptation effect alone is subject to development during (late) adolescence. To investigate this further, future studies should focus on the late adolescence and early adulthood. Possibly, the differences between individuals with ASD and TDs vanish around that time.

Some criticism has been made against studies investigating adaptation in ASD using social stimuli such as faces (eg. Ewing et al., 2013; Pellicano et al., 2007). Since individuals with ASD have problems in the social domain (American Psychiatric Association, 2013), it has been argued that the reduced adaptation after-effect could be specific to social stimuli. However, one study showed the same reduced adaptation after-effect in children with ASD, using nonsocial stimuli (Turi et al., 2015). Specifically, the children saw two patches of dots and were asked to indicate which patch contained more dots. The children with ASD were less influenced by the size of the patch in the adaptation phase when making that decision. Therefore, it can be argued that the reduced adaptation after-effect is reflecting a general processing difference which is not specific to social stimuli.

Action Prediction Task

The results from the action prediction task only seem partly in line with our hypotheses. The first hypothesis regarded the influence of Action Step on predictive eye movements: in line with past research (Braukmann et al., 2017; Poljac et al., 2013), we expected to replicate an increase in predictive eye

movements over the action steps for the TD group. This replication, however, was not successful. When investigating the TD group alone, no significant effect of Action Step could be established. One explanation for this is the underestimation of an apparently important predictor: Duration of Time Window of Interest (DoTOI). Unfortunately, DoTOI differed significantly between the first and the last two action steps. Ignoring DoTOI led to a significant effect of Action Step (see Table 9 in the Appendix). However, this significant effect vanished when DoTOI was controlled for (see Tables 5 and 6). This finding is striking since it raises the question whether past studies using the same stimulus material confounded the effect of DoTOI with the effect of Action Step (Braukmann et al., 2017). Therefore, the question arises whether an effect of Action Step can be found in eye tracking data at all. An indication to answering this might be found in the results of the models for the ASD and TD group combined. There, we see a significant effect of DoTOI but also a significant effect of Action Step for the duration of predictive fixations. The effect of Action Step in the onset of predictive fixations, however, was not significant. These findings together indicate that the duration of predictive fixations might be longer in TDs when they understand the displayed action, whereas the onset of those fixations seems to remain unaffected by this understanding. An important recommendation for future studies is to consider the effect of DoTOI already in the stimulus construction, making them equally long for all action steps.

Based on the effect of Action Step in the TD group, we also expected an interaction of Action Step with Group, namely that Action Step would influence predictive eye movements to a lesser extent in the ASD group. Indeed, we saw a marginally significant interaction of Group and Action Step in the onset and the duration of predictive fixations (Table 3). This seems again to be in line with the hypothesis that predictions should be facilitated in later action steps only for the TD group. A definite conclusion, however, is not possible since the effect did not reach significance in either group when investigated separately (Tables 4 and 5). This might be due to insufficient statistical power when splitting the data into two groups and additionally due to the small effects we expected for the ASD group.

The second hypothesis aimed at the effect of being able to integrate background knowledge using the displayed objects. We expected that by hiding parts of the action, the TD should show decreased predictive eye-movements. This effect should be

smaller in the ASD group since the integration of background knowledge should be impaired. This is indeed what we found for the onset and duration of predictive fixations (see Table 3, 5, and 6). This indicates that TD individuals used cues from the presented objects to inform their prediction. In the absence of those cues (in the occluded condition) their ability to make predictions was impaired. This difference was absent for the ASD group, indicating that they use the additional information less or not at all to inform their predictions. This result is in line with the predictive processing account of ASD (Pellicano & Burr, 2012; Van de Cruys et al., 2014) that posits that individuals with ASD rely less on previous knowledge and more on direct sensory input in their perceptual process.

However, both the effect of Action Step and the effect of Condition were only observed for two of the three eye tracking measures. For the third measure, the planned regression model did not converge making it difficult to draw conclusions, especially when comparing the two groups. The group-wise results show that when comparing predictive against reactive predictions, neither of the two groups showed more predictive fixations in later action steps. However, the occlusion of objects seems to influence both groups (see Table 4). This indicates that it is not the ability to make predictive fixations, per se, that is impaired in adolescents with ASD, but rather the quality of the predictive fixations (eg. onset and duration). This is an important finding that should be taken into account in future studies investigating predictive eye movements in ASD: only looking at whether a fixation is predictive might hide important aspects of the data. Concerning the (absent) influence of the Action Step in this measure, two possibilities can be considered: either it is again a power problem, similar to the other two eye tracking measures, or this measure is not sensitive to the influence of Action Step. Previous studies analysed this measure in a slightly different way, computing a ratio between predictive and reactive fixations per action step per participant (Braukmann et al., 2017; Poljac et al., 2013). This difference in analysis could account for the unsuccessful replication.

In sum, parts of the eye tracking results are in line with the hypotheses. The effect of Condition generally presents itself as predicted. In two of the three measures, it influenced the TD group but not the ASD group. The effect of Action Step is more difficult to assess. Since it is mostly absent when controlling for the duration of the TOI, it is not possible to determine whether the manipulation did not work in this sample, or whether it did not work

in any of the previous studies who did not control for DoTOI. The only measure that did not show the expected pattern at all was the measure *Predictive versus Reactive Fixations*. This might be because only some qualities of predictive fixations are impaired in ASD, not the ability to make predictive fixations per se.

Results from the EEG data seem to partly confirm the prior hypothesis: we expected an increase of beta-power desynchronisation over the action steps for the TD group but not for the ASD group. A marginally significant increase in beta-desynchronization can indeed be observed over the three action steps. This result, on its own, only shows that while observing someone's action, the MNS engages. To assess the predicting function of the MNS, we included the occluded condition where prediction should be hindered. Contrary to the hypothesis, however, beta-desynchronisation does not seem to be influenced by condition which gives no indication that the MNS's predictive function was successfully measured. It seems unlikely that the occluded condition failed completely as a control condition since differences have been observed in the eye tracking data. Interestingly, the interaction between Group and Action Step approached significance, indicating a greater activation of the TD motor cortex than the ASD motor cortex. However, since it could not be distinguished whether the activation is reflecting or predicting the displayed action, no conclusions can be drawn for differences in predictive processing between ASD and TD.

An additional striking finding is that the random effects of the model explain a large amount of variance (21% for the fixed effects only, 81% for all effects combined). The big discrepancy between the variance explained by fixed effects only and by both effects indicates that there are large inter-individual differences. This additionally shows that on the one hand, a multilevel model is very powerful in capturing those effects, and that on the other hand a large sample size is necessary to capture the relatively small effects of our hypothesised predictors.

General Discussion

Results from both tasks, adaptation and action prediction, seem to point in the same direction: predictive processing seems to be impaired in adolescents with ASD. However, results from the adaptation task seem much stronger than in the action prediction task. Capturing a highly significant effect in such a small sample size speaks for large effects. This implies that differences in predictive

processing in low-order processes are more pronounced than in higher-order processes. This goes against the notion proposed by Van de Cruys and colleagues (2014). They argue that differences in low-level perception should get carried over into higher areas, with the effects adding up. Results from this study however, point to larger differences in the low-level areas compared to higher levels. Although this could point to a compensatory mechanism that prevents differences adding up, a somewhat more likely alternative is the difference in tasks: In the adaptation paradigm, we tested how much the participant's perception is influenced by prior expectations. In the action prediction paradigm, we tested the participant's ability to make predictions. The influence of prediction on perception, and the ability to make predictions could be affected separately by ASD.

Limitations

Although this study provided some interesting insights into predictive processing mechanisms in ASD, all results must be treated with the utmost caution. The main reason for this is the inadequate control group. Clearly, the two groups were not matched in age, and probably not in IQ either. Age was included as a predictor in all analyses and it reached significance only once. However, age could also have a nonlinear effect on the outcome variables which would not have been captured by the (generalized) linear models that were performed here. Also, the relationship between Age and Group is problematic, and hardly controllable for with the analyses performed here. It is therefore paramount to include a suitable, matched control group and to exclude the student controls before drawing any definite conclusions from this dataset.

Another limitation is the small sample size. Especially when investigating the plots for the eye tracking data, it becomes obvious that the data is very noisy, particularly for the ASD group. This is no surprise, since less eye tracking data were available for the ASD group and since variability in performance is probably higher in ASD compared to TDs. Some results do indeed show a trend towards a significant result that could become significant with more power.

Another problem stemming from the small power, especially in the ASD group, is that results from the eye tracking data in the ASD group never reached significance (with one exception being the effect of Condition on *Predictive versus Reactive Fixations*). We expected a smaller effect here, which

is more difficult to detect in small sample sizes. However, the effect could also be completely absent. A bigger sample size and possibly a Bayesian statistics approach would be necessary to assess a small effect or its absence.

Conclusion

The present study is to the best of our knowledge the first investigation of predictive processing mechanisms of adolescents with ASD. Although there are many serious limitations to this study, such as an insufficient control group and a small sample size, it does provide some interesting first results. Specifically, results from the adaptation task seem to show that the reduced adaptation after-effect in individuals with ASD is observable not only in children but also in adolescents. This evidence supports the recently proposed predictive processing accounts of ASD. Results from the action prediction task, especially the eye tracking results, also seem to partly be in line with this account. However, differences in group effects seem much smaller and therefore in need of confirmation in a much bigger sample. Together these results support the predictive processing account in ASD by providing evidence in a previously untested age range.

References

American Psychiatric Associaton. (2013). *Diagnostic and Statistical Manual of Mental Disorders*.

Arain, M., Haque, M., Johal, L., Mathur, P., Nel, W., Rais, A., … Sharma, S. (2013). Maturation of the adolescent brain. *Neuropsychiatric Disease and Treatment*.

Barton, K. (2016). MuMIn: Multi-Model Inference. Retrieved from https://cran.r-project.org/package=MuMIn

Bates, D., Maechler, M., Bolker, B., & Walker, S. (2015). Fitting Linear Mixed-Effects Models Using lme4. *Journal of Statistical Software*, *67*(1), 1–48.

Bekkering, H., De Bruijn, E. R. A., Cuijpers, R. H., Newman-Norlund, R., Van Schie, H. T., & Meulenbroek, R. (2009). Joint Action: Neurocognitive Mechanisms Supporting Human Interaction. *Topics in Cognitive Science*, *1*(2), 340–352.

Blakemore, S. J., & Choudhury, S. (2006). Development of the adolescent brain: Implications for executive function and social cognition. *Journal of Child Psychology and Psychiatry and Allied Disciplines*, *47*(3-4), 296-312.

Bliese, P. (2016). multilevel: Multilevel Functions. R package version 2.6. Retrieved from https://cran.r-project.org/package=multilevel

Boucher, J. (1989). The theory of mind hypothesis of autism: explanation, evidence and assessment. *The*

British Journal of Disorders of Communication, 24(2), 181-198.

Braukmann, R., Bekkering, H., Hidding, M., Poljac, E., Buitelaar, J. K., & Hunnius, S. (2017). Neuropsychologia Predictability of action sub-steps modulates motor system activation during the observation of goal-directed actions. *Neuropsychologia, 103*(February), 44–53.

Burd, L., Kerbeshian, J., Westerland, A., Labine, J., Barth, A., Klug, M. G., … Burd, N. (2002). Prospective Long-Term Follow-Up of Patients With Pervasive Developmental Disorders From the Departments of Pediatrics. *Journal of Child Neurology, 17*(9), 681–688.

Caggiano, V., Fogassi, L., Rizzolatti, G., Casile, A., Giese, M. A., Thier, P., … Rizzolatti, G. (1996). Premotor cortex and the recognition of motor actions. *Current Biology, 3*(2), 131-141.

Cattaneo, L., Fabbri-Destro, M., Boria, S., Pieraccini, C., Monti, A., Cossu, G., & Rizzolatti, G. (2007). Impairment of actions chains in autism and its possible role in intention understanding. *Proceedings of the National Academy of Sciences U S A, 104*(45), 17825–17830.

Chambon, V., Farrer, C., Pacherie, E., Jacquet, P. O., Leboyer, M., & Zalla, T. (2017). Reduced sensitivity to social priors during action prediction in adults with autism spectrum disorders. *Cognition, 160*, 17–26.

Christensen, R. H. B. (2015). ordinal - Regression Models for Ordinal Data. Retrieved from http://www.cran.r-project.org/package=ordinal/

Clark, A. (2013). Whatever next? Predictive brains, situated agents, and the future of cognitive science. *Behavioral and Brain Sciences, 36*, 181– 253.

Cook, R., Brewer, R., Shah, P., & Bird, G. (2014). Intact facial adaptation in autistic adults. *Autism Research, 7*(4), 481-490.

Elsner, C., D'Ausilio, A., Gredebäck, G., Falck-Ytter, T., & Fadiga, L. (2013). The motor cortex is causally related to predictive eye movements during action observation. *Neuropsychologia, 51*(3), 488-492.

Ewing, L., Pellicano, E., & Rhodes, G. (2013). Atypical updating of face representations with experience in children with autism. *Developmental Science, 16*(1), 116-123.

Falck-Ytter, T. (2010). Young children with autism spectrum disorder use predictive eye movements in action observation. *Biology Letters, 6*(3), 375–378.

Flanagan, J. R., & Johansson, R. S. (2003). Action plans used in action observation. *Nature, 424*(6950), 769–771.

Fox, J., & Weisberg, S. (2011). *An R Companion to Applied Regression, Second Edition*. SAGE Publications.

Friston, K. (2010). The free-energy principle: a unified brain theory? *Nature Review Neuroscience, 11*(2), 127–138.

Halekoh, U., & Hojsgaard, S. (2014). A Kenward-Roger Approximation and Parametric Bootstrap Methods for Tests in Linear Mixed Models - The R Package pbkrtest. *Journal of Statistical Software, 59*(9), 1-32.

Happé, F., & Frith, U. (2006). The weak coherence account: Detail-focused cognitive style in autism spectrum disorders. *Journal of Autism and Developmental Disorders, 36*(1), 5-25.

Hooker, C. I., Paller, K. A., Gitelman, D. R., Parrish, T. B., Mesulam, M. M., & Reber, P. J. (2003). Brain networks for analyzing eye gaze. *Cognitive Brain Research, 17*(2), 406-418.

Jaeger, T. F. (2009). Categorical Data Analysis: Away from ANOVAs (transformation or not) and towards Logit Mixed Models. *Journal of Memory and Language, 59*(4), 434–446.

Jenkins, R., Beaver, J. D., & Calder, A. J. (2006). I Thought You Were Looking at Me. *Psychological Science, 17*(6), 506–513.

Kenward, M. G., & Roger, J. H. (1997). Small Sample Inference for Fixed Effects from Restricted Maximum Likelihood. *Biometrics, 53*(3), 983–997.

Kilford, E. J., Garrett, E., & Blakemore, S.-J. (2016). The development of social cognition in adolescence: An integrated perspective. *Neuroscience and Biobehavioral Reviews, 70*, 106-120.

Kilner, J. M., Friston, K. J., & Frith, C. D. (2007). Predictive coding: An account of the mirror neuron system. *Cognitive Processing, 8*(3), 159-166.

Kilner, J. M., Vargas, C., Duval, S., Blakemore, S.-J., & Sirigu, A. (2004). Motor activation prior to observation of a predicted movement. *Nature Neuroscience, 7*(12), 1299.

Knoll, L. J., Magis-Weinberg, L., Speekenbrink, M., & Blakemore, S.-J. (2015). Social influence on risk perception during adolescence. *Psychological Science Online First, 26*(5), 583-592.

Kwisthout, J., Bekkering, H., & van Rooij, I. (2017). To be precise, the details don't matter: On predictive processing, precision, and level of detail of predictions. *Brain and Cognition, 112*, 84–91.

Maranesi, M., Livi, A., Fogassi, L., Rizzolatti, G., & Bonini, L. (2014). Mirror Neuron Activation Prior to Action Observation in a Predictable Context. *Journal of Neuroscience, 34*(45), 14827–14832.

Meijer, E., & York, S. N. (2008). Handbook of Multilevel Analysis. In J. de Leeuw & E. Meijer (Eds.) (pp. 237–274). Springer New York.

Meyer, M., Bekkering, H., Paulus, M., & Hunnius, S. (2010). Joint Action Coordination in 2½- and 3-Year-Old Children. *Frontiers in Human Neuroscience, 4* (December), 1–7.

Nordt, M., Hoehl, S., & Weigelt, S. (2015). The use of repetition suppression paradigms in developmental cognitive neuroscience. *Cortex, 80*, 61-75.

O'Hearn, K., Schroer, E., Minshew, N., & Luna, B. (2010). Lack of developmental improvement on a face memory task during adolescence in autism. *Neuropsychologia, 48*(13), 3955-3960.

O'Hearn, K., Tanaka, J., Lynn, A., Fedor, J., Minshew, N., & Luna, B. (2014). Developmental plateau in visual object processing from adolescence to adulthood in autism. *Brain and Cognition, 90*, 124-134.

Oostenveld, R., Fries, P., Maris, E., & Schoffelen, J. (2011). FieldTrip : Open Source Software for Advanced Analysis of MEG , EEG , and Invasive Electrophysiological Data. *Computational Intelligence and Neuroscience, 2011*, 1.

Pellicano, E., & Burr, D. (2012). When the world becomes "too real": A Bayesian explanation of autistic perception. *Trends in Cognitive Sciences*, *16*(10), 504-510.

Pellicano, E., Jeffery, L., Burr, D., & Rhodes, G. (2007). Abnormal Adaptive Face-Coding Mechanisms in Children with Autism Spectrum Disorder. *Current Biology*, *17*(17), 1508–1512.

Pellicano, E., Rhodes, G., & Calder, A. J. (2013). Reduced gaze aftereffects are related to difficulties categorising gaze direction in children with autism. *Neuropsychologia*, *51*(8), 1504-1509.

Pfeifer, J. H., & Blakemore, S.-J. (2012). Adolescent social cognitive and affective neuroscience: past, present, and future. *Social Cognitive and Affective Neuroscience*, *7*(1), 1-10.

Poljac, E., Dahlslätt, K., & Bekkering, H. (2013). Shared predictive decision-making mechanisms in action and language. *Language, Cognition and Neuroscience*, *29*(4), 424–434.

R Development Core Team. (2017). R: A language and environment for statistical computing. R Foundation for Statistical Computing. Vienna, Austria. Retrieved from http://www.r-project.org.

Sarkar, D. (2008). *Lattice: Multivariate Data Visualization with R*. New York: Springer.

Schuwerk, T., Sodian, B., & Paulus, M. (2016). Cognitive Mechanisms Underlying Action Prediction in Children and Adults with Autism Spectrum Condition. *Journal of Autism and Developmental Disorders, 46*(12), 3623-3639.

Sebanz, N., & Knoblich, G. (2009). Prediction in Joint Action: What, When, and Where. *Topics in Cognitive Science*, *1*(2), 353–367.

Sevgi, M., Diaconescu, A. O., Tittgemeyer, M., & Schilbach, L. (2016). Social Bayes: Using Bayesian Modeling to Study Autistic Trait-Related Differences in Social Cognition. *Biological Psychiatry*, *80*(2), 112–119.

Shattuck, P. T., Seltzer, M. M., Greenberg, J. S., Orsmond, G. I., Bolt, D., Kring, S., … Lord, C. (2007). Change in autism symptoms and maladaptive behaviors in adolescents and adults with an autism spectrum disorder. *Journal of Autism and Developmental Disorders*, *37*(9), 1735–1747.

Sinha, P., Kjelgaard, M. M., Gandhi, T. K., Tsourides, K., Cardinaux, A. L., Pantazis, D., … Held, R. M. (2014). Autism as a disorder of prediction. *Proceedings of National Academy of Sciences USA*, *111*(42), 15220–15225.

Turi, M., Burr, D. C., Igliozzi, R., Aagten-Murphy, D., Muratori, F., & Pellicano, E. (2015). Children with autism spectrum disorder show reduced adaptation to number. *Proceedings of National Academy of Sciences U S A*, *112*(25), 7868–7872.

Van De Cruys, S., Evers, K., Van Der Hallen, R., Van Eylen, L., Boets, B., De-Wit, L., … Leuven, K. (2014). Precise Minds in Uncertain Worlds: Predictive Coding in Autism. *Psychological Review*, *121*(4), 649–675.

Wahlstrom, D., Collins, P., White, T., & Luciana, M. (2010). Developmental changes in dopamine neurotransmission in adolescence: Behavioral implications and issues in assessment. *Brain and Cognition*, *72*(1), 146-159.

Walsh, J. A., Vida, M. D., Morrisey, M. N., & Rutherford, M. D. (2015). Adults with autism spectrum disorder show evidence of figural aftereffects with male and female faces. *Vision Research*, *115*, 104-112.

Walsh, J. A., Vida, M. D., & Rutherford, M. D. (2014). Strategies for perceiving facial expressions in adults with autism spectrum disorder. *Journal of Autism and Developmental Disorders*, 44(5), 1018-1026.

Warnes, G. R., Bolker, B., Gorjanc, G., Grothendieck, G., Korosec, A., Lumley, T., … Rogers, J. (2017). gdata: Various R Programming Tools for Data Manipulation. R package version 2.18.0.

Warnes, G. R., Bolker, B., Lumley, T., & Johnson, R. C. (2015). gmodels: Various R Programming Tools for Model Fitting. R package version 2.16.2. Retrieved from https://cran.r-project.org/package=gmodels

Webster, S., & Potter, D. D. (2008). Brief report: Eye direction detection improves with development in autism. *Journal of Autism and Developmental Disorders*, *38*(6), 1184-1186.

Wickham, H. (2009). *ggplot2: Elegant Graphics for Data Analysis*. New York: Springer.

Zalla, T., Labruyère, N., Clément, A., & Georgieff, N. (2010). Predicting ensuing actions in children and adolescents with autism spectrum disorders. *Experimental Brain Research*, *201*(4), 809–819.
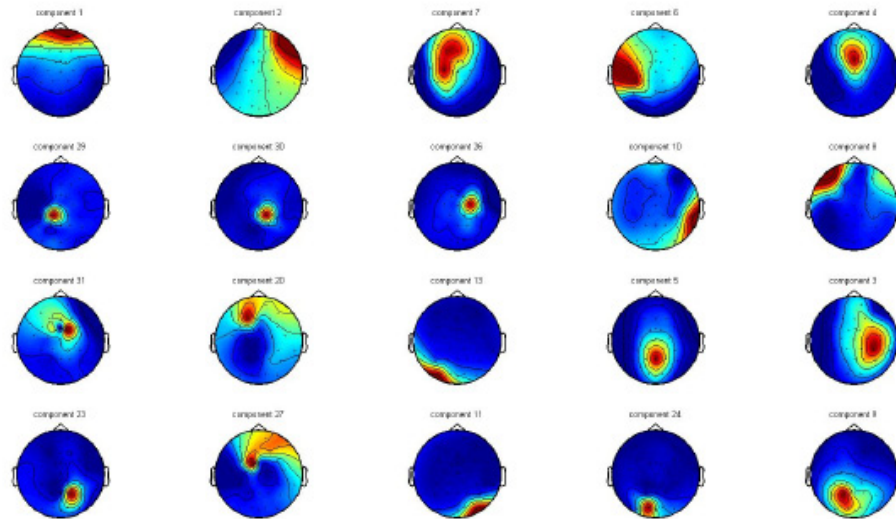
Appendix

Fig. 1. Example of the spatial distribution of a vertical (component 1) and horizontal (component 2) eye movement component, identified in the ICA.

Table 1.

Summary of the linear model investigating the differences in Duration of Time Window for the three different action steps.

Variable	b	SE	p
Action Step 1 – (2+3)	**137.28*****	20.97	< .001
Action Step 2 – 3	-17.78	36.33	.626

Note: *** indicates a significant result to a level < .001.
Significant results are printed in bold.
Note that this linear model investigated the differences of DoTOI between action steps using two contrasts:
action step one versus two and three, and action step two versus three.
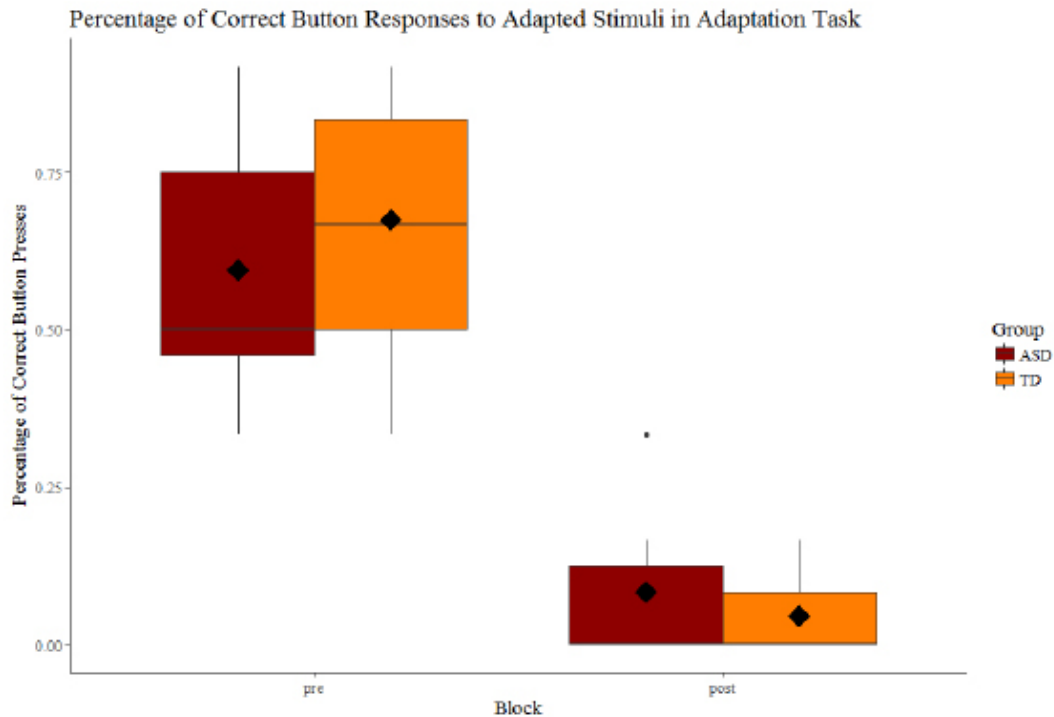
Fig. 2. Button Responses to Adapted Stimuli in Adaptation Task These boxplots show parts of the behavioural results from the adaptation task. Diamonds indicate means. This graph shows that both groups are comparable in their performance in classifying gaze direction in the preadaptation block. Interestingly, both groups seem to be similarly affected by the adaptation block, performing worse in the post adaptation block.
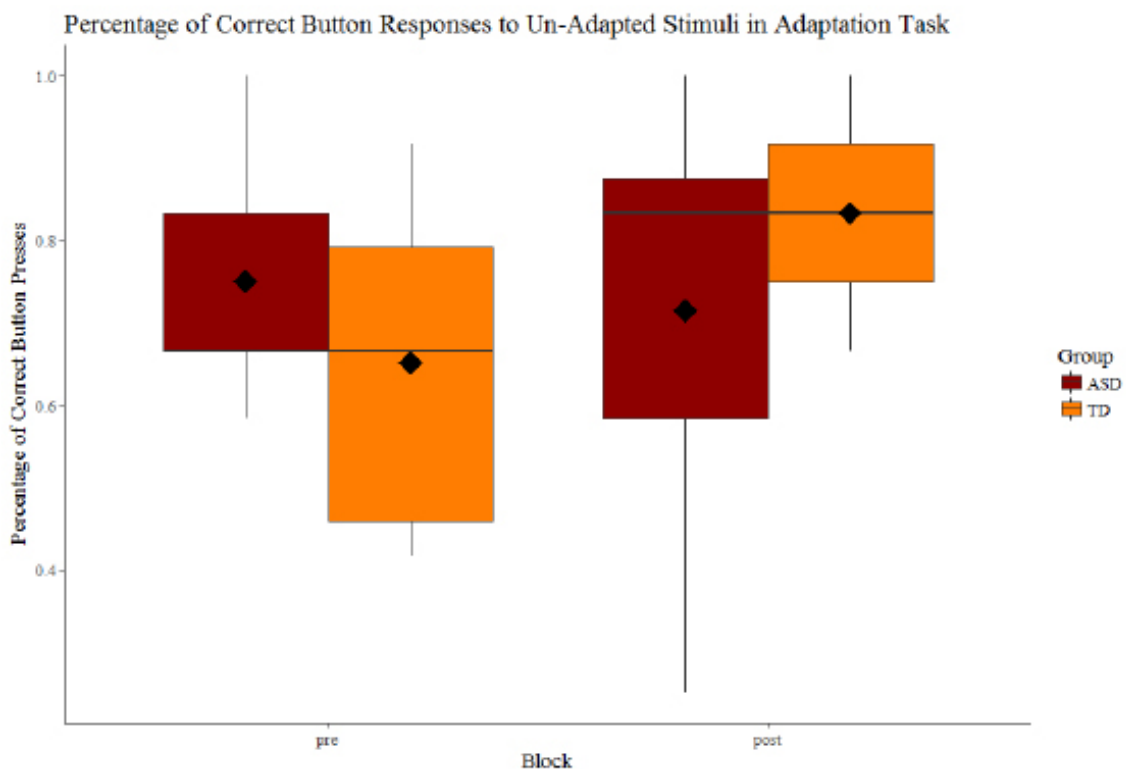

Fig. 3. Button Responses to Unadapted Stimuli in Adaptation Task. These boxplots show parts of the behavioural results from the adaptation task. Diamonds indicate means. This graph shows performances in classifying gazes in the un-adapted direction. Performance should not differ in either group between pre and postadaptation block, since the bias is towards the un-adapted direction. Therefore, stimuli in this direction should be classified as looking even more in this direction, a bias that cannot be captured by the behavioral response.

Table 2.

Summary of the fixed effects from the multilevel regressions using the student TD group, without DoTOI as a predictor.

Variable	Onset of Predictive Fixation[a]					Duration of Predictive Fixation[a]				
	b	*SE*	*t*	Appr. dfs	*p*	*b*	*SE*	*t*	Appr. *dfs*	*p*
Action Step	**2.87***	.68	4.23	668.54	< .001	**1.87***	.52	3.61	666.41	< .001
Condition	**6.63***	1.90	3.50	450.35	< .001	**4.54***	.52	3.61	511.80	.001
Action Step * Condition	-1.48	.83	-1.78	669.99	.077	-1.04	.64	-1.64	669.58	.103

Note: * indicates a significant result to a level < .05, ** indicates a significant result to a level < .01, *** indicates a significant result to a level < .001.

Significant findings to either of those levels are printed in bold.

[a] The outcome variable of this model was transformed using a square root transformation.

Note that Predictive versus Reactive Fixations was not analyzed since it did not reveal significant effects of DoTOI in the previous analysis (see Table 4).

R^2 for fixed effects:

R^2 (Onset of Predictive Fixation) = .06

R^2 (Duration of Predictive Fixation) = .05

R^2 for fixed and random effects combined:

R^2 (Onset of Predictive Fixation) = .24

R^2 (Duration of Predictive Fixation) = .17

Abstracts

Proceedings of the Master's Programme Cognitive Neuroscience is a platform for CNS students to publish their Master thesis. Given the number of submissions, we select the articles that received the best reviews, under recommendation of our editors, for the printed edition of the journal. The abstracts of the other articles are provided below, and for interested readers a full version is available on our website: www.ru.nl/master/cns/journal.

Relative Clauses In Context

An EEG study on the influence of topicality cues on grammatical role assignment

J.A. (Thijs) Trompenaars, Herbert Schriefers, Dorothee Chwilla

Relative clauses in Dutch provide an ideal environment for testing the relative strength of syntactic, semantic and pragmatic cues the listener might employ to link subject- and object roles to sentence constituents. This thesis investigates the interplay between two such cues – discourse topicality and inherent topicality – in an EEG experiment using short discourse contexts. The Topichood Hypothesis, introduced by Mak (2001) and reported in Mak et al. (2002, 2006, 2008), will be refined and further explored by directly contrasting two types of topicality introduced to account for processing biases in relative clause processing: the discourse topicality of a nominal referent and the inherent topicality of a pronominal referent. Despite behavioural evidence for an effect of both topicality factors on relative-clause processing in Dutch, we did not find a clear reflection of processing preferences in ERPs.

Structural integrity of midbrain nuclei in tremor-dominant and non-tremor Parkinson's disease

Margot Heijmans, Annelies van Nuland, Rick Helmich, Ivan Toni

Background

The reason for clinical variability between tremor-dominant and non-tremor Parkinson's Disease (PD) patients is still unclear. Post-mortem evidence suggests that some of this variability may be explained by differences in neurodegeneration patterns in the substantia nigra (SN) and retro-rubral area (RRA). The aim of this study is to in vivo relate patterns of neurodegeneration in the SN and RRA to PD subgroups and resting tremor.

Methods

Using high-resolution diffusion tensor imaging scans of 71 subjects (38 tremor-dominant, 10 non-tremor and 23 healthy controls), we test whether fractional anisotropy (FA) values in the SN and RRA differ between PD subgroups and healthy controls. Circular regions of interest were manually drawn by two raters in sub-regions of the SN, in the RRA, and in the cerebral peduncles as control areas.

Results

FA values for the different type of regions [region of interest (SN posterior and RRA) or control region (cerebral peduncles)] did not differ between PD patients and healthy controls (p = 0.400). This was the same between tremor-dominant, non-tremor and healthy controls (p = 0.306). When solely looking at the SN and RRA, there were no non-specific FA decreases in PD patients compared to healthy controls in both the SN (p = 0.090) and the RRA (p = 0.174). No correlation was found between resting tremor scores and FA values for the RRA (r = 0.064, p = 0.648).

Conclusions

Our findings question whether FA values can be used as a consistent proxy for structural integrity. Other promising measures, like free-water, may provide more reliable measures of neurodegeneration patterns in PD patients.

Habit Propensity as a Vulnerability Factor for Dependence in Experimentally Smoking Adolescents and Non-Smoking Controls

An Exploratory fMRI Study Investigating Group Differences

Rozemarijn Erdbrink, Maartje Luijten

Many Dutch adolescents have tried smoking, thereby risking the chance to become dependent on nicotine. In dependence, individuals show more habitual behaviour and less goal-directed behaviour. Dependent individuals might also activate the goal-directed brain system (the ventromedial prefrontal (VMPFC) cortex and ventral striatum) less and the habitual system (dorsal striatum) more. However, it is still unclear whether there are pre-existing differences in brain and behaviour that might indicate susceptibility to dependence. To test this, in the current study 8 experimentally smoking adolescents and 10 non-smoking controls participated in the slips-of-action task in the fMRI scanner to test differences in goal-directed and habitual behaviour and their corresponding brain systems between the two groups. It was expected that experimental smokers would be more habitual and less goal-directed compared to the non-smokers, indicating that habit propensity could be indicated as a risk factor to dependence. In addition, experimental smokers were expected to activate the goal-directed brain system (VMPFC and ventral striatum) less and the habitual (dorsal striatum) brain system more. However, there were no behavioural differences between both groups, nor were there differences in activity in the VMPFC, ventral and dorsal striatum between the groups. These findings may suggest that the differences between dependent and non-dependent individuals are not pre-existing, thus habit propensity might not indicate vulnerability to dependence. Due to the very small sample size and the difficulty of the task, however, validation of these results in a bigger sample is highly warranted.

Towards layer specific fMRI: investigating feed forward and feedback processing in area V5/MT

Alexis Joyaux, David Norris, Floris de Lange, Tim van Mourik

High-resolution fMRI has been used to investigate layer specific feedback responses in V1. Currently, no paradigm exists for high-resolution fMRI which enables to investigate both feedforward and feedback processing in an area higher in the visual information processing hierarchy than V1. This study aimed to establish a paradigm with which those processes can be selectively elicited and manipulated in motion sensitive area V5/MT. Two different manipulations of a moving dot stimulus were used to selectively manipulate feedforward and feedback processes. To manipulate feedforward processing, three different motion coherence levels were used. Feedback processing was manipulated using an attentional task where either the motion or the color of the stimulus had to be attended. The results showed that increased motion coherence elicited increased percent signal change in V5/MT while no attention effect was observed in V5/MT. The absence of such an effect might be explained by confounds of task difficulty that could have weakened attentional influences on V5/MT activity. The proposed paradigm demonstrates an interesting approach to investigate layer specific feedforward and feedback processes in V5/MT. However, additional investigations and improvements of the current paradigm are necessary before using it in a high-resolution fMRI setting.

Mechanisms of activity modulation in V1 during illusory shape perception: predictions or amodal completion?

Patricia Romero Verdugo, Matthias Ekman, Peter Kok, Floris P. de Lange

Perception is proposed to arise as a generative process in which early areas of the visual stream receive predictions from later areas, allowing for a faster and more efficient processing of visual input. In a recent study using Kanizsa illusory configurations, Kok & de Lange (2014) found that a pattern of BOLD activity resembling predictions and prediction errors could be found in primary visual cortex (V1), providing support for a predictive coding account of perception. However, an alternative interpretation has been suggested to explain these effects (Moors, 2015). We conducted an fMRI experiment to test the two proposed interpretations. Our results fail to provide conclusive evidence for either of the accounts, but provide insight into key aspects to consider for further research into the mechanisms of illusory shape perception.

Spatiotemporal Context-Generalization of Object Category Representations during Fear Conditioning.

Yannick P. J. Murray, Lycia D. de Voogd, Erno J. Hermans

Generalization of emotional arousing experiences to other contexts is adaptive. Fear-related disorders are often characterized by excessive generalization, indicating an impaired integration of cue and context information. Neocortical representations of emotional experiences show increased spontaneous reactivations during post-learning rest, which lead to better memory. However, it remains unclear whether context spontaneously reactivates these neocortical representations of emotional experiences during rest and how this affects generalization. We hypothesize that increased context generalization is associated with heightened activity of neocortical representations of emotional experiences in a safe context. To test this, participants underwent a categorical localizer paradigm, followed by a categorical differential delay cue/contextual fear conditioning paradigm. We used a virtual reality environment that contained a threat and safe context to acquire context specific activity patterns of CS+ and CS- object category representations from blood-oxygen-level dependent functional magnetic resonance imaging (BOLD fMRI). An exemplar of the CS+ category was paired with a mild electrical stimulation, but only when it was presented in a threat context. We found differential skin conductance responses (SCR) in the threat context, indicating successful conditioning, but also in the safe context, indicating context generalization. Using representational similarity analyses we found increased differential representations in the threat context compared to the safe context. This was driven by reduced representation of the CS- in the threat context. Critically, we found that the more participants inhibited CS- representations in the threat context, the more they exhibited fear generalization, measured with SCR. In conclusion, our data show that suppression of neutral objects underlies individual differences in fear generalization.

The role of suboptimal mitochondrial function in stress adaptation and depression pathogenesis

Elisavet Vasileiou, Tamas Kozicz, Tim Emmerzaal

The brain requires massive amounts of energy to operate optimally. These demands are almost exclusively covered by the powerhouses of neurons, the mitochondria. Recently, a considerable body of evidence implicates impaired mitochondrial bioenergetics in psychopathology, although the mechanism behind this link remains elusive. Here we test the hypothesis that the interaction of suboptimal mitochondrial function with chronic stress confers vulnerability to depression, using the novel Ndufs4 deficient transgenic mouse model. To this end, we subjected wild type and transgenic adult male mice to the well-established chronic variable stress (CVS) paradigm and assessed its effects on physiological parameters and affective behavior. We found that chronically stressed Ndufs4 deficient mice showed reduced exploration behavior and a markedly higher preference for the outer zone in the open field arena that is not decreased with time, a greater propensity to passive coping and earlier signs of behavioral despair in the forced swim test, but no significant loss of interest in self-care in the splash test and no weight change alterations. Moreover, cFos imaging analysis revealed that impaired mitochondrial function was linked with higher activity in the dorsomedial hypothalamic nucleus (DMH) in response to acute stress and aberrant spontaneous activity in significant stress-related areas, i.e DMH and the ventral portions of hippocampal CA1 and dentate gyrus, under conditions of chronic stress. Taken together, these results provide evidence that compromised mitochondrial function mediates effects of chronic stress on mood and may be a vulnerability factor to maladaptive stress-coping. Our research could be the basis for the development of novel antidepressant pharmaceuticals that target brain metabolic processes and could benefit at least a portion of currently treatment-resistant patients.

Interaction of Stroke and Alzheimer's disease in the APPswe/ PS1dE9 Mouse Model

Lieke Bakker, Nienke Timmer, Maximilian Wiesmann, Amanda J. Kiliaan

While the most well-known pathology associated with Alzheimer's disease (AD) is the accumulation of beta-amyloid protein, more and more studies indicate a strong interaction of vascular risk factors with AD, such as hypertension, atherosclerosis and stroke. With this study, we strived to clarify the link between AD and ischemic stroke in vivo, by means of a longitudinal study in transgenic AD mice in which ischemic stroke was induced. Systolic blood pressure (SBP) measurements have been performed next to a variety of behavioral paradigms, such as the open field, rotarod and Morris water maze. Results one month after surgery suggest a larger motor impairment in the AD stroke mice compared to the other groups. At the age of 9-10 months, the AD mice showed a higher SBP, in combination with higher activity levels in the open field, in contrast to measurements performed in the wildtype mice. At 12 months of age however, this hyperactive behavior was only observed in the AD stroke mice. Moreover, throughout the study, a higher incidence of epileptic seizures was observed in these same AD stroke mice, together with higher mortality rates. It seems that the combination of AD and ischemic stroke leads to a higher sensibility to stressors than either pathology alone, resulting in pathological and behavioral alterations that vary during the different stages of the disease. The combination of AD and ischemic stroke thus deserves more attention, since more insight in the underlying mechanisms of this combination can contribute to the development of preventatives or treatments.

Sex Differences in Affective Processing

Taking a Comparative and Evolutionary Approach

Victoria Heng, Eliza Bliss-Moreau, Rogier Mars

Across domains ranging from clinical to evolutionary psychology, and well engrained in the public's perception, is the idea that women are the more emotional sex in comparison to men. However, the extent to which perceived sex differences are real and rooted in biology (and therefore evolutionary processes) and not the result of social factors is not entirely clear. In order to investigate whether sex differences in affective processing are rooted in biology, we adopted an evolutionary and comparative approach and studied 7 male and 7 female rhesus macaques (Macaca mulatta) in 4 different experiments that used behavioral, physiological and attentional measures to quantify sex differences in affective processing. We did not observe sex differences in the majority of our experiments – including experiments that measured affective reactivity to threatening humans (Experiment 1) and live animal stimuli (Experiment 2) and an experiment that measured monkeys' toy preference (Experiment 3). We did observe some sex differences in an experiment that measured autonomic nervous system activity and visual attention to passively viewed movies that varied in affective content (Experiment 4) We observed that in comparison to females, males has significantly higher Respiratory Sinus Arrhythmia values, a measure that reflects parasympathetic nervous system activity, and attended movies that showed neutral affective content significantly more than females. We did not observe any sex differences in measures that reflected sympathetic nervous system activity (i.e., Dark-Adapted Pupil Diameter) or in measures that reflected mixed parasympathetic and sympathetic nervous system activity (i.e., heart rate and respiration rate). These results suggest that males overall were less engaged with the movie stimuli compared to females and were possibly less anxious compared to females. Our findings are not in line with results from human studies, which generally do not report sex differences in physiological measures relating to affective processing. This could mean that human sex differences are largely the result of social and cultural processes and are not rooted in biology. However, to our knowledge we are the first ones to study sex differences in rhesus macaques across tasks using various measures for affective processing, and more research using a wider variety of animal models and translational tools is warranted.

Acquisition of Novel Concept Spaces

Adrian Jodzio, Stephanie Theves, Christian Doeller

The hippocampus is known to play a key role in spatial navigation as well as declarative memory. More recently, hippocampal circuitry has been shown to map more abstract spaces such as social space (Tavares et al., 2015) or the mapping of frequency tones (Aronov et al. 2017). Here we test whether novel concepts are also acquired with a map-like representation in the hippocampus. We create a novel concept map comprising symbols spanning two feature dimensions. Participants learn to categorize symbols into A & B concepts, as well as associate real-world objects with some of these symbols. By means of showing them the objects in the scanner both before and after the learning phase, we are able to examine changes in neural representations as a function of learning. Participants are able to learn the novel concept along with the concept space. fMRI data indicate a repetition suppression effect in the right body of the hippocampus for objects that are close together compared to those that are further apart within the concept space.

Institutes associated with the
Master's Programme Cognitive Neuroscience
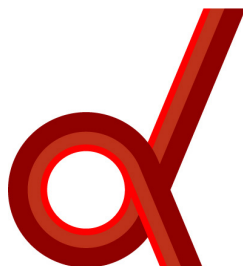
Donders Institute for Brain, Cognition
and Behaviour:
Centre for Cognitive Neuroimaging
Kapittelweg 29
6525 EN Nijmegen

P.O. Box 9101
6500 HB Nijmegen
www.ru.nl/donders

Max Planck Institute for Psycholinguistics
Wundtlaan 1
6525 XD Nijmegen

P.O. Box 310
6500 AH Nijmegen
http://www.mpi.nl

Radboudumc
Geert Grooteplein-Zuid 10
6525 GA Nijmegen

P.O. Box 9101
6500 HB Nijmegen
http://www.radboudumc.nl

Baby and Child Research Center
Montessorilaan 3
6525 HR Nijmegen

P.O. Box 9101
6500 HB Nijmegen
http://www.babyandchild.nl